

**A Novel Antimalarial Lead Compound:
In Vitro Properties and Mode of Action Studies**

INAUGURALDISSERTATION

zur

Erlangung der Würde eines Doktors der Philosophie

vorgelegt der

Philosophisch-Naturwissenschaftlichen Fakultät

der Universität Basel

von

Ralf Oskar Brunner

aus Therwil (BL)

Basel, 2011

Genehmigt von der Philosophisch - Naturwissenschaftlichen Fakultät auf Antrag
von Prof. Reto Brun, Prof. Nicole Schaeren-Wiemers und Prof. Till Voss.

Basel, den 24. Mai 2011

Prof. Martin Spiess

Dekan

Table of contents

Acknowledgments.....	4
Abstract.....	6
Zusammenfassung.....	7
Table of abbreviations.....	8
1 Introduction.....	10
1.1 A general introduction to malaria.....	10
1.2 Treatment of malaria.....	13
1.3 Resistance to antimalarials.....	16
1.4 The need for novel antimalarial agents.....	19
1.5 Discovery of a novel antimalarial chemotype.....	20
1.6 Objectives.....	21
2 Materials.....	22
2.1 Chemicals and proteins.....	22
2.2 Chemical probes and antimalarials.....	24
2.3 Solutions, buffers and experimental devices.....	24
2.4 <i>Plasmodium falciparum</i> strains.....	27
3 Methods.....	28
3.1 Parasite cultivation.....	28
3.2 [³ H]hypoxanthine incorporation assays.....	29
3.3 Methods based on UV-activatable compounds.....	31
3.4 Fluorescent imaging.....	32
3.5 SDS-PAGE.....	33
3.6 Far Western blotting.....	33
3.7 Pull-down experiments based on UV-activatable compounds.....	34
3.8 Pull-down experiments using monomeric avidin systems.....	37
3.9 Pull-down experiments using streptavidin systems.....	38

Table of contents

3.10	Pull-down experiments using compounds directly linked to beads.....	39
3.11	Mass spectrometry	40
3.12	Validation of target candidates	42
3.13	Hematin interaction studies.....	46
3.14	Microarray.....	48
3.15	qPCR.....	50
4	Results.....	55
4.1	<i>In vitro</i> activities of test compounds.....	55
4.2	Panel of resistant <i>Plasmodium falciparum</i> strains	56
4.3	<i>In vitro</i> pharmacodynamics.....	57
4.4	Fluorescent imaging.....	60
4.5	Far Western blotting	64
4.6	Pull-down experiments based on UV-activatable compounds	65
4.7	Pull-down experiments using monomeric avidin systems.....	72
4.8	Early pull-down experiments.....	73
4.9	Overlap of target candidates	74
4.10	Validation of target candidates	75
4.11	Hematin interaction studies.....	85
4.12	Microarray.....	89
4.13	Overlap of pull-down and microarray results	93
4.14	qPCR.....	94
5	Discussion.....	96
5.1	<i>In vitro</i> activity of ACT-AM and derivatives	96
5.2	UV-activatable compounds.....	97
5.3	Fluorescent imaging.....	98
5.4	Far Western blotting	99
5.5	Pull-down experiments	99
5.6	Microarray.....	103
5.7	Mode of action	104
5.8	Outlook	108

Table of contents

5.9	Conclusion	110
6	Appendix.....	112
6.1	Microarray.....	112
6.2	qPCR: Primer validation.....	116
7	References.....	117
	Curriculum vitae	128

Acknowledgments

First and foremost, I would like to thank Reto Brun for taking me on as a PhD student, for his experienced guidance and for always having an open door. It has been a pleasure and a privilege to work with such an expert in the field.

I am very grateful to Sergio Wittlin who did an excellent job as a supervisor for allowing me a lot of freedom but at the same time always being there when support was needed.

A special thanks must go to Richard Welford; I very much appreciate his scientific advice and his critical look at the thesis.

I am indebted to Christoph Binkert for enthusiastically driving the antimalaria project forward, for enabling and backing collaborations and for many stimulating discussions.

Till Voss got involved in numerous methodological Q&A sessions; I am very thankful that he untiringly shared his vast expertise.

I would also like to express my gratitude to Nicole Schaeren-Wiemers and Hans-Peter Beck for joining the thesis committee meetings and for scientific suggestions.

To Pascal Mäser I would like to thank for precious input, especially concerning transporters.

Many thanks to Christoph Boss whose unfailing effort was of key importance. He and his team provided the chemical probes which were the base of all relevant experiments; I individually acknowledge Claire-Lise Ciana, Olivier Corminboeuf and Bibia Heidmann.

I am greatly appreciative to Walter Fischli for a very positive and motivating attitude towards the project.

Amélie Le Bihan needs to be thanked for coordinating the whole antimalaria venture.

I sincerely acknowledge the following collaborators for

The analysis of the microarray experiment:

Enghow Lim and Zbynek Bozdech (Nanyang Technological University, Singapore)

In vitro tests of target candidates:

David Fidock and Corinna Mattheis (Columbia University, NY); I.J. Frame (Albert Einstein College, NY); Michael Lanzer and Sebastiano Bellanca (Universitätsklinikum

Acknowledgments

Heidelberg); Colin Stack (University of Western Sydney); Ingrid Müller and Rolf Walter (Bernhard Nocht Institut, Hamburg)

Mass Spectrometry:

Paul Jenö and Suzette Moes (Biocenter, Basel)

I wish to thank several people who specifically contributed to this project in the following ways:

In vivo experiments: Karin Gysin, Christoph Fischli, Jolanda Kamber, Petros Papastogiannidis and Pascale Steiger

TDR panel related experiments: Marcel Kaiser, Monica Cal, Sonja Keller-Märki, Christoph Stalder

Advice and help in the laboratory: Ulf Eidhoff, Christian Flück, Igor Niederwieser, Esther Pachlatko, Sebastian Rusch, Patrick Seitz, Christian Scheurer, Annette Trébaul

Providing Pfaldolase: Jürgen Bosch and Heinz Döbeli

qPCR: Dania Müller and Kathrin Widmer

Bioinformatics: Philipp Ludin

Statistics: Christian Schindler

Many thanks must also go to a number of people who provided an unforgettable and welcoming atmosphere:

Urs, Benjamin, Céline, Christian, Katrin, Lucienne, Marie, Marco, Matthias, Mireille, Nicolas, Pax, Sarah, Sophie and Theresia.

I am deeply grateful to Korinna, my family and friends for their support and encouragement.

Abstract

Malaria remains a major public health problem and the increasing number of resistant strains underscores the need for new drugs with new modes of action (MOAs).

It was the aim of the present thesis to characterize a novel antimalarial lead compound with respect to MOA and *in vitro* properties.

The lead compound, ACT-AM, inhibited *in vitro* proliferation of all tested *P. falciparum* strains, irrespective of their drug resistance properties, with IC₅₀ values in the low single-digit nanomolar range. ACT-AM was further shown to equally and rapidly affect all asexual blood stages of the parasite. The novel molecule is therefore comparable to the most efficacious registered antimalarial drugs in terms of *in vitro* activity.

To investigate the MOA of ACT-AM, a chemical derivative of the compound able to form covalent bonds upon UV activation was utilized. This advantageous UV-dependent system was adapted and implemented for *P. falciparum*- notably for the use in intact cells and proved to be appropriate for various biochemical methods including pull-down experiments, fluorescent imaging and Far Western blotting. Pull-down experiments revealed numerous target candidates, three of which were shown to interact with ACT-AM *in vitro*, namely MDR (multidrug resistance protein), ENT4 (equilibrative nucleoside transporter 4) and CRT (chloroquine resistance transporter). These proteins could represent actual targets or might confer resistance to the compound.

Microarray and hematin interaction studies suggested that ACT-AM has an MOA distinct from that of several registered antimalarials, a factor that bodes well for possible combination therapies.

The promising *in vitro* activity of the compound and the indication of a novel MOA emphasize the potential of ACT-AM or analogues of the same chemical class as therapeutic agents for the treatment of malaria.

Zusammenfassung

Malaria ist noch immer eines der grössten Gesundheitsprobleme weltweit und die Zunahme an resistenten Stämmen unterstreicht die Notwendigkeit neuer Medikamente mit neuen Wirkmechanismen.

Das Ziel der vorliegenden Arbeit war, eine neuartige Leitstruktur gegen Malaria hinsichtlich Wirkmechanismus und *in vitro* Eigenschaften zu charakterisieren.

Diese Leitstruktur, ACT-AM, hemmte *in vitro* das Wachstum aller getesteten *P. falciparum*-Stämme, unabhängig von deren Resistenzeigenschaften und wies IC₅₀-Werte im niedrigen einstelligen nanomolaren Bereich auf. Zudem zeigte ACT-AM eine schnelle Wirksamkeit gegen alle asexuellen Blutstadien des Parasiten und ist somit bezüglich *in vitro* Aktivität vergleichbar mit den effizientesten zugelassenen Malariamedikamenten.

Um den Wirkmechanismus von ACT-AM zu untersuchen, wurden chemische Derivate der Verbindung eingesetzt, die nach UV-Aktivierung kovalente Bindungen eingehen können. Dieses vorteilhafte UV-abhängige System wurde adaptiert und implementiert für den Gebrauch mit *P. falciparum* – insbesondere für intakte Zellen und erwies sich als geeignet für verschiedene biochemische Methoden wie „Pull-down“-Experimente, „Fluorescent Imaging“ und „Far Western Blotting“. Mittels „Pull-down“-Experimenten wurden mehrere Zielstruktur-Kandidaten identifiziert, wovon bei den folgenden drei eine *in vitro* Interaktion mit ACT-AM nachgewiesen werden konnte: MDR (multidrug resistance protein), ENT4 (equilibrative nucleoside transporter 4) und CRT (chloroquine resistance transporter). Diese Proteine könnten tatsächliche Zielstrukturen sein oder aber Resistenz gegen ACT-AM bewirken.

„Microarray-Studien“ und Hematin-Interaktionsexperimente lassen vermuten, dass die neue Leitstruktur einen Wirkmechanismus aufweist, der sich von diversen registrierten Malariamedikamenten unterscheidet, was eine Voraussetzung für potenzielle Kombinationstherapien ist.

Die vielversprechende *in vitro* Aktivität von ACT-AM sowie der Hinweis auf einen neuartigen Wirkmechanismus betonen das Potenzial dieser Verbindung oder analoger Substanzen derselben chemischen Klasse als Therapeutika zur Behandlung von Malaria.

Table of abbreviations

AS	artesunate
Bis-Tris	bis (2-hydroxyethyl) aminotris (hydroxymethyl) methane
BSA	bovine serum albumin
CAPS	n-cyclohexyl-3-aminopropanesulfonic acid
cDNA	complementary DNA
CM	culture medium
CQ	chloroquine
CRT	chloroquine resistance transporter
C _T	threshold cycle
Da	dalton
DAPI	4'-6-diamidino-2-phenylindol
DEPC	Diethylpyrocarbonate
DHFR	dihydrofolate reductase
DHPS	dihydropteroate synthase
DIS	distomer
DMSO	dimethylsulfoxid
DNA	deoxyribonucleic acid
DTT	Dithiothreitol
DV	digestive vacuole
EDTA	ethylenediaminetetraacetic acid
ER	endoplasmic reticulum
EU	eutomer
FACS	fluorescence activated cell sorting
FIC	fractional inhibitory concentration
FLC	fluorescein
GAPDH	glyceraldehyde 3-phosphate dehydrogenase

Abbreviations

α -GDH/TPI	glycerophosphate dehydrogenase- triosephosphate isomerase
gDNA	genomic DNA
HEPES	4-(2-hydroxyethyl)-1-piperazine- ethanesulfonic acid
HRP	horse radish peroxidase
iRBC	(infected) red blood cell
MES	2-(N-morpholino)ethanesulfonic acid
MOPS	3-(N-morpholino)propanesulfonic acid
MQ	mefloquine
MS	mass spectrometry
N.A.	not applicable
NAD	nicotinamide adenine dinucleotide
NP-40	Nonidet P-40
PAGE	polyacrylamide gel electrophoresis
PBS	phosphate buffered saline
p.i.	post infection
PYR	pyrimethamine
RBC	red blood cell
SD	standard deviation
SDS	sodium dodecyl sulfate
SM	screening medium
TBS	tris-buffered saline
TEMED	tetramethylethylenediamine
vs.	versus
WHO	world health organization
wt	wild type
mt	mutant

1 Introduction

1.1 A general introduction to malaria

Malaria, caused by protozoan parasites of the genus *Plasmodium* was first scientifically described by Laveran in 1880 (Laveran 1880) and is still a major health problem. More than 240 million cases of malaria occur every year and the number of fatalities is estimated at over 800'000 (World Health Organization 2010). The disease accounts for 20% of all childhood deaths in Africa (WHO 2010). There are four malaria species that commonly infect humans: *P. falciparum*, *P. vivax*, *P. ovale*, and *P. malariae* (reviewed by Tuteja 2007). Isolated cases of transmission of nonhuman primate malaria parasites such as *P. knowlesi* to humans have been reported, but do not seem to be a major threat (Singh et al. 2004; Van den Eede et al. 2009). Malaria is endemic in 99 countries (Feachem et al. 2010) and occurs mainly in sub-Saharan Africa, Asia, Latin America, and to a lesser extent in the Middle East and parts of Europe, as shown for the most common species, *P. falciparum* and *P. vivax* (Figure 1.1).

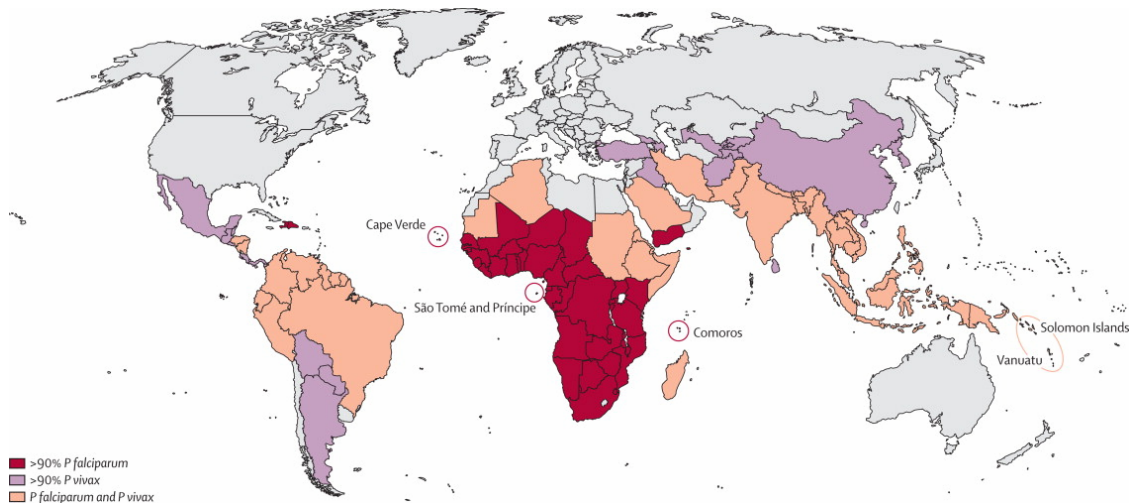


Figure 1.1. Categorization of countries according to whether human malaria is predominantly caused by *P. falciparum*, *P. vivax*, or both. Adapted from Feachem et al. 2010.

Malaria tropica, the most severe and potentially fatal form of malaria, is caused by *P. falciparum* (WHO 2010). The parasite is transmitted through the bites of female mosquitoes of the genus *Anopheles*. In the human host, the complex life cycle of *P. falciparum* (Figure 1.2) begins upon injection of sporozoites from the salivary gland of the mosquito into the subcutaneous tissue or directly into blood vessels (reviewed by Miller et al. 2002). Via the bloodstream, sporozoites are transported to the liver where they infect hepatocytes (reviewed by Kappe et al. 2010). On their way to the liver, the motile sporozoites are able to traverse several cell types of the host (Mota et al. 2001). Sporozoites remain for 9–16 days in the liver and undergo asexual replication (reviewed by Tuteja 2007) whereby each sporozoite develops into thousands of first generation merozoites which are released into the bloodstream (reviewed by Kappe et al. 2010). Each merozoite can rapidly invade a red blood cell (RBC), (reviewed by Cowman & Crabb 2006) and initiate the intraerythrocytic cycle: *P. falciparum* develops over 48 hours in RBCs, exhibiting three morphologically distinct forms (Elmendorf & Haldar 1993): Rings [0-24h post invasion (p.i.)], trophozoites (24-36h p.i.), and schizonts (36-48h p.i.). Each mature schizont produces 8 - 32 merozoites which can infect new RBCs. After several rounds of asexual replication, up to 10% of all RBCs can become infected and most clinical features of malaria (see below) are associated with this intraerythrocytic cycle of the parasite (reviewed by Wirth 2002). Eventually, a small fraction of merozoites differentiates into sexual blood stages, micro- and macrogametocytes (male and female, respectively), which are taken up by mosquitoes during another blood meal. Upon nuclear division and exflagellation in the midgut of the mosquito, microgametocytes form microgametes and fuse with female macrogametes to form a zygote. The zygote in turn develops into the ookinete, capable of penetrating the gut wall and forming an oocyst. After sporogony and rupture of the oocyst, sporozoites are released and migrate to the salivary gland rendering the mosquito infective for 1-2 months. The mosquito vector can then initiate a new *P. falciparum* infection (reviewed by Tuteja 2007).

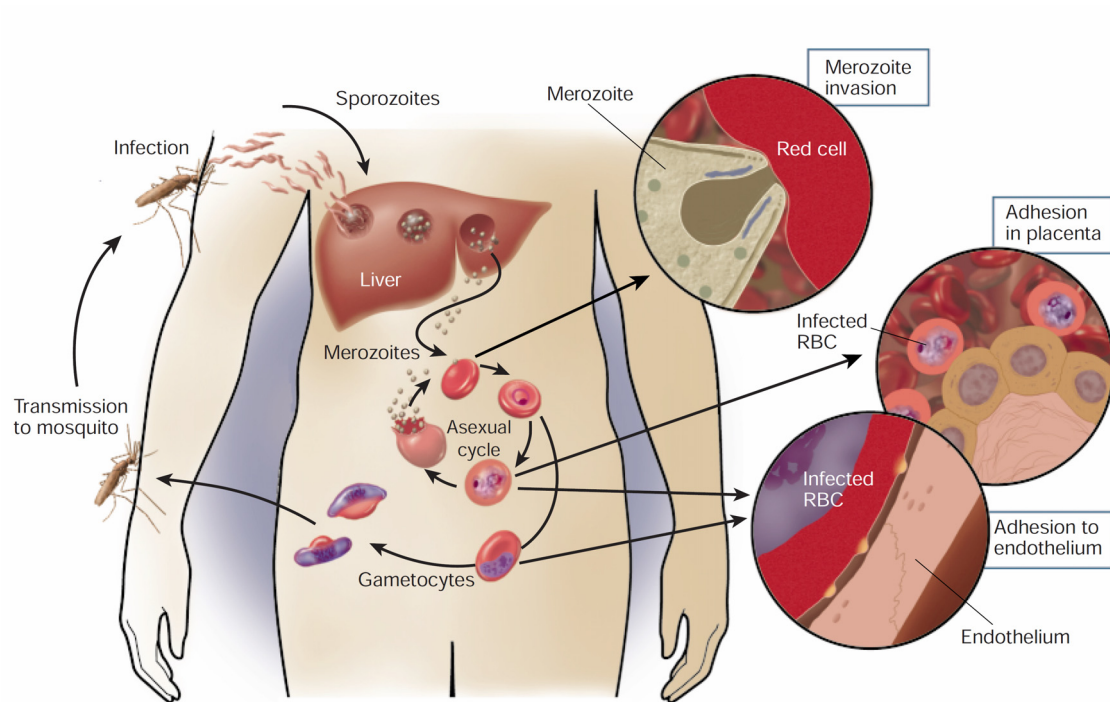


Figure 1.2. Life cycle of *Plasmodium falciparum*. Adapted from Miller et al. 2002.

Malaria symptoms appear approximately one week after infection. Regular symptoms include fever, shivering, cough, respiratory distress, pain in the joints, headache, watery diarrhea, vomiting and convulsions (reviewed by Miller et al. 2002). Untreated malaria fevers are typically periodic (48h for *P. falciparum*) because they coincide with the synchronous release of merozoites and cytokines into the bloodstream (reviewed by Tuteja 2007).

In most cases of malaria, there are no fatal complications. The factors triggering the transition from an uncomplicated to a severe (life-threatening) malaria are still unknown (Snow & Marsh 1998). A key-characteristic of *P. falciparum* leading to potentially fatal symptoms such as severe anaemia, impaired consciousness, and renal failure (reviewed by Miller et al. 2002) is termed sequestration. Infected RBCs display adhesive parasite-derived proteins on their surface causing them to adhere to uninfected RBCs, endothelial cells of small blood vessels and in some cases to placental cells (Baruch 1999) thereby sequestering the parasite from being cleared in the spleen. Additionally, adherence of

infected RBCs to small blood vessels or organs gives rise to serious forms of the disease (reviewed by Tuteja 2007), namely placental or cerebral malaria (Figure 1.2.). Due to these two potential complications, malaria is especially dangerous for pregnant women and small children (van Geertruyden et al. 2004). In sub-Saharan Africa, where transmission rates are high, people gradually become semi-immune after repeated exposure to the parasite (McGregor 1974); it is children under the age of five, too young to develop semi-immunity, who are most at risk of severe malaria (WHO 2010).

1.2 Treatment of malaria

The phenomenon of semi-immunity (see 1.1) offers a plausible rationale for the development of malaria vaccines. Nevertheless, after decades of research, no registered vaccine is available (reviewed by Crompton et al. 2010). Therefore, malaria treatment today is still solely reliant on parasite chemotherapy.

The most widely used antimalarial compounds belong to the classes of quinolines, antifolate drugs, artemisinins, atovaquone, and antibiotics (reviewed by Cunha-Rodrigues et al. 2006).

Quinoline-based compounds, such as quinine, piperaquine, chloroquine and mefloquine are historically among the most successful antimalarial agents. Quinine-containing extracts from the bark of the South American cinchona tree were introduced to Western medicine as early as the 17th century (reviewed by Toovey 2004).

In spite of extensive use since 1947 (reviewed by Solomon & H. Lee 2009), the molecular target of chloroquine, the most famous member of the quinolines, is still a matter of debate (reviewed by Cunha-Rodrigues et al. 2006). An often discussed mode of action of chloroquine and other quinolines is thought to involve interference of the compound with the detoxification of heme (reviewed by Sullivan 2002): Intraerythrocytic *P. falciparum* parasites enzymatically digest hemoglobin in special acidic compartments, called food vacuoles, whereby toxic heme is released and spontaneously converted to a less reactive dimer, the “malaria pigment” or hemozoin (Slater et al. 1991; Egan et al. 2002; Pagola et al. 2000). Chloroquine and related compounds have been shown to inhibit synthetic

hemozoin (beta-hematin) formation *in vitro* (Slater & Cerami 1992; Egan et al. 1994; Dorn et al. 1995; Sullivan et al. 1996). However, a number of other targets have been proposed for the quinoline family, including tyrosine kinases (Sharma & Mishra 1999), DNA (Ciak & Hahn 1966), and phospholipases (Kubo & Hostetler 1985).

The most well-known antifolates, designed to affect nucleotide synthesis and amino acid metabolism, are pyrimethamine, chloroguanide (proguanil), and sulfadoxine (reviewed by Cunha-Rodrigues et al. 2006). Type-1 antifolates, e.g. sulfadoxine (Y. Zhang & Meshnick 1991), inhibit dihydropteroate synthase (DHPS), whereas type-2 antifolates, e.g. pyrimethamine and proguanil, affect dihydrofolate reductase (DHFR), (Ferone et al. 1969). The mode of action of this class of antimalarials is based on the inability of the parasite to salvage certain folate cofactors from their human host. Inhibiting the synthesis of these essential cofactors is therefore an attractive point of attack (reviewed by Olliaro 2001). As the name implies, antifolates, or folate antagonists, are believed to mimic the substrates of their target enzymes thereby competing for the active site of the latter: Type-1 antifolates mimic p-aminobenzoic acid inhibiting DHPS. Likewise, type-2 antifolates mimic dihydrofolic acid and compete for the active site of DHFR (reviewed by Olliaro 2001). Compared to quinolines, antifolates act in general less rapidly and, as shown for sulfadoxine and pyrimethamine (Dieckmann & Jung 1986), affect late forms of the asexual *P. falciparum* blood stage that undergo nuclear division (reviewed by Cunha-Rodrigues et al. 2006).

A different mode of action is attributed to the antimalarial drug atovaquone which apparently interferes with plasmodial mitochondria. The exact mechanism leading to inhibition of parasite proliferation is yet not fully understood. However, atovaquone is thought to affect mitochondria at the level of the plasmodial cytochrome bc1 complex which differs structurally from its human counterpart (Vaidya et al. 1993). Atovaquone probably interferes with the cytochrome bc1 complex by mimicking ubiquinone (Fry & Pudney 1992; Hudson 1993; Srivastava et al. 1997), which was shown to inhibit mitochondrial electron transport (Fry & Beesley 1991) and to collapse mitochondrial membrane potential (Srivastava et al. 1997; Painter et al. 2007).

Artemisinin-based compounds, e.g. artemether, artesunate, and dihydroartemisinin, are currently among the most important antimalarials (reviewed by Fidock 2010). The excellent effectiveness of these molecules is largely attributable to their fast onset of action and their activity against all three asexual blood stages (ter Kuile et al. 1993; White 2008). In addition, artemisinins counteract malaria transmission because they are active against gametocytes (Chen et al. 1994). The starting material of this class of compounds, artemisinin, is purified from sweet wormwood (*Artemisia annua*), extracts of which have been in use for more than 2000 years in China (reviewed by Meshnick et al. 1996). Chemically, artemisinins belong to the class of sesquiterpene lactones and have an endoperoxide bridge which is essential for antimalarial activity (reviewed by White 2008). Studies on how artemisinins exert their action, are numerous but controversial (reviewed by Ding et al. 2011). An often proposed mode of action involves iron-mediated activation of artemisinins whereby the endoperoxide bridge is thought to be decomposed upon contact with ferrous heme leading to the formation of free radicals (reviewed by Meshnick 2002). This mechanism would also explain the selective activity against parasites (reviewed by Meshnik 2002). On the other hand, this often cited hypothesis is in contradiction to findings that all blood stages of the parasite – even early rings (Skinner et al. 1996) and gametocytes (Chen et al. 1994) which are apparently devoid of hemozoin- are susceptible to these drugs. Other potential modes of action include more specific targets such as PfATP6, a SERCA (sarco/endoplasmic reticulum)-type Ca^{2+} dependent ATPase (Eckstein-Ludwig et al. 2003) or cysteine protease (Pandey et al. 1999).

Antibiotics define another class of antimalarials.

Several apicomplexan parasites are believed to be susceptible to antibiotics due to their special organelle, the apicoplast, which carries transcription and translation machineries similar to those of prokaryotes (reviewed by Cunha-Rodrigues et al. 2006). A well studied member of this class is the slowly acting prokaryotic translation inhibitor azithromycin which has been used in numerous clinical trials (van Eijk & Terlouw 2011). In bacteria, azithromycin binds to the 50S ribosomal subunit thereby inhibiting protein synthesis. For *P. falciparum*, in contrast, the MOA remains unknown but the molecule is

believed to affect house keeping functions of the apicoplast (Dahl & Rosenthal 2008). Van Eijk and coworkers have recently published an analysis of 15 clinical antimalarial trials involving azithromycin. Their findings suggest that “azithromycin is a weak antimalarial” which depends on the activity of combination partners. The authors concluded that this antibiotic’s “future for the treatment of malaria does not look promising” (van Eijk & Terlouw 2011).

1.3 Resistance to antimalarials

Malaria is a potentially fatal but, if treated correctly, curable disease. However, worldwide emerging resistance to the existing antimalarial drugs has been threatening current treatment regimens (reviewed by Fidock 2010).

In the case of chloroquine, the scale of the problem becomes apparent, as areas of reported resistance have been shown to more and more overlap with endemic regions (Figure 1.3).

The molecular mechanism underlying resistance to chloroquine is mostly assigned to mutant forms of the chloroquine resistance transporter (pfCRT). Mutant transporters are thought to lead to a decrease in chloroquine concentration inside the food vacuole, allegedly the site of action of the antimalarial (Fidock et al. 2000; Martin et al. 2009). Another transporter, the multidrug resistance protein (pfMDR), seems to play a role in both resistance to mefloquine and chloroquine. *In vitro*, variants of this p-glycoprotein homologue were shown to transport chloroquine (Sanchez et al. 2008) and *in vitro* susceptibility to mefloquine and quinine apparently correlates with the copy number of the transporter (Sidhu et al. 2006).

Spread of resistance to the antifolates pyrimethamine and sulfadoxine is probably as pronounced as for chloroquine (reviewed by Wongsrichanalai et al. 2002; Mita et al. 2009), (Figure 1.3).

In contrast to chloroquine resistance, mutations of the actual target enzymes, DHFR and DHPS, lead to increased tolerance to pyrimethamine and sulfadoxine, respectively (Plowe et al. 1997).

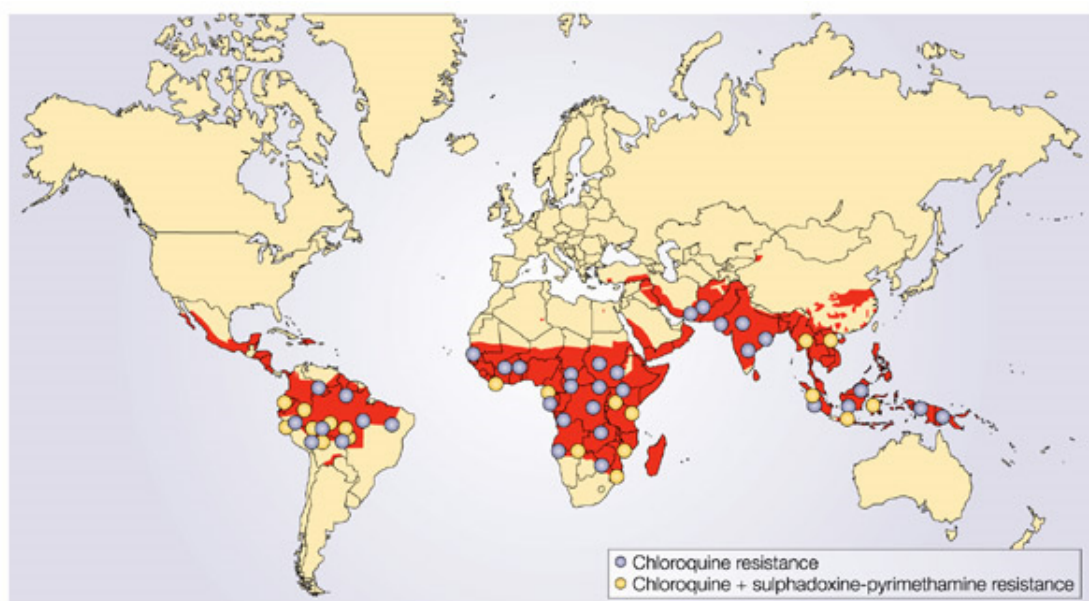


Figure 1.3. Resistance to chloroquine and chloroquine + sulphadoxine-pyrimethamine. Malaria-endemic regions are colored in red. Source: Fidock et al., 2004. Data are from the World Health Organization and are adapted from Ridley, 2002 © Macmillan Magazine Ltd (2002).

Atovaquone is also prone to resistance development, as monotherapies with the generally very potent substance rapidly led to elevated *in vitro* tolerance and to early observed recrudescence in clinical trials (Looareesuwan et al. 1996). To counter this weakness of atovaquone, the compound was developed in combination with proguanil (1.2), a compound with a different mode of action (Looareesuwan et al. 1996). The genetic basis of resistance to the drug seems to stem from point mutations in the cytochrome b complex of the parasite (Korsinczky et al. 2000; Peters et al. 2002).

Even for the current mainstay of antimalarial treatment, the artemisinins (reviewed by Fidock 2010), the first cases of reduced effectiveness were recently published (Dondorp

et al. 2009), questioned (Taylor et al. 2009) and confirmed for the Thai–Cambodia border (Dondorp et al. 2010; Enserink 2010). The mechanism behind these first signs of artemisinin resistance is a matter of intense investigation but remains obscure (White 2010; Ding et al. 2011). In order to protect artemisinin-based therapies, the WHO has launched an unprecedented action plan to try and stop possibly emerging resistance at an early stage (Burr 2011).

Table 1.1. provides an overview of currently used drugs and their status of resistance.

Table 1.1. Existing antimalarial drugs, their use and status of resistance.

Common name	Chemical class	Clinical use	Resistance
Artemisinins: Artemether, Artesunate, Dihydroartemisinin	Sesquiterpene lactone endoperoxide	In artemisinin-based combination therapies (ACTs)	Possibly emerging
Lumefantrine	Arylamino alcohol	Most common first-line antimalarial therapy in Africa, in combination with artemether	No evidence
Amodiaquine	Quinoline	In combination with artesunate in parts of Africa	Limited crossresistance with chloroquine
Piperaquine	Quinoline	In combination with dihydroartemisinin in parts of southeast Asia	Observed in China following single-drug therapy
Mefloquine	Quinoline	In combination with artesunate in parts of southeast Asia	Prevalent in southeast Asia
Quinine/quinidine	Quinoline	Mainly for treating severe malaria, often with antibiotics	Exists at a low level
Atovaquone	Naphthoquinone	In combination with proguanil for treatment or prevention	Has been observed clinically
Chloroquine	Quinoline	Former first-line treatment for uncomplicated malaria	Widespread
Pyrimethamine	Diaminopyrimidine	For intermittent preventive treatment, combined with sulphadoxine	Widespread

Adapted from Fidock 2010.

1.4 The need for novel antimalarial agents

In many temperate areas such as Western Europe or North America, malaria has been controlled or eliminated (reviewed by Tuteja 2007). In contrast, poor regions face two main problems fighting the disease: High-priced antimalarials (Laxminarayan et al. 2010) and the increasing drug resistance of the parasite (1.3). Therefore, the need for new and affordable drugs is urgent and indisputable.

In 2007, the Bill and Melinda Gates Foundation unveiled an agenda with the overall goal of the extinction of all *Plasmodium* species causing human malaria (Okie 2008). This goal is pursued in conjunction with several other institutes such as the Roll Back Malaria partnership of the WHO (www.rollbackmalaria.org) and one main nonprofit private public partnership Medicines for Malaria Venture (MMV, www.mmv.org). Such strong partnerships were a boost for antimalarial research leading to an encouraging MMV antimalarial portfolio (MMV 2011) which currently contains over 10 projects (preclinical to phase IV). Furthermore, a plenitude of chemical structures, potentially serving as starting points for new antimalarial lead substances, was recently disclosed after extensive compound screenings (Gamo et al. 2010; Guiguemde et al. 2010).

Nevertheless, since 1996, not a single new chemical class of antimalarials has been registered (Gamo et al. 2010) and the current global drug portfolio (MMV 2011) relies largely on novel combinations – not novel compounds, underscoring the urgent need for drugs with new modes of action.

1.5 Discovery of a novel antimalarial chemotype at Actelion Ltd.

In the quest for a novel antimalarial compound, researchers at Actelion Ltd initially confined their drug screening activities on food-vacuolar plasmepsins (PM) as drug targets. These efforts resulted in very potent plasmepsin inhibitors which showed only poor activity against *in vitro*-cultured *P. falciparum* parasites (Boss et al. 2003; Corminboeuf et al. 2006). Therefore, cell-based antimalarial screens were performed in order to find new lead structures independent of molecular targets. In a library with an assortment of aspartic protease inhibitors and compounds with undefined targets, novel piperazine-containing compounds were identified. These compounds were considerably more potent than the previously known PM inhibitors that served as positive controls for the screen. Medicinal chemistry efforts at Actelion led to improved potency of the piperazine-containing compounds with IC₅₀ values in the low nanomolar range. Herein, a lead compound, representative of this novel class of antimalarial agents will be further described: ACT-AM (for Actelion antimalarial).

1.6 Objectives

As described above, antimalarial drugs with new MOAs are urgently needed.

It was the main goal of this thesis to investigate the MOA of a novel antimalarial chemotype. To this end, six major groups of experiments were performed:

- 1) Pull-down assays using several chemical derivatives of the lead compound aimed at identifying possible interaction partners of the latter.
Potential targets were then tested for sensitivity to ACT-AM *in vitro*.
- 2) Microarray studies: *In vitro* gene expression of ACT-AM-treated vs. untreated *P. falciparum* parasites was compared to expression under treatment with 20 known antimalarial compounds.
Microarray results were confirmed with quantitative real-time PCR (qPCR).
- 3) Fluorescent imaging: To determine the intracellular localization of the site of action of the compound, fluorescent imaging experiments using derivatives of the new pharmacophore were conducted.
- 4) Hematin-interaction studies: To exclude the often cited MOA of certain quinolines (see above), the *in vitro* interaction of the compound with hematin was investigated.
- 5) *In vitro* pharmacodynamic experiments: Time-, stage-, and concentration-dependent effects of ACT-AM were assessed using synchronous cultures of the parasite.
- 6) In order to exclude cross-resistance, the *in vitro* activity of ACT-AM against a panel of resistant and sensitive *P. falciparum* strains was determined by means of [³H]-hypoxanthine incorporation assays.

2 Materials

2.1 Chemicals and proteins

Acetic acid 96%	Synopharm, Schweizerhalle, Basel, CH
Albumax	Gibco-BRL life tech. AG, Basel, CH
Artesunate	Guilin Pharma corporation, China
β -mercaptoethanol	Fluka, Buchs, CH
Bromophenolblue	Merck, Darmstadt, D
Bovine Serum Albumin (BSA)	Sigma, Buchs, CH
CAPS	Sigma, Buchs, CH
Chlorophorm	Sigma, Buchs, CH
Chloroquine	Sigma, Buchs, CH
DAPI	Sigma, Buchs, CH
d-Biotin	Sigma, Buchs, CH
DMSO	Sigma, Buchs, CH
DTT	Sigma, Buchs, CH
Ethanol	Merck, Darmstadt, D
Ethanolamine-HCL	Sigma, Buchs, CH
EDTA	Merck, Darmstadt, D
D-Fructose 1,6-bisphosphate	
Trisodium salt hydrate	Sigma, Buchs, CH
Gas mixture for parasite cultivation	Garbogaz, Basel, CH
Giemsa solution	Sigma, Buchs, CH
Glutaraldehyde	Sigma, Buchs, CH
Glycerol	Merk, Darmstadt, D
Glycine	Sigma, Buchs, CH
α -GDH/TPI	Sigma, Buchs, CH
Glycine	Merk, Darmstadt, D
HCl	Merk, Darmstadt, D

Materials

Hemin	Sigma, Buchs, CH
HEPES	Fluka, Buchs, CH
Hypoxanthine	Fluka, Buchs, CH
[8- ³ H]-hypoxanthine	ANAWA trading SA, CH
Isopropanol	Sigma, Buchs, CH
KH ₂ PO ₄	Merk, Darmstadt, D
KCl	Sigma, Buchs
KOH	Merk, Darmstadt, D
Methanol	Merk, Darmstadt, D
NaCl	Merk, Darmstadt, D
β-NADH, disodium salt hydrate	Sigma, Buchs, CH
NaHCO ₃	Merk, Darmstadt, D
Na ₂ HPO ₄	Merk, Darmstadt, D
NaOH	Merk, Darmstadt, D
Neomycin	Sigma, Buchs, CH
NP-40 (Nonidet P-40)	Fluka, Buchs, CH
Protease inhibitor cocktail tablet	Roche applied Science, CH
Pyrimethamine	Roche, Basel, CH
RPMI 1640	Gibcobl life tech. AG, Basel, CH
Saponin	Sigma, Buchs, CH
Scintillation fluid	Perkin Elmer, Schwerzenbach, CH
SDS	Sigma, Buchs, CH
d-Sorbitol	Fluka, Buchs, CH
Tris/Trizma-base	Sigma, Buchs, CH
Triton X-100	Sigma, Buchs, CH
Trizol (TRI Reagent)	Ambion, Rotkreuz, CH
Tween 20	Merk, Darmstadt, D
Vectashield mounting solution	Vector laboratories, USA

2.2 Chemical probes and antimalarials

Table 2.1 Chemical probes and reference antimalarials.

Compound	Description	Solvent
ACT-AM	novel antimalarial compound from Actelion	DMSO
ACT-AM-EN2	less active enantiomer of ACT-AM	DMSO
ACT-AM-UV	derivative of ACT-AM linked to UV-activatable capture group (forms nitrene upon activation) and to sorting group (biotin)	DMSO
ACT-AM-UV-Neg	less active derivative of ACT-AM-UV: same capture and sorting group, different (incomplete) parent scaffold	DMSO
ACT-AM-Biotin	derivative of ACT-AM linked to biotin	DMSO
ACT-AM-Fluo	derivative of ACT-AM linked to fluorescein	DMSO
ACT-Seph	precursor of ACT-AM conjugatable to sepharose beads	DMSO
Artesunate	R.A.	DMSO
Chloroquine	R.A.	ddH ₂ O
Pyrimethamine	R.A.	DMSO

Mainly used chemical probes from Actelion and reference antimalarials (R.A.). Compounds were dissolved in the indicated solvent.

2.3 Solutions, buffers and experimental devices

2.3.1 Frequently used stock solutions

10x PBS

137mM NaCl, 2.7mM KCl, 10mM Na₂HPO₄ and 2mM KH₂PO₄ in ddH₂O. The pH was adjusted to 7.4 with HCl and the solution autoclaved.

10x TBS

137mM NaCl, 2.7mM KCl, and 24.8mM Tris-base in ddH₂O. The pH was adjusted to 7.4 with HCl.

T-PBS

0.1% Tween 20 in PBS

10mM d-biotin

10mM d-biotin in DMSO.

2.3.2 Parasite cultivation and growth assays

Culture medium (CM)

10.44g RPMI 1640, 5.94g HEPES, 50mg hypoxanthine, 5.0g Albumax, 2.1g NaHCO₃, 10ml neomycin solution 10µg/l, filled up to 1l with ddH₂O. After 2h stirring, the medium was sterile-filtered through a 0.22µm filter into autoclaved bottles under sterile conditions. The medium was stored up to two weeks at 4°C.

Screening medium

10.44g RPMI 1640, 5.94g HEPES, 5.0g Albumax, 2.1g NaHCO₃, 10ml neomycin solution 10µg/l, filled up to 1l with ddH₂O. After 2h stirring, the medium was sterile-filtered through a 0.22µm filter into autoclaved bottles under sterile conditions. The medium was stored up to two weeks at 4°C.

Giemsa solution

Giemsa buffer contains 4.2g KH₂PO₄, 12.5g Na₂HPO₄ in 10l ddH₂O. 10ml of Giemsa stock solution was mixed with 100ml of Giemsa buffer.

[³H]-hypoxanthine working solution

Stock solution: [³H]-hypoxanthine was diluted 1:2 in 50% EtOH/ddH₂O, aliquoted (1ml) and stored at -20°C. The working solution was obtained by mixing 1ml stock solution with 49ml screening medium (resulting in 0.5mCi).

2.3.3 SDS-PAGE, (Far-) Western blotting and silver staining

5x SDS-PAGE sample buffer

500mM Tris pH6.8, 10% SDS, 25% Glycerol, 5% β-mercaptoethanol, 0.2% bromophenolblue

Polyacrylamide gels and protein size marker

4-12% Bis-Tris polyacrylamide pre-cast gels
SeeBlue Plus2 Standard (both Invitrogen)

SDS-PAGE and protein transfer

Gel running chambers, protein transfer devices, nitrocellulose membranes as well as all needed chemicals were from Invitrogen and used according to the manufacturer.

Coomassie staining

InstantBlue, Expedeon

Silver staining

SilverQuest Staining Kit, Invitrogen

2.3.4 Pull-down assays

Monomeric avidin beads

Pierce Monomeric Avidin Kit

Biotin Blocking and Elution buffer

2mM d-biotin/ PBS (Pierce Monomeric Avidin Kit)

Regeneration buffer

0.1M glycine, pH 2.8 (Pierce Monomeric Avidin Kit)

2.4 *Plasmodium falciparum* strains

Table 2.2. List of used *Plasmodium falciparum* strains.

Isolate	Origin	Provider	Resistance
NF54	Airport, Netherlands	SwissTPH (Roche Ltd, MRA-1000)	–
3D7	Airport, Netherlands	Cloned from NF54 by limiting dilution (MRA-102)	–
D6	Sierra Leone	D. Kyle (MRA-285)	–
K1	Thailand	SwissTPH (MRA-159)	CQ, PYR
W2	Indochina	SwissTPH (Roche, MRA-157)	CQ, PYR
7G8	Brazil	SwissTPH (MRA-152)	CQ, PYR
TM90C2A	Thailand	D. Kyle (MRA-202)	CQ, PYR
V1/S	Vietnam	L. Vivas (MRA-176)	CQ, PYR

Plasmodium falciparum strains, their origin, provider and sensitivity / resistance to chloroquine and pyrimethamine are indicated. MR4 numbers according to mr4.org.

3 Methods

3.1 Parasite cultivation

All used *P. falciparum* strains were cultivated by standard methods (Trager & Jensen 1976). Parasites were kept in culture medium containing AB type RBCs (hematocrit 5%). Cultures were incubated at 37°C in an atmospheric chamber (standard conditions: 3% O₂, 4% CO₂ and 93% N₂). The culture medium was changed daily if parasitemia exceeded 2%.

3.1.1 Giemsa slide preparation

To determine parasitemia and life cycle stages of parasite cultures, a sample of 200µl was pelleted and 10µl of the pellet was smeared on glass slides. After fixation for > 10sec in 100% MeOH, staining was performed by incubation in Giemsa solution for > 15min.

3.1.2 Culture synchronization

Cultures were synchronized as described previously (Lambros & Vanderberg 1979):

All solutions were pre-warmed to 37°C. RBCs were pelleted by centrifugation at 1500rpm for 5min. After removal of the supernatant, the pellet was resuspended in 5% d-sorbitol/ddH₂O solution (five pellet volumes) and incubated for 5min at 37°C. The culture was then centrifuged a second time at 1500rpm for 5min followed by removal of the supernatant. The pellet was resuspended in culture medium and the hematocrit adjusted to 5% with fresh RBCs. Synchronized cultures were then either washed twice with 10ml culture medium if immediately used for experiments or washed once and transferred to new dishes for further cultivation.

3.1.3 Saponin lysis

Cultures were pelleted at 1500rpm for 5min. The supernatant was removed and pellets were resuspended in 0.15% Saponin/PBS solution (4°C, four pellet volumes). The suspension was incubated for 10min on ice. Lysed RBCs were removed by centrifugation for 10min at 4000rpm (4°C). Parasites were washed 3x in 1x PBS (> 10 pellet volumes) until supernatant became clear.

3.2 [³H]hypoxanthine incorporation assays

3.2.1 *In vitro* growth assay

In vitro growth assays were performed as described previously (Desjardins et al. 1979): *P. falciparum* growth was determined by measuring incorporation of the nucleic acid precursor [³H]hypoxanthine. Test compounds were diluted in screening medium and titrated over a 64-fold range in 96-well plates (Figure 3.1):

After adding 100µl screening medium to each well, 100µl of dissolved compounds, containing 4x the highest test concentration, were added to wells of row B in duplicates.

2x serial drug dilutions were prepared using a multichannel pipette: 100µl were taken from wells of row B and transferred, after mixing, to wells of row C and so forth down to row H. The 100µl removed from wells of row H were discarded. Infected erythrocytes (2.5% hematocrit and 0.3% parasitemia) were then added to each well except for A9-A12, to which 100µl uninfected RBCs (diluted in screening medium to 2.5% hematocrit) were added as a negative control. The final culture parameters of the assay were thus 1.25% hematocrit and 0.3% parasitemia. Wells A1-A8 served as positive controls. After a 48h incubation period (parasite cultivation, 3.1), 50µl of [³H]hypoxanthine working solution was added to each well (0.5µCi per well). Plates were incubated for an additional 24h period then frozen at -20°C. After thawing, the content of the plates was harvested onto glass-fiber filters using a Betaplate cell harvester (1295-004 Betaplate; Wallac Perkin Elmer). The micro wave-dried filters were drenched in 10ml of scintillation fluid in a plastic foil and the [³H]hypoxanthine incorporation was measured using a Betaplate liquid scintillation counter (1205 Betaplate; Wallac Perkin Elmer). The result of each

well was recorded as counts/min and expressed as percentage of the untreated (positive) control. The negative control was used for background subtraction. Fifty percent inhibitory concentrations (IC₅₀s) were estimated by linear interpolation (Huber & Koella 1993).

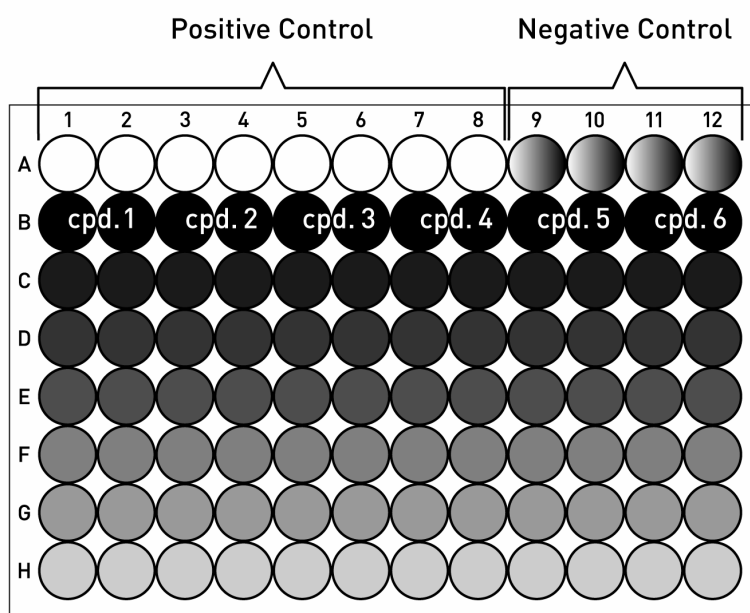


Figure 3.1. Schematic plate layout of the [³H]hypoxanthine incorporation assay. Test compounds were added in duplicate to 96-well plates (row B). Compounds were then titrated (6 times a 2-fold dilution). The positive control contained infected RBCs in absence of antimalarial compounds, whereas the negative control consisted of uninfected RBCs.

3.2.2 *In vitro* activities of test compounds against a panel of resistant *Plasmodium falciparum* strains

IC₅₀s of test compounds against resistant *P. falciparum* strains were determined as described in the above paragraph (3.2.1).

3.2.3 *In vitro* pharmacodynamics

Stage specificity and onset of action of test compounds were assessed as described previously (Maerki et al. 2006; Hofer et al. 2008): Synchronized cultures (two synchronization steps, 7h apart) of young 3D7 trophozoites (approx. 20h p.i.) with parasite counts of 0.15% and a hematocrit of 5% were divided into three 10ml petri dishes. Two dishes were further incubated for 16h and 32h (cultivation of parasites, 3.1) for maturation into early schizonts (approx. 36h p.i.) and early ring stages (approx 4h p.i.), respectively. Parasite stages were monitored using Giemsa stained cells. Early trophozoites were directly exposed to test compounds for a 1, 6, 12 or 24h period. Compounds were diluted in screening medium to a final starting concentration of approx. 100x the respective IC₅₀s and titrated over a 64-fold concentration range. The subsequent *in vitro* growth assay was performed as described above (3.2.1) with the following modifications:

The final assay parasitemia and hematocrit were adjusted to 0.15% and 2.5%, respectively. After incubation in presence of compounds, the plates were washed four times with 150µl screening medium (centrifugation steps: 2000rpm, 3min) and in a final step, 150µl screening medium and 50µl [³H]hypoxanthine working solution were added resulting in a 1280-fold dilution of free compound. After another incubation period of 24h, the plates were frozen at -20°C. For the IC₅₀ determination, plates were thawed and harvested as described above (3.2.1).

3.3 Methods based on UV-activatable compounds

UV-activatable compounds (see materials section) were used for several biochemical methods and are trifunctional probes consisting of

1. A selectivity function (the compound of interest)
2. A reactivity function forming a nitrene upon UV-activation, which enables the compound to irreversibly form covalent bonds with nearby molecular structures
3. A sorting function (biotin)

3.4 Fluorescent imaging

All used parasites were of the *P. falciparum* 3D7 strain. Incubation steps with living parasites were always carried out under standard incubation conditions (3.1). A Leica DM5000B fluorescence microscope and a Leica DC200 camera were used.

3.4.1 Fluorescent imaging using acetone/MeOH fixed cells

1ml iRBCs (5% hematocrit, 2-5% parasitemia) were incubated with 500nM ACT-AM-UV or with ACT-AM-UV-Neg (negative control) in a 24-well plate for 2h. Cultures were transferred to 1.5ml Eppendorf tubes and washed 3x with 1ml culture medium (centrifugation steps: 1500rpm for 0.5min). Cultures were resuspended in 1ml ice cold PBS and UV-irradiated at 4°C for 3x 3min on the cover of a 6-well plate using a Caprotec UV device. The suspension was mixed after every 3min irradiation period. As a second negative control, iRBCs incubated with ACT-AM-UV were stored at 4°C while the respective samples were UV-irradiated. The pelleted iRBCs were smeared on glass slides, air dried and fixed in pre-cooled (-20°C) acetone/MeOH solution (40:60 v/v) for 2min. Fixed slides were air dried. After blocking for 1h in blocking solution (1% BSA/PBS), Alexa488-streptavidin, 2mg/ml (Invitrogen) diluted 1/200 in blocking solution was added and the slides were incubated in the dark for 1h at room temperature. Samples were washed 3x with 1ml 0.05% Tween20/TBS before mounting with Vectashield (Vector laboratories) containing 1.5µg/ml DAPI.

3.4.2 Fluorescent imaging using living cells

To assess the fluorescence pattern of ACT-AM in living cells, a derivative of the compound covalently linked to fluorescein was used (ACT-AM-Fluo).

1ml iRBCs (2.5% hematocrit, 2-5% parasitemia) were incubated in presence of 20µM (ACT-AM-Fluo) or 40µM fluorescein (negative control) in screening medium in a 24-well plate for 4h. Cultures were transferred to 1.5ml Eppendorf tubes and washed 4x with 1ml TBS (centrifugation steps: 1500rpm for 0.5min). Pellets were resuspended in 500µl TBS containing DAPI (1µg/ml) and incubated for 30min in the dark.

Cells were washed with 1ml TBS and 3 μ l of pelleted cells were mixed with 10 μ l Vectashield mounting medium (Vector laboratories) and directly mounted on glass slides.

3.5 SDS-PAGE

Samples for SDS-PAGE were resuspended in 5x SDS-PAGE sample buffer (e.g. 20 μ l sample + 5 μ l of 5x SDS-PAGE sample buffer) and incubated for 4min at 95°C. 18 μ l of denaturated samples were separated on a 4-12% Bis-Tris polyacrylamide pre-cast gel (Invitrogen) for 75min (30mA, 150V) using 1x MOPS as a running buffer.

3.6 Far Western blotting

3.6.1 Lysate Preparation

Lysates were prepared as described below (3.7 pull-downs, i) with the following exceptions:

1. One sample consisted of 30ml 3D7 culture (5% hematocrit, approx. 5% parasitemia)
2. Four different samples were used:
 - A) sample treated with ACT-AM-UV, irradiated with UV light
 - B) same as A) without UV-irradiation
 - C) sample treated with ACT-AM-UV-Neg, irradiated with UV light
 - D) sample treated with DMSO, irradiated with UV light
3. Samples were lysed in 150 μ l of 1% SDS lysis buffer (3.7.i)

3.6.2 Blotting procedure

After gel electrophoresis (3.5.), samples were transferred to a nitrocellulose membrane using an iBlot device (Invitrogen) according to the protocol of the manufacturer.

The membrane was blocked in 10ml of blocking solution (2% membrane blocking agent, GE in T-PBS) for 1h at room temperature. After removal of the solution, the membrane was incubated with HRP-labeled streptavidin (Pierce, 1mg/ml, diluted 1:2000 in 10ml blocking solution) for 45min at RT. The membrane was washed 5x (2x for 10sec with 30ml, 3x for 5min with 50ml T-PBS).

10ml of blotting substrate (Western Lightning, Perkin Elmer) was pipetted directly on the membrane. After incubation for 1min, films (Amersham Hyperfilm ECL, 18 × 24 cm, GE Healthcare) were exposed to the membrane in a dark room and developed after 1 to 60min exposure.

3.7 Pull-down experiments based on UV-activatable compounds

3.7.1 UV-activation of compounds in parasites after saponin lysis

i) Protocol used for whole gel analysis

Lysate preparation

One sample consisted of 60ml 3D7 culture (5% hematocrit, 5-10% parasitemia).

Samples were treated with 100nM (approx. 2x IC₉₀) of ACT-AM-UV and incubated under normal culture conditions for 2h at 37°C.

Two pairs (sample and respective negative control) were used:

Negative control A: Competition: Cultures were incubated for 15min with 10μM of ACT-AM prior to the addition of ACT-AM-UV.

Sample A: Cultures were treated with the respective amount of DMSO for 15min prior to the addition of ACT-AM-UV.

Negative control B: Cultures were incubated with 100nM of ACT-AM-UV-Neg instead of ACT-AM-UV.

Sample B: Cultures were directly incubated with ACT-AM-UV.

After incubation, samples were centrifuged at 2000rpm for 5min. Pelleted cells were resuspended in 4 pellet volumes of a 0.15% Saponin/PBS solution and incubated for 8min on ice. Lysed RBCs were separated from parasites by centrifugation (4000rpm, 8min, 4°C). Pelleted parasites were washed 3x with 10ml PBS, (4000rpm, 5min, 4°C). Pellets were resuspended in 1ml of ice cold PBS and transferred to a cover of a petri dish (6cm in diameter) which was placed in the cover of a 96-well plate filled with ddH₂O (for efficient cooling). Parasites were UV-irradiated (UV device of Caprotec) at 4°C for 3x 3min, the suspension was mixed after every 3min irradiation period.

Irradiated samples were transferred to 1.5ml Eppendorf tubes and centrifuged (5000rpm, 5min, 4°C). Pellets were resuspended in 50µl PBS by vortexing and lysed in 1ml SDS lysis buffer for 10min at room temperature. Lysates were stored at -80°C.

1% SDS lysis buffer consisted of 1% SDS, 1x protease inhibitors, 1mM DTT in PBS.

Pull-down procedure

For 1 sample:

After thawing, lysates were passed 5x through a needle (0.6mm in diameter) and centrifuged for 5min at 13000rpm. 900µl of supernatant was transferred to 200µl resuspended beads (magnetic Dynabeads MyOne Streptavidin C1, Invitrogen) which were washed twice with 1ml PBS before usage. The suspension was incubated for 1h at room temperature on a rotating wheel. Beads were washed with 1ml of 1) 1% SDS in PBS, 2) 1x wash buffer of Caprotec, 3) see 2), 4) 1% SDS in PBS, 5) ddH₂O.

Beads were then incubated in 25µl of 1.5x SDS loading buffer for 10min at 94°C. The supernatant was centrifuged for 5min at 13000rpm to remove all remaining beads. 18µl of the upper fraction of the supernatant was loaded on a polyacrylamide gel which was run as described above (3.5) and stained for 2h with 50ml of InstantBlue Coomassie stain.

The gel was washed 3x in 50ml ddH₂O and every lane was cut into 10 bands which were used for mass spectrometry; the samples and their respective negative controls were cut in parallel.

ii) Protocol used for partial gel analysis

As described above under i) with the following modifications:

Lysate preparation

1. One sample consisted of 120ml 3D7 culture (5% hematocrit, 5-10% parasitemia).
2. Parasites treated with ACT-AM-UV-Neg instead of ACT-AM-UV were used as a negative control.
3. SDS lysis buffer consisted of 2% SDS and 1mM DTT in PBS.

Pull-down procedure

1. 300µl of resuspended beads were used.
2. The gel was silver stained, washed 3x in 50ml ddH₂O and areas which differed in the amount of protein (sample vs. control) were cut out for mass spectrometry.

3.7.2 UV-activation of compounds in living cells before saponin lysis

As described above under i) with the following modifications:

Lysate preparation

1. One sample consisted of 60ml 3D7 culture (5% hematocrit, 5-10% parasitemia).
2. Negative control A: Competition: Cultures were incubated for 30min with 1µM of ACT-AM prior to the addition of ACT-AM-UV.
3. Before UV-irradiation, parasites were washed 2x with 12ml culture medium and resuspended in 15ml PBS.

4. Parasites in PBS were transferred to the cover of a 96-well plate and UV-irradiated before saponin lysis.
5. SDS lysis buffer consisted of 2% SDS and 1mM DTT in PBS

Pull-down procedure

1. Lysates were not passed through a needle.
2. The gel was silver stained, washed 3x in 50ml ddH₂O and bands which differed in the amount of protein (sample vs. control) were cut out for mass spectrometry.

3.8 Pull-down experiments using monomeric avidin systems

3.8.1 Triton lysates

Pellets of six 30ml dishes of a mixed 3D7 culture and of six 30ml dishes of a once synchronized 3D7 culture (parasitemia > 8%, hematocrit 5%) were pooled. After Saponin lysis and 3x 10ml PBS washes (3.1.3), parasites were resuspended in 6.5ml Triton lysis buffer and incubated for 30min on ice. The solution was centrifuged for 5min at 4000rpm. The supernatant was aliquoted in 1.5ml Eppendorf tubes (6x 1ml) and stored at -80°C.

After thawing, lysates were centrifuged for 5min at 13000rpm. The clear supernatant was used for pull-down assays.

The Triton lysis buffer consisted of 20mM Hepes pH7.9, 150mM NaCl, 10% glycerol, 1x protease inhibitors, 1% Triton X-100, 1mM EDTA, 1mM DTT.

3.8.2 Pull-down procedure

100µl of settled beads (monomeric avidin beads, Pierce) were used per sample. 200µl of settled beads were washed with 2x 1ml PBS and non-reversible biotin binding sites were blocked with 3x 250µl of Biotin Blocking and Elution buffer. Biotin was removed from the reversible binding sites by washing the beads with Regeneration Buffer (0.5 / 1.0 / 0.5ml), followed by 3 washes with 1ml PBS. Beads were divided into two 1.5ml

Eppendorf tubes (sample and negative control). The biotinylated compounds (ACT-AM-Biotin) and the negative control (less active derivative of ACT-AM-Biotin: same biotin group, different i.e. incomplete parent scaffold) were coupled to the reversible binding sites: Suspensions of beads and biotinylated compounds (approx. 15 μ M in 900 μ l PBS) were incubated for 1h at room temperature on a rotating wheel. Coupled beads were washed with 2x 900 μ l PBS before incubation with 900 μ l of lysate for 1h at room temperature on a rotating wheel. Beads were then washed 6x with 1ml PBS and elution was performed 4x for 2min with 150 μ l of Biotin Blocking and Elution buffer. Pooled elutions were concentrated/dried using a Vacufuge (Eppendorf).

3.9 Pull-down experiments using streptavidin systems

3.9.1 Triton lysates

Triton lysates were prepared as described above (3.8.1).

3.9.2 Pull-down procedure

50 μ l of settled beads (streptavidin beads, GE) were used per sample. 100 μ l of settled beads were washed with 3x 0.5ml PBS and coupled to ACT-AM-Biotin (30 μ M in 900 μ l PBS) for 1h at room temperature on a rotating wheel. After 3 washes with 0.8ml PBS, beads were divided into two 0.5ml Eppendorf tubes (sample and negative control). For the negative control, 450 μ l of lysate was blocked with a more active non-biotinylated precursor of ACT-AM-Biotin (approx. 10 μ M) whereas the lysate for the sample was treated with the corresponding amount of DMSO. Lysates were added to beads and incubated for 1h at room temperature on a rotating wheel. After incubation, beads were washed 6x with 800 μ l PBS in mini columns (1ml, Pierce). In order to break the biotin:streptavidin bond, 35 μ l of drained beads were incubated with 25 μ l of 1.5x SDS sample buffer for 4min at 95 $^{\circ}$ C. The supernatant was used for gel electrophoresis.

3.10 Pull-down experiments using compounds directly linked to beads

3.10.1 Covalent coupling of compounds to Sepharose beads

600µl of settled beads (activated Sepharose 4 Fast Flow, GE) were washed with 13ml of ice cold ddH₂O and activated with 10ml of an ice cold 1mM HCl solution.

Activated beads were coupled to ACT-Seph (12µmoles in 600µl DMSO, negative control: 600µl DMSO only) for 3h at room temperature on a rotating wheel. Beads were washed with 2x 10ml ddH₂O and blocked with 10ml of blocking solution (0.5M ethanolamine-HCL, 0.5 M NaCl, pH8.3) overnight at 4°C. Beads were washed with 5ml of a 0.1M Tris-HCl buffer, pH8 followed by 5ml of a 0.1M acetate buffer, 0.5M NaCl, pH4. The washing procedure was repeated 4 times. Before storage in 20% ethanol, beads were washed with 10ml ddH₂O.

3.10.2 Lysate preparation

Lysates were prepared as described above (3.8.1) but parasites were lysed for 5min only and the lysis buffer consisted of 20mM Hepes pH7.9, 10mM KCl, 1mM EDTA, 1mM DTT, 1 X protease inhibitors and 0.65% NP-40.

3.10.3 Pull-down procedure

50µl of settled beads per sample were washed 2x with 450µl ddH₂O and equilibrated 3x with 450µl equilibration buffer. 450µl of lysate was added to the beads and incubated for 2h at room temperature on a rotating wheel. Beads were washed 8x with equilibration buffer, 2x with 1M KCl buffer, 2x with 2M KCl buffer and equilibrated 5x with equilibration buffer (always 450µl per step). Competition with a relatively soluble precursor of ACT-AM was performed using 2x 2nM and 2x 50µM solutions in 100µl equilibration buffer. Beads were again equilibrated with 3x 100µl equilibration buffer. Beads were washed 3x with low pH buffer, pH3.0, 2x with equilibration buffer, pH7.9

and 3x with high pH buffer, pH10.0 (always 100µl per wash). 10µl of drained beads were incubated with 25µl of 1x SDS sample buffer for 4min at 95°C. The supernatant was used for gel electrophoresis.

Buffers

Equilibration buffer:

20mM Hepes, 10mM KCl, 1mM EDTA, 1mM DTT, 0.1% NP-40, pH7.9

KCl buffer:

20mM Hepes, 1 and 2M KCl, 0.1% NP-40, pH7.9

Low pH buffer:

20mM Glycine, 10mM KCL, 0.1% NP-40, pH3.0

High pH buffer:

20mM CAPS, 10mM KCL, 0.1% NP-40, pH10.0

3.11 Mass spectrometry

Mass spectrometry was carried out by Suzette Moes in the laboratory of Paul Jenö at the Biocenter in Basel.

3.11.1 Protein digestion

Solutions:

Trypsin solution: Sequencing grade (Promega), 12.5ng/µl in 50mM NH₄HCO₃

10mM DTT in 100mM Tris-HCl, pH8.0

50mM iodoacetamide in 100mM Tris-HCl, pH8.0

Gel slices were cut into small cubes and washed once with 50µl of 40% n-propanol and five times with 50µl of 50% acetonitrile/0.1M NH₄HCO₃. Gel pieces were then completely immersed in 50% acetonitrile/0.1M NH₄HCO₃ and incubated for 2h at room temperature. Residual liquid was left to evaporate at room temperature. Proteins were reduced with 50µl of 10mM DTT for 2h at 37°C and alkylated with 50µl of 50mM iodoacetamide for 15min at room temperature in the dark. Gel pieces were washed five times with 50µl of 50% acetonitrile/0.1M NH₄HCO₃ and air dried at room temperature. For digestion, gel pieces were soaked in 10µl trypsin solution, completely covered with additional 50mM NH₄HCO₃ solution and incubated overnight at 37°C. Peptides of the supernatant were collected and gel pieces were extracted with 50µl of 0.1% acetic acid/50% acetonitrile. The extract was pooled with the tryptic peptides, the pooled digest was dried in a speed vac and redissolved in 50µl of 0.1% trifluoroacetic acid.

3.11.2 LC-MS/MS Analysis

LC-MS/MS (Liquid Chromatography Tandem Mass Spectrometry) analysis was performed as previously described (Soulard et al. 2010).

3.11.3 Protein identification, databank searching

LC-MS/MS data were searched using the SEQUEST search engine, version 3.3 (Eng et al. 1994) against the *P. falciparum* databank (PlasmoDB version 5.5, July 2008) and the NCBI human databank (version June 2010). The precursor ion and fragment ion mass tolerances were set to 10ppm (parts per million) and 0.6Da, respectively. Two missed cleavages were allowed.

3.12 Validation of target candidates

3.12.1 Multidrug resistance protein

In vitro interactions of ACT-AM with the multidrug resistance protein (MDR or MDR1, gene ID: PFE1150w) were studied by Corinna Mattheis in the laboratory of David Fidock in New York.

IC₅₀ values of ACT-AM against *P. falciparum* strains exhibiting either one or two gene copies of *mdr* were determined as described previously (Sidhu et al. 2006) and essentially as above (3.2). Mefloquine was used as a positive control. Statistical analysis of the results was performed by Christian Schindler in the following way:

Data were log-transformed for analysis. 95%-confidence intervals for the means of the log-transformed data were determined by using appropriate quantiles (0.975) of the t-distribution. Data were then backtransformed to provide 95%-confidence intervals for the geometric mean of the untransformed data which coincides with the median for variables with a log-symmetric distribution.

3.12.2 Equilibrative Nucleoside Transporter 4

Interactions of the Equilibrative Nucleoside Transporter 4 (ENT4 gene ID: PFA0160c: nucleoside transporter, putative) with ACT-AM were investigated *in vitro* by I. J. Frame in the laboratory of Myles Akabas in New York.

Transport studies were conducted using *Xenopus laevis* oocyte expression systems (Downie et al. 2006). Oocytes were injected with mRNA for PfENT4, PvENT4 (*Plasmodium vivax*), PfENT1, or with diethylpyrocarbonate-treated ddH₂O and were incubated for expression at 16°C for 72h. mRNA for PfENT4 was expressed using a synthetic gene that has been optimized for expression in *Xenopus laevis*. The sequence of the synthetic gene is not yet published. Before exposure to radiolabeled adenine, oocytes were preincubated for 15min in transport buffer in presence of 1μM and 10μM ACT-AM / ACT-AM-EN2 or solvent control. Oocytes were then transferred to transport buffer containing 150nM [³H]adenine with either compounds or solvent control. After

incubation for 60min, oocytes were washed 5x with ice-cold transport buffer and solubilized individually in 5%-SDS. Uptake of [³H]adenine was measured using liquid scintillation spectrometry. Background levels of [³H]adenine accumulation from ddH₂O-injected oocytes were subtracted from uptake values obtained from oocytes injected with mRNA. Baseline-subtracted uptake values were then normalized to % of solvent controls.

Transport buffer composition:

96mM NaCl, 1mM MgCl₂, 2mM KCl, 1.8mM CaCl₂, 10mM HEPES, 10mM MES pH 7.4.

3.12.3 Chloroquine Resistance Transporter

Chloroquine Resistance Transporter (CRT, gene ID: MAL7P1.27) was tested for *in vitro* activity under treatment with ACT-AM by Sebastiano Bellanca in the laboratory of Michael Lanzer in Heidelberg.

Transport studies using *Xenopus* oocytes were essentially performed as described in the above paragraph, with the following modifications:

1. The CRT of the chloroquine-resistant *P. falciparum* strain Dd2 (Wellems et al. 1990) was expressed at 18°C.
2. Oocytes were simultaneously exposed to the substrate (50nM of [³H]CQ) and to ACT-AM / ACT-AM-EN2.
3. Transport buffer composition:
96mM NaCl, 1mM MgCl₂, 2mM KCl, 1.8mM CaCl₂, 10mM TRIS, 10mM MES pH 6.0.

3.12.4 Aldolase

Fructose-bisphosphate aldolase (ID: PF14_0425) was kindly provided by J. Bosch: wt aldolase (Bosch et al. 2007) and by H. Doebeli: mt aldolase: K365 to N (Döbeli et al. 1990). Both enzymes were tested; the protocols and results were similar and are shown for wt aldolase.

In vitro assay

The *in vitro* assay was performed according to the manufacturer (Sigma):

The biochemical principle of this method is:

Aldolase: fructose 1,6-diphosphate + H₂O → G3-P + DHAP

TPI: G3-P → DHAP

α-GDH: 2 DHAP + 2 β-NADH → 2 α-glycerophosphate + 2 β-NAD

The decrease in A_{340nm} (of β-NADH) / t is proportional to the activity of aldolase and was monitored in Fisherbrand cuvettes (336-850nm) using a UV-visible spectrophotometer (Cary50, Varian).

Abbreviations:

Aldolase: fructose-bisphosphate aldolase

G3-P: glyceraldehyde 3-phosphate

DHAP: dihydroxyacetone phosphate

TPI: triosephosphate isomerase

α-GDH: glycerophosphate dehydrogenase

β-NADH: nicotinamide adenine dinucleotide, reduced form

β-NAD: nicotinamide adenine dinucleotide, oxidized form

Kinetics and Michaelis Constant (K_M)

One reaction, final concentration in 725 μ l:

86mM Tris pH7.4

140 μ M β -NADH

1.25 units of α -GDH/ TPI (based on α -GDH units)

0.5 μ g aldolase

Increasing substrate (fructose 1,6-diphosphate) concentrations were used.

Before adding aldolase, the solution was mixed and the $A_{340\text{nm}}$ was monitored until constant. After adding aldolase, the solution was mixed again and the decrease in $A_{340\text{nm}}$ was recorded for 4min. The activity ($\Delta A_{340\text{nm}}/t$) was expressed as (μ M NADH/min*mg) Curve fitting and K_M determination was performed using Prism software.

Validation of enzyme activity

One reaction, final concentration in 725 μ l, as described in the above paragraph with the following modifications:

1. Fructose 1,6-diphosphate concentration: 2x K_M (42 μ M)
2. Variable aldolase concentrations were used
3. Enzyme activity was plotted against enzyme concentration

Inhibition assay

One reaction, final concentrations in 725 μ l, as described in the above paragraph with the following modifications:

1. Fructose 1,6-diphosphate concentration: K_M (21 μ M)
2. Enzyme activity was measured in presence and absence (DMSO) of ACT-AM

3.12.5 M17 leucyl aminopeptidase

M17 leucyl aminopeptidase (PF14_0439) was tested for *in vitro* activity under treatment with ACT-AM in the laboratory of Colin Stack in Sydney. The assay was performed as previously described (Stack et al. 2007) measuring the release of the fluorogenic leaving group, NHMec (aminomethyl coumarylamide), from several fluorogenic peptide substrates.

3.12.6 Spermidine synthase, S-adenosylmethionine synthetase, and secreted acid phosphatase

In vitro activities of spermidine synthase (PF11_0301), S-adenosylmethionine synthetase (PF11090w), and secreted acid phosphatase (PFI0880c) under treatment with ACT-AM were tested according to (Haider et al. 2005; Dufe et al. 2007), (Das Gupta 2005), (Müller et al. 2010), respectively. All tests were performed by Ingrid Müller in the laboratory of Rolf Walter in Hamburg.

3.13 Hematin interaction studies

3.13.1 Inhibition of beta-hematin formation

The following assay was carried out with Sandra Vargas who had adapted the method from (Ncokazi & Egan 2005) in the laboratory of Karine Ndjoko in Geneva.

10µl of test compound stock solutions, 100µl of a hematin solution and 10µl of a 1M HCl solution were added in triplicate to 96-well plates (2ml-wells) and mixed at 900rpm for 10min. 10µl of a chloroquine stock solution / 10µl solvent were used as a positive / negative control. 60µl of saturated acetate solution (60°C) was added and the mixture was stirred for 1min. After incubation at 60°C for 90min, 750µl of pyridine solution was added. The mixture was incubated for 10min at 900rpm and allowed to settle during

15min at room temperature. Formation of a red complex indicated inhibition of beta-hematin formation whereas solutions without inhibition remained colorless.

Solutions especially used for the above assay:

- Stock solutions of compounds (50mM) were prepared in HCl (Merck), 0.1M / MeOH (Chromanorm) / DMSO (Acros Organics): (5/3/2).
- Hematin solution (1.68mM): 6.8mg of bovine hemin (Sigma) adjusted to 10ml with 0.1M NaOH (Merck)
- Saturated acetate solution, pH5.0: 18g of sodium acetate (Fluka), 24ml of glacial acetic acid (Acros Organics) and 10ml ddH₂O
- 15% pyridine (Acros Organics) in 20mM Hepes (Fluka)

3.13.2 Spectrophotometric measurement of hematin interactions

Interaction of hematin with test compounds was studied as described previously (Egan & Ncokazi 2004).

Hematin solutions were prepared as 2 μ M hematin in 40% aqueous DMSO (v/v) containing 0.02M Hepes buffer, pH7.4.

Solutions of test compounds were prepared in 80% aqueous DMSO (v/v) containing 0.02M Hepes buffer, pH7.4. The background absorbance of the test compounds was subtracted (obtained from blank titrations performed in the absence of hematin). The measuring procedure was:

1. Baseline: solvent: 40% aqueous DMSO (v/v) containing 0.02M Hepes buffer, pH7.4
2. Baseline: compounds at test concentrations (0, 2, 4, 8, 16 μ M) in solvent (1)
3. Spectrophotometric measurement of hematin solutions in presence of 0, 2, 4, 8 or 16 μ M of test compounds

The absorbance of the test solutions was monitored from 300 to 500nm in Eppendorf cuvettes (UVette, 220-1600nm) using a UV-visible spectrophotometer (Cary50, Varian).

3.14 Microarray

3.14.1 Experimental conditions for microarray

1. 3D7 parasites were tightly synchronized as described above (3.1.3). The time window (oldest - youngest parasites) was 6h.
2. The experiment was initiated at $t_0 = 32\text{h p.i.}$
3. Samples were treated with an IC_{90} (13nM) of ACT-AM and control samples with the respective amount of DMSO for 1h, 2h, 4h, 6h and 8h.
4. One sample consisted of a 50ml culture (in flasks), 5.0% hematocrit and 2.0% parasitemia.

3.14.2 IC_{90} determination under microarray conditions

Feasibility-study of IC_{90} determination experiment under microarray conditions

In order to test whether IC_{50} determination was possible under microarray conditions, $\text{IC}_{90/50}$ tests of ACT-AM were performed as described above (3.2) with the following exceptions:

1. Synchronization, t_0 , hematocrit and parasitemia as described under 3.14.1.
2. After 16h of compound exposure, 150 μl of screening medium was replaced to prevent starvation of the parasites as their number was higher than the one used in regular IC_{50} experiments.

IC_{90} determination experiment under microarray conditions

The actual IC_{90} determination experiment was performed as described in the above paragraph. To ensure that the conditions were comparable to the situation described under 3.14.1, the following changes were applied:

1. All volumes were scaled-up 10-fold.
2. 6-well plates were used instead of 96-well plates.
3. For harvesting, 250 μl of each well were transferred to the corresponding wells of 96-well plates.

3.14.3 Sample preparation for microarray and RNA extraction

For every timepoint, treated and untreated samples (described under 3.14.1) were processed as follows:

After centrifugation (2000rpm, 5min, 4°C), pelleted cells were resuspended in 10ml of a 0.15% Saponin/PBS solution and incubated for 10min on ice. Lysed RBCs were separated from parasites by centrifugation (4000rpm, 10min, 4°C). Pelleted parasites were immediately lysed in 6ml Trizol (TRI Reagent) and incubated for 5min at room temperature. 500µl of lysate was separated for later qPCR validation and samples were stored at -80°C.

For RNA extraction, samples were thawed and 1.1ml of chlorophorm was added. Samples were shaken vigorously for 1min and left at room temperature for 5min. After centrifugation (4000rpm, 30min, 4°C), 2ml of the upper aqueous phase was transferred to 1.6ml isopropanol for RNA precipitation. After moderate vortexing for 10sec and incubation for 5min at room temperature, the RNA samples were stored at -80°C.

3.14.4 Reference RNA extraction for microarray

11x 30ml of synchronized cultures (time window: 10h, ca 5% parasitemia, 5% hematocrit) together spanning the whole life cycle of asexual parasite blood stages were processed as described under 3.14.3 for RNA extraction.

3.14.5 Microarray analysis

Microarray hybridization, analysis and comparison of transcriptional profiles (ACT-AM vs. 20 different antimalarial compounds) were performed by Zbyinek Bozdech and Enghow Lim in Singapore.

Hybridization and genome-wide gene expression profiling was carried out using long oligonucleotides representing all 5.363 *P. falciparum* genes as previously described (Hu et al. 2007). The microarray results were compared to those obtained for 20 previously assessed antimalarial compounds by means of functional enrichment and hierarchical clustering analysis (Hu et al. 2010).

For the in-house analysis of microarray data and the generation of array heatmaps, genes were clustered by average linkage clustering using Gene Cluster 3.0 (Eisen et al. 1998). The similarity score of two joined elements was calculated by uncentered Pearson correlation. Heatmaps were generated using Java Treeview (Saldanha 2004).

3.15 qPCR

3.15.1 Total RNA isolation

Total RNA for qPCR was isolated according to the protocol of the manufacturer (Qiagen, RNeasy):

250µl Trizol lysate of microarray samples (corresponding to approx. 0.2×10^8 parasites) were incubated for 5min at 37°C. After adding 50µl chloroform, the solution was shaken vigorously for 1min and centrifuged at 13000rpm for 10min.

100µl of the aqueous phase was added to 400µl Lysis buffer RLT and the solution was mixed by pipetting and vortexing. The solution was transferred to a gDNA Eliminator spin column placed in a 2ml collection tube and centrifuged for 30s at 8000g. The flow-through was saved, 500µl of 70% ethanol was added and the solutions were mixed by pipetting. The resulting 1000µl were transferred in 2 steps (2x 500µl) to an RNeasy spin column placed in a 2ml collection tube. The column was centrifuged for 15s at 8000g and the flow-through was discarded. 700µl Buffer RW1 was added to the spin column which was centrifuged for 15s at 8000g to wash the spin column membrane. The flow-through was discarded. 500µl Buffer RPE was added to the spin column which was again centrifuged for 15s at 8000g. The RPE washing step was repeated once and the flow-through was discarded. The spin column was placed in a new 2ml collection tube and centrifuged at full speed for 1 min. The spin column was placed in a new 1.5ml collection tube. 45µl of RNase-free ddH₂O was directly added to the spin column membrane and the RNA was eluted by spinning for 1min at 8000g.

3.15.2 cDNA preparation

Unless stated otherwise, all subsequent steps were performed on ice, reagents were from Ambion.

Removal of contaminating gDNA from total RNA (1 reaction):

45µl total RNA

5µl of 10x TURBO DNA-free buffer

1.5µl TURBO DNase

The solution was mixed and incubated for 30min at 37°C.

DNase was inactivated by adding 5µl DNase inactivation reagent and incubation for 5min at room temperature with repeated mixing by flicking the tube. The inactivation reagent was pelleted by centrifugation at 13000rpm for 3min. 40µl total RNA was transferred to a fresh 1.5ml Eppendorf tube. 5µl total RNA was stored separately as a negative control for qPCR to prove absence of contaminating gDNA.

Reverse transcription (1 reaction)

10µl RNA

1.6µl random decamers

16.8µl RNase-free ddH₂O

After mixing, RNA was denatured for 3min at 80°C and immediately chilled on ice.

Added were:

4µl of 10x reverse transcription buffer

6µl dNTPs

0.8µl MMLV (Moloney Murine Leukemia Virus) reverse transcriptase

0.8µl RNase inhibitor

Reverse transcription was performed at 43°C for 1h and stopped by incubation at 92°C for 2min.

cDNA for qPCR was diluted ½ by adding 40µl ddH₂O and stored at 4°C.

3.15.3 qPCR procedure

qPCR was performed using a Step One Plus System (qPCR device and reagents from Applied Biosystems).

1 qPCR reaction mixture consisted of:

3µl ddH₂O

6µl SYBR Green Mix

1µl primer mix (forward and reverse primers, 5µM)

2µl cDNA

The qPCR program is shown below (Figure 3.2).

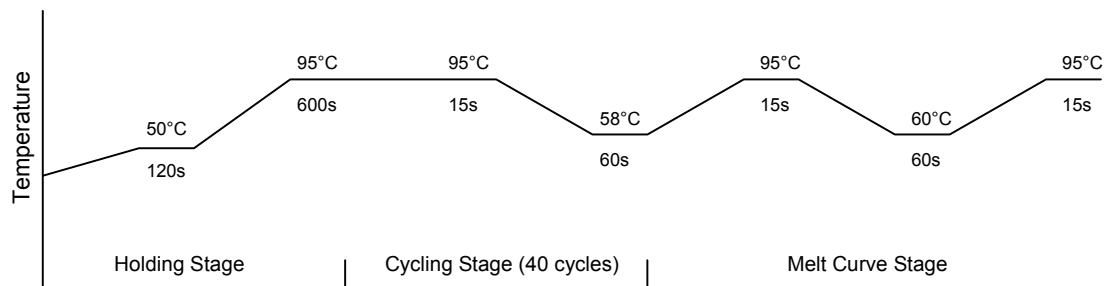


Figure 3.2. qPCR run method. Ramp rates were set at 100%. The last temperature increment for the melt curve was set at + 0.3°C.

Primers

Primer pairs used for qPCR are shown in Table 3.1.

Table 3.1. Primers used for qPCR.

Gene ID Product description	Forward primer (5' to 3')	Reverse primer (5' to 3')
PFL0035c acyl-CoA synthetase, PfACS7	TGTGGAGAACCCGAAAATTA	TCTGGAACACCAGTACCTTCA
PF10_0380 serine/threonine protein kinase, FIKK family	GGTTTGACGGAGATCAAGAA	CATTGCTTTCTGCCTCACTT
PF13_0196 MSP7-like protein	ACAAACGTCTAGTCCCGATG	TCGATCCTCTTGTTGTGAT
PF14_0545 thioredoxin, putative	TTGCCCATTTTATGAAGAA	TTTAAAGGTTGGCATGGAAG
PFA0310c calcium-transporting ATPase	ATTAAATGCTGCCGTAGGTG	AATTTCCCACTTCCCATCTC
PFL1550w lipoamide dehydrogenase	TTGGAGGTGGTGTATAGGG	TCAGCATCAAGAAAACCACA
PFL0900c arginyl-tRNA synthetase adapted from Frank et al. 2006	AAGAGATGCATGTTGGTCATTT	GAGTACCCCAATCACCTACA

Primer pairs used for qPCR and respective gene identification.

Primer validation

All primers were validated with respect to the melting curve patterns of their products and with respect to their amplification efficiencies. Primers were used for qPCR if they yielded 1 amplification product only as judged by their melting curves and if their amplification efficiencies were comparable. Amplification efficiencies were compared as follows: For every gene, C_T values were determined with gDNA templates spanning 5 logs (base 10). ΔC_T values (C_T of target gene – C_T of endogenous control) were calculated for every log of template amount. According to Applied Biosystems, the

absolute value of the slope of the graph (ΔC_T vs. log of template amount) should not exceed 0.1.

Comparative C_T ($\Delta\Delta C_T$) method

The $\Delta\Delta C_T$ method is used to determine the relative target (gene X) quantity in samples. For this method, amplification of gene X and of the endogenous control (e.g. a housekeeping gene) in samples (here: treated with a substance) and in a reference sample (here: untreated) are measured and normalized using the endogenous control. The relative quantity of gene X in every sample is determined by comparing normalized gene X quantity in every sample to normalized gene X quantity in the reference sample.

The amount of target (treated), relative to a reference (untreated) and normalized to an endogenous control (housekeeping gene: HK), is given by:

$$2^{-\Delta\Delta C_T} \text{ whereby}$$

$$\Delta\Delta C_T = \Delta C_{T, \text{ treated}} - \Delta C_{T, \text{ untreated}} =$$

$$(C_T \text{ of gene X, treated} - C_T \text{ of HK, treated}) - (C_T \text{ of gene X, untreated} - C_T \text{ of HK, untreated})$$

4 Results

4.1 *In vitro* activities of test compounds

During the course of this project, a number of chemical derivatives of ACT-AM were used as tool compounds for mode of action studies. The introduction of functional groups such as biotin into pharmacophores may significantly reduce their activity, implying that the derivative no longer hits the target of its precursor. Prior to further experiments, all chemically derivatized tool compounds of ACT-AM as well as negative controls were thus tested for their *in vitro* activities against *P. falciparum* using [³H]hypoxanthine incorporation assays (3.2). Activities against the sequenced 3D7 strain (Gardner et al. 2002) are expressed as IC₅₀ values and summarized in Table 4.1. Chloroquine was used as a reference antimalarial; IC₅₀ values obtained for chloroquine were in the range of those published (Vennerstrom et al. 2004; Maerki et al. 2006).

All tested compounds showed desirable activities i.e. extensively modified compounds largely retained the activity of their precursors, whereas compounds used as negative controls were significantly less active.

Table 4.1 *In vitro* activities of test compounds against *P. falciparum* 3D7.

Compound	Description	IC ₅₀ [mean ± SD (nM)]
ACT-AM	novel antimalarial compound from Actelion	3.8 ± 0.3
ACT-AM-EN2	less active enantiomer of ACT-AM	186.7 ± 26.7
ACT-AM-UV	derivative of ACT-AM linked to UV-activatable capture group (forms nitrene upon activation) and to sorting group (biotin)	34.1 ± 2.9
ACT-AM-UV-Neg	less active derivative of ACT-AM-UV: same capture and sorting group, different (incomplete) parent scaffold	11785.1 ± 3411.0
ACT-AM-Biotin	derivative of ACT-AM linked to biotin	25.4 ± 5.0
ACT-AM-Fluo	derivative of ACT-AM linked to fluorescein	607.5 ± 124.0
ACT-Seph	precursor of ACT-AM conjugatable to sepharose beads	161.9 ± 12.9

Chloroquine	reference antimalarial	8.1 ± 0.1
-------------	------------------------	-----------

Mean IC₅₀ values of test compounds against *P. falciparum* 3D7 ± standard deviations (n ≥ 3 independent experiments) measured by [³H]hypoxanthine incorporation. CQ was used as a control in every experiment, representative values for CQ were determined simultaneously with values for ACT-AM.

4.2 Panel of resistant *Plasmodium falciparum* strains

Prove of activity against key drug resistant *P. falciparum* strains is a progression criterion for novel antimalarial compounds (MMV 2008). Therefore, IC₅₀ values of ACT-AM and reference compounds were determined as described above (4.1) for five resistant and two sensitive strains.

ACT-AM was shown to be very potent (comparable to artesunate) against all tested strains (Table 4.2).

Table 4.2. Mean IC₅₀ values for ACT-AM, CQ, PYR and AS against a panel of several resistant and sensitive *P. falciparum* strains.

Isolate	Origin	Resistance	IC ₅₀ [mean ± SD (nM)]			
			CQ	PYR	AS	ACT-AM
NF54	Airport, NL	--	11 ± 2	18 ± 1	3.7 ± 0.5	1.0 ± 0.1
K1	Thailand	CQ, PYR	303 ± 37	10138 ± 705	2.7 ± 0.4	0.46 ± 0.04
W2	Indochina	CQ, PYR	326 ± 38	13923 ± 3525	2.4 ± 0.7	0.42 ± 0.09
7G8	Brazil	PYR	137 ± 21	10484 ± 2574	1.8 ± 0.2	1.2 ± 0.2
TM90C2A	Thailand	CQ, PYR	174 ± 19	19248 ± 3876	4.6 ± 1.7	2.7 ± 0.4
D6	Sierra L.	--	16 ± 1	5.4 ± 1.3	7.1 ± 1.9	1.3 ± 0.2
V1/S	Vietnam	CQ, PYR	458 ± 66	21936 ± 1072	3.2 ± 0.5	0.65 ± 0.12
Max			458	21936	7.1	2.7
Min			11	5.4	1.8	0.42
Max/Min			42	4062	4	7

IC₅₀ values were determined by [³H]hypoxanthine incorporation. Data are the means ± SD of n = 3 independent experiments.

4.3 *In vitro* pharmacodynamics

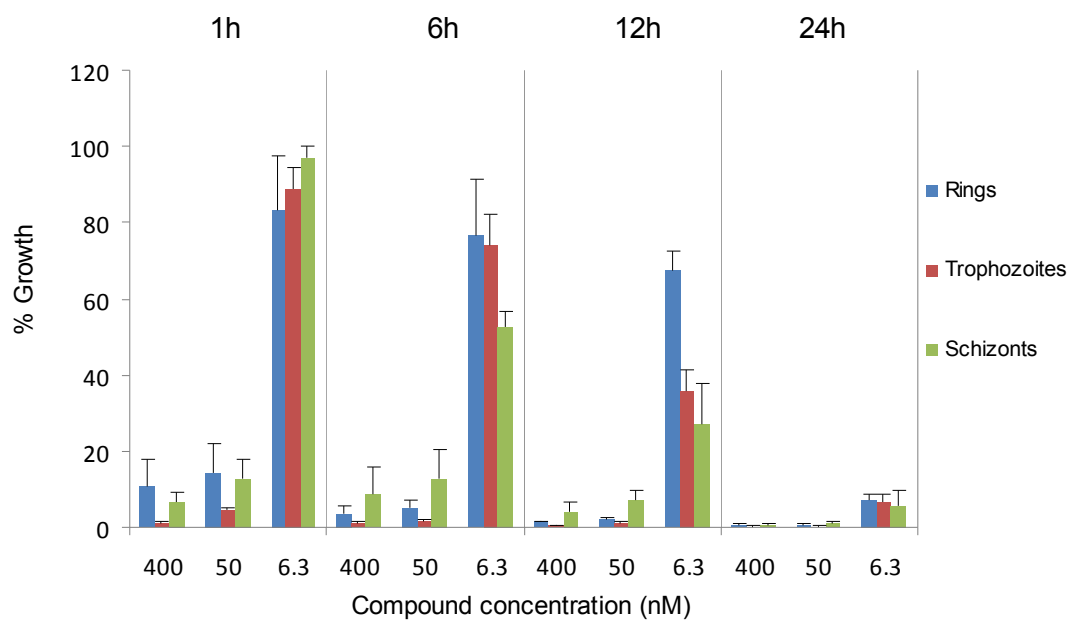
Stage specificity and onset of action of ACT-AM and ACT-AM-UV were assessed with synchronous 3D7 cultures. Pyrimethamine served as a stage (schizont) specific control (Dieckmann & Jung 1986; Maerki et al. 2006). All compounds were tested in three independent experiments. Growth was quantified relative to untreated controls after incubation for 1, 6, 12 or 24h in presence of approx. 1x, 10x and 100x the IC₅₀ values of the respective compounds. After these incubation periods, parasites were extensively washed resulting in a 1280x dilution of free compound before growth was measured.

ACT-AM rapidly reduced parasite growth (onset of action already after 1h of compound exposure) and affected all blood stages equally in a time- and concentration-dependent manner (Figure 4.1.A).

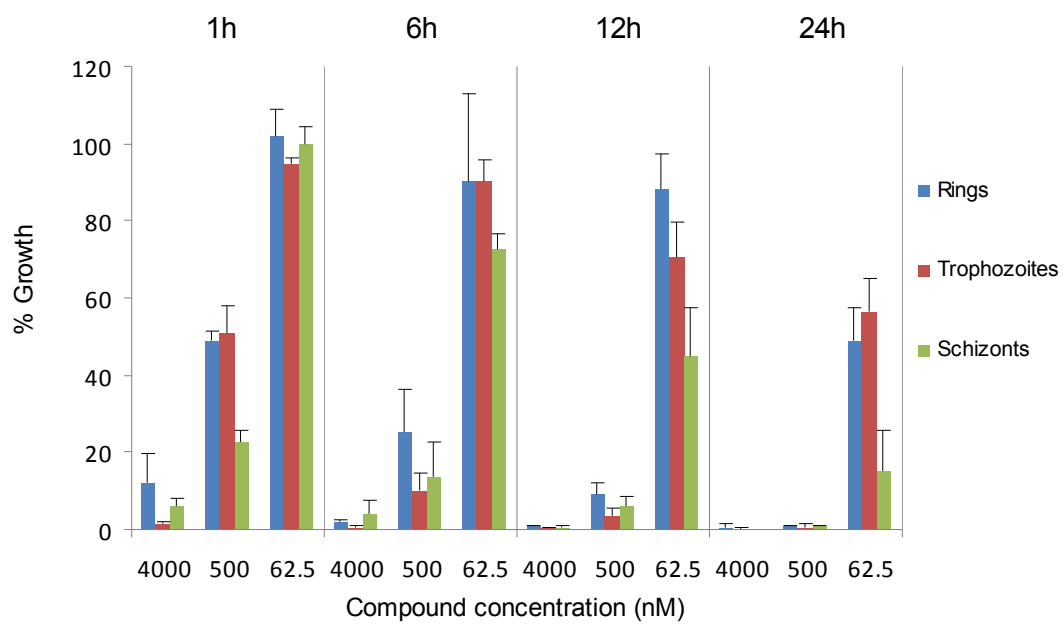
ACT-AM-UV displayed a similar pattern but seemed not to be as potent and fast acting as its precursor (Figure 4.1.B). The control experiment showed the characteristic specificity of pyrimethamine for late parasite stages (Figure 4.1.C).

Results

A



B



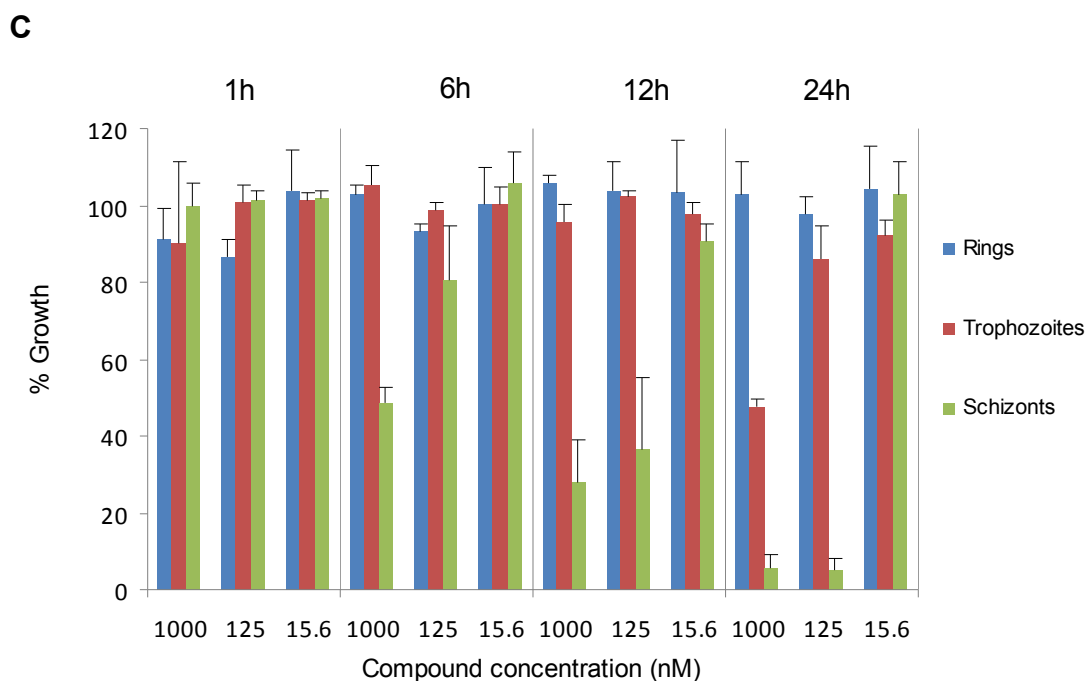


Figure 4.1. *In vitro* concentration- and stage-dependent effects of A) ACT-AM, B) ACT-AM-UV, C) Pyrimethamine (~1x, ~10x and ~100x the IC_{50}) on the growth of synchronous cultures of *P. falciparum* strain 3D7 determined by [3H]hypoxanthine incorporation. Parasites were exposed to compounds for 1, 6, 12 or 24h. After removal of the compounds, parasites were incubated for 24h in the presence of [3H]hypoxanthine. Results are expressed as the percentage of growth of the respective development stage relative to an untreated control. Each bar represents the mean + SD of $n = 3$ independent experiments.

4.4 Fluorescent imaging

4.4.1 Fluorescent imaging with acetone/MeOH fixed cells

To investigate the cellular localization of ACT-AM and to probe whether UV-activatable compounds are applicable for *P. falciparum*, fluorescent imaging was performed. Using UV-activatable compounds, cells had to be fixed with acetone/MeOH, since the applied fluorescent probe (Alexa488-streptavidin) was unable to penetrate intact membranes.

Living 3D7 parasites were incubated with either ACT-AM-UV or ACT-AM-UV-Neg (first negative control) before activation of the compounds with UV light. (In this context, UV-activation means formation of a nitrene which enables the compounds to form covalent bonds with nearby molecular structures, detailed in methods 3.3). As a second negative control, UV-activation was omitted. Cells were washed and after fixation and blocking, the biotin moieties of the compounds were detected using Alexa488-streptavidin.

For all parasite stages, the fluorescent signal was restricted to the parasite and suggested a cytosolic distribution of the compound (Figure 4.2). Fluorescence could also be detected in membranous structures, most notably for schizonts. Both negative controls gave only weak signals which clearly differed from those of the samples.

Furthermore, the results show that UV light reaches into the parasite and that the applied fluorescent imaging method depends on UV-irradiation, since compounds which were incapable of covalent bond formation (absence of UV light) were presumably washed away in the experimental process (Figure 4.2).

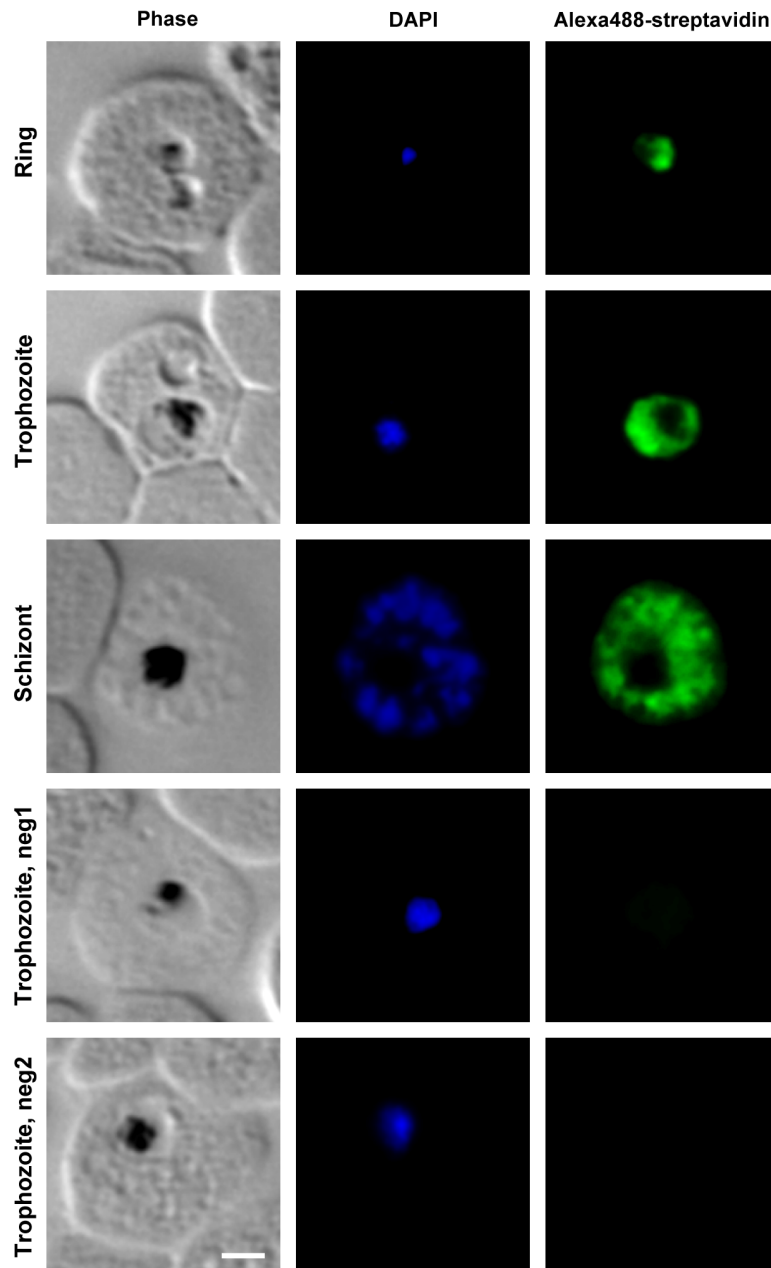


Figure 4.2. Fluorescent imaging with acetone/MeOH fixed cells using UV-activatable compounds. Living *P. falciparum* 3D7 cultures were incubated with ACT-AM-UV prior to fixation with acetone/MeOH. Cells were then washed, UV-irradiated and blocked. After incubation with Alexa488-Streptavidin, cells were mounted in DAPI-containing mounting medium and examined under a fluorescence microscope. Negative control 1: No UV-activation. Negative control 2: UV-activatable mock substance (ACT-AM-UV-Neg). Bar: 1 μ m.

4.4.2 Fluorescent imaging with living cells

The cellular localization of ACT-AM in living cells was studied using the fluorescein-labeled derivative ACT-AM-Fluo.

Living 3D7 parasites were incubated with ACT-AM-Fluo or fluorescein only (negative control). Cells were washed in TBS and directly mounted on glass slides.

Fluorescence was visible in infected red blood cells and seemed to peak in parasites (all stages, Figure 4.3). The observed signal was more diffuse than for the UV-activatable compound (Figure 4.2). This is presumably a result of the shorter half-life of the fluorescein signal (compared to Alexa488) and the fact that living cells were used. Nevertheless, the results seemed to be comparable to those obtained with fixed cells (4.4.1), since the main signals also appeared to be cytosolic.

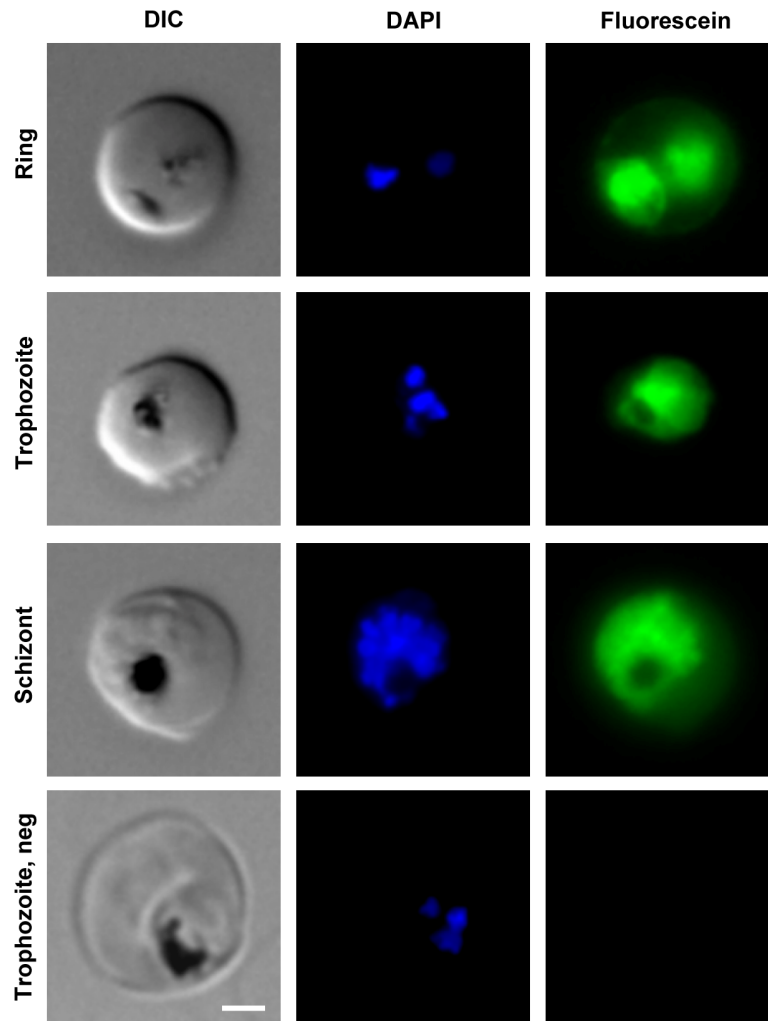


Figure 4.3. Fluorescent imaging with living cells using ACT-AM-Fluo. Living 3D7 cultures were incubated with ACT-AM-Fluo (negative control: fluorescein) and washed. After nuclear staining with DAPI, cells were mounted and examined under a fluorescence microscope. Bar: 1 μ m.

4.5 Far Western blotting

Far Western blotting was used to validate that UV-activatable compounds covalently bind to proteins within *P. falciparum* parasites upon activation with UV light.

Four different samples (differently treated 3D7 parasites) were used:

- A) Sample treated with ACT-AM-UV, irradiated with UV light
- B) Same as A) without UV-irradiation
- C) Sample treated with ACT-AM-UV-Neg, irradiated with UV light
- D) Sample treated with DMSO, irradiated with UV light

Parasite cultures were treated with saponin prior to UV-irradiation to reduce the absorbance of UV light by RBCs. After blotting, proteins bound to UV-activatable compounds were detected with HRP-labeled streptavidin. The resulting signals were weak, probably due to the low concentrations of ACT-AM-UV (approx. 2x IC₉₀) and the limited loading capacity of the protein gel. However, the signal was stronger in lane A than in lane B, indicating that covalent linking of ACT-AM-UV to proteins is dependent on UV light (Figure 4.4). Furthermore, no defined bands were detected in lane C or D, which suggests that the signals of lane A were attributable to ACT-AM-UV only.

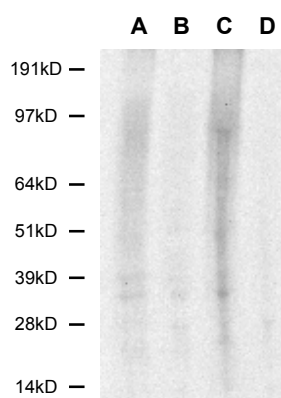


Figure 4.4. Far Western assay. Lysates were separated on a polyacrylamide gel and subsequently blotted on a nitrocellulose membrane. Biotinylated probes were detected with streptavidin-HRP. All samples except for B were UV irradiated. A) sample treated with ACT-AM-UV, B) A without UV-irradiation, C) sample treated with ACT-AM-UV-Neg, D) sample treated with DMSO.

4.6 Pull-down experiments based on UV-activatable compounds

To identify potential targets of ACT-AM, various pull-down experiments were performed using several chemical probes, lysates and beads.

Target candidates were obtained from mass spectrometric analysis of pull-down results. Listed are proteins that were detected in treated samples only, i.e. proteins found in negative controls were subtracted from the respective candidate lists.

4.6.1 UV-activation of compounds in parasites after saponin lysis

i) Whole gel analysis

Whole gel analysis was performed to gain information about the maximal number of proteins potentially binding to ACT-AM.

Samples (3D7 *P. falciparum* cultures) for pull-down experiments were treated with ACT-AM-UV and incubated under normal culture conditions. Two pairs of samples and respective negative controls were used:

-Negative control A:

Competition: Cultures were incubated with an excess of ACT-AM prior to the addition of ACT-AM-UV.

-Sample A:

Cultures were treated with DMSO (to compensate for the DMSO-effects of the ACT-AM treatment of the negative control) prior to the addition of ACT-AM-UV.

-Negative control B:

Cultures were incubated with the mock substance ACT-AM-UV-Neg instead of ACT-AM-UV.

-Sample B:

Cultures were directly incubated with ACT-AM-UV.

After saponin treatment (removal of RBCs), samples were UV-irradiated and lysed in SDS lysis buffer. For pull-downs, lysed samples were incubated with magnetic streptavidin beads which were rigorously washed with SDS buffer before elution (94°C) of captured proteins. Eluted proteins were separated on a polyacrylamide gel which was entirely cut into small fragments used for mass spectrometry. Identified proteins are listed in Tables 4.3 and 4.4.

Table 4.3. Target candidates from pull-downs with UV-activatable compounds using a competitive control and whole gel analysis.

Gene ID	Protein Length	Product Description	Annotated GO Function
PFA0375c	1470	lipid/sterol:H ⁺ symporter	hedgehog receptor activity
PFB0210c	504	hexose transporter, PfHT1	monosaccharide transmembrane transporter activity
PFD1050w	450	alpha-tubulin ii	structural molecule activity, GTP binding, GTPase activity
PFE1050w	479	adenosylhomocysteinase(S-adenosyl-L-homocystein e hydrolase)	binding, adenosylhomocysteinase activity
PFE1150w	1419	multidrug resistance protein	ATP binding, multidrug efflux pump activity, ATPase activity, coupled to transmembrane movement of substances
PFE1195w	1123	karyopherin beta	binding
PFF0690c	853	organic anion transporter	null
PFF0940c	828	cell division cycle protein 48 homologue, putative	ATP binding, ATPase activity
PF07_0029	745	heat shock protein 86	ATP binding, unfolded protein binding
PF07_0033	873	Cg4 protein	ATP binding
PF07_0101	2190	conserved Plasmodium protein, unknown function	null
PFI0880c	396	glideosome-associated protein 50	null
PFI1090w	402	S-adenosylmethionine synthetase	methionine adenosyltransferase activity, ATP binding
PF10_0084	445	tubulin beta chain, putative	structural constituent of cytoskeleton, GTP binding, GTPase activity
PF11_0172	455	folate/biopterin transporter, putative	molecular function
PFL1070c	821	endoplasmic homolog precursor, putative	ATP binding, unfolded protein binding

Results

PFL2215w	376	actin I	structural constituent of cytoskeleton, protein binding
PF13_0272	208	thioredoxin-related protein, putative	protein disulfide isomerase activity
PF14_0352	847	ribonucleoside-diphosphate reductase, large subunit	molecular function, ribonucleoside-diphosphate reductase activity, protein binding
PF14_0425	369	fructose-bisphosphate aldolase	fructose-bisphosphate aldolase activity
PF14_0528	282	hemolysin, putative	molecular function

Target candidates are listed according to gene IDs. Protein characteristics are from PlasmoDB.org. The sample was treated with ACT-AM-UV, the negative control with an excess of ACT-AM. Proteins detected in samples and negative controls were excluded.

Table 4.4. Target candidates from pull-downs with UV-activatable compounds using a non-competitive control and whole gel analysis.

Gene ID	Protein Length	Product Description	Annotated GO Function
PFA0160c	434	nucleoside transporter, putative	null
PFA0375c	1470	lipid/sterol:H ⁺ symporter	hedgehog receptor activity
PFB0585w	365	Leu/Phe-tRNA protein transferase, putative	transferase activity, transferring amino-acyl groups, catalytic activity
PFC0120w	1417	Cytoadherence linked asexual protein 3.1	cell adhesion molecule binding
PFD1110w	372	conserved Plasmodium membrane protein, unknown function	null
PFE0065w	337	skeleton-binding protein 1	null
PFE0080c	398	rhoptry-associated protein 2, RAP2	null
PFE1285w	300	membrane skeletal protein IMC1-related	null
PFF0435w	414	ornithine aminotransferase	pyridoxal phosphate binding, ornithine-oxo-acid transaminase activity
PFF1300w	511	pyruvate kinase	magnesium ion binding, potassium ion binding, pyruvate kinase activity
MAL7P1.228	661	Heat Shock 70 KDa Protein, (HSP70)	ATP binding
MAL7P1.27	424	chloroquine resistance transporter	drug transporter activity
PF07_0101	2190	conserved Plasmodium protein, unknown function	null
MAL8P1.53	514	conserved Plasmodium protein, unknown function	null
PFI0880c	396	glideosome-associated protein 50	null
PFI1090w	402	S-adenosylmethionine synthetase	methionine adenosyltransferase activity, ATP binding

Results

PF11270w	217	conserved Plasmodium protein, unknown function	null
PF11445w	1378	High molecular weight rhopty protein-2	null
PF11_0069	266	conserved Plasmodium protein, unknown function	molecular function
PF11_0098	343	endoplasmic reticulum-resident calcium binding protein	calcium ion binding
PF11_0281	287	protein phosphatase, putative	phosphatase activity
PF11_0301	321	spermidine synthase	spermidine synthase activity
PF11_0506	6093	Antigen 332, DBL-like protein	molecular function, receptor activity
PFL2215w	376	actin I	structural constituent of cytoskeleton, protein binding
PF13_0143	437	phosphoribosylpyrophosphate synthetase	ribose phosphate diphosphokinase activity, magnesium ion binding
PF13_0272	208	thioredoxin-related protein, putative	protein disulfide isomerase activity
PF14_0075	449	plasmepsin IV	aspartic-type endopeptidase activity
PF14_0076	452	plasmepsin I	aspartic-type endopeptidase activity
PF14_0077	453	plasmepsin II	aspartic-type endopeptidase activity
PF14_0105	334	conserved Plasmodium protein, unknown function	molecular function
PF14_0486	832	elongation factor 2	translation elongation factor activity, GTP binding, GTPase activity
PF14_0541	717	V-type H(+)-translocating pyrophosphatase, putative	hydrogen-translocating pyrophosphatase activity, hydrogen ion transmembrane transporter activity, inorganic diphosphatase activity
PF14_0598	337	glyceraldehyde-3-phosphate dehydrogenase	glyceraldehyde-3-phosphate dehydrogenase (phosphorylating) activity, NAD or NADH binding
PF14_0655	398	helicase 45	translation initiation factor activity, RNA cap binding, ATP binding, mRNA binding, ATP-dependent helicase activity

Target candidates are listed according to gene IDs. Protein characteristics are from PlasmoDB.org. The sample was treated with ACT-AM-UV, the negative control with ACT-AM-UV-Neg. Proteins detected in samples and negative controls were excluded.

ii) Partial gel analysis

Pull-downs for partial gel analysis were essentially performed as described above under i) with the modifications that parasites treated with ACT-AM-UV-Neg instead of ACT-AM-UV were used as a negative control, the resulting protein gel was silver stained and

only the areas which differed in the amount of protein (sample vs. control, Figure 4.5) were cut out for mass spectrometry. Partial gel analysis thus enabled the visual exclusion of probably unspecific binding partners of ACT-AM prior to mass spectrometry. Identified proteins are listed in Table 4.5.

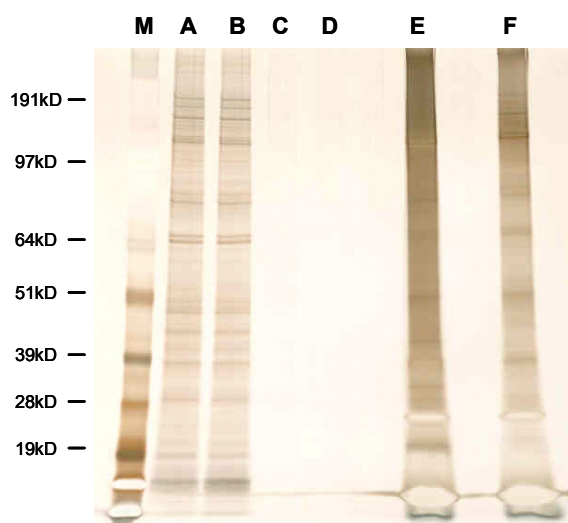


Figure 4.5. Silver staining of pull-down experiments using compounds UV-activated after saponin lysis. The sample was treated with ACT-AM-UV, the negative control with ACT-AM-UV-Neg. M) marker, A) first wash, B) first wash of negative control, C) last wash, D) last wash of negative control, E) elution, F) elution of negative control. Differentially stained areas of the gel (in lanes E and F) were cut out for mass spectrometry.

Table 4.5. Target candidates from pull-downs with UV-activatable compounds using partial gel analysis and a non-competitive control.

Gene ID	Protein Length	Product Description	Annotated GO Function
PFA0160c	434	nucleoside transporter, putative	null
PFA0760w	379	rifin	molecular function
PFB0210c	504	hexose transporter, PfHT1	monosaccharide transmembrane transporter activity
PFB0220w	354	ubiE/COQ5 methyltransferase family, putative	quinone cofactor methyltransferase activity
PFC0730w	221	HVA22/TB2/DP1 family protein, putative	molecular function

Results

PFC0775w	161	40S ribosomal protein S11, putative	structural constituent of ribosome
PFD1055w	170	40S ribosomal protein S19, putative	structural constituent of ribosome
PFE1155c	534	mitochondrial processing peptidase alpha subunit, putative	ubiquinol-cytochrome-c reductase activity, zinc ion binding
PFE1285w	300	membrane skeletal protein IMC1-related	null
PFF0435w	414	ornithine aminotransferase	pyridoxal phosphate binding, ornithine-oxo-acid transaminase activity
PFF0690c	853	organic anion transporter	null
PFF0815w	521	malate:quinone oxidoreductase, putative	malate dehydrogenase (acceptor) activity
PFF0825c	377	mitochondrial import receptor subunit tom40	voltage-gated anion channel activity
PFF0870w	795	conserved Plasmodium membrane protein, unknown function	null
PFF1025c	301	pyridoxine/pyridoxal 5-phosphate biosynthesis enzyme	catalytic activity
PFF1300w	511	pyruvate kinase	magnesium ion binding, potassium ion binding, pyruvate kinase activity
MAL7P1.229	1394	Cytoadherence linked asexual protein	null
MAL7P1.27	424	chloroquine resistance transporter	drug transporter activity
PF07_0088	195	40S ribosomal protein S5, putative	structural constituent of ribosome
MAL8P1.69	262	14-3-3 protein, putative	protein domain specific binding
PF08_0054	677	heat shock 70 kDa protein	ATP binding
PFI0385c	416	P1 nuclease, putative	hydrolase activity, acting on ester bonds
PFI0880c	396	glideosome-associated protein 50	null
PFI0930c	269	nucleosome assembly protein	null
PFI1270w	217	conserved Plasmodium protein, unknown function	null
PFI1310w	839	NAD synthase, putative	ATP binding, NAD ⁺ synthase (glutamine-hydrolyzing) activity
PFI1370c	353	phosphatidylserine decarboxylase	phosphatidylserine decarboxylase activity
PF10_0068	246	RNA binding protein, putative	nucleic acid binding
PF10_0212a	2072	conserved Plasmodium protein, unknown function	null
PF10_0366	301	ADP/ATP transporter on adenylate translocase	ATP:ADP antiporter activity, binding
PF11_0069	266	conserved Plasmodium protein, unknown function	molecular function
PF11_0246	1336	conserved Plasmodium protein, unknown function	molecular function
PF11_0313	316	60S ribosomal protein P0	structural constituent of ribosome
PFL0210c	161	eukaryotic initiation factor 5a, putative	translation initiation factor activity
PFL0720w	245	conserved Plasmodium membrane protein, unknown function	molecular function
PFL1720w	442	serine hydroxymethyltransferase	glycine hydroxymethyltransferase activity
PFL2005w	336	replication factor C subunit 4	ATP binding, DNA clamp loader activity
PFL2060c	459	rabGDI protein	Rab GDP-dissociation inhibitor activity, Rab GTPase activator activity

Results

PFL2275c	304	FK506-binding protein (FKBP)-type peptidyl-propyl isomerase	FK506 binding, peptidyl-prolyl cis-trans isomerase activity
PF13_0033	393	26S proteasome regulatory subunit, putative	ATP binding, nucleoside-triphosphatase activity, endopeptidase activity
PF13_0143	437	phosphoribosylpyrophosphate synthetase	ribose phosphate diphosphokinase activity, magnesium ion binding
MAL13P1.221	375	aspartate carbamoyltransferase	amino acid binding, aspartate carbamoyltransferase activity
MAL13P1.413	249	membrane associated histidine-rich protein, MAHRP-1	null
PF14_0105	334	conserved Plasmodium protein, unknown function	molecular function
PF14_0201	969	surface protein, Pf113	molecular function
PF14_0439	605	M17 leucyl aminopeptidase	manganese ion binding
PF14_0541	717	V-type H(+)-translocating pyrophosphatase, putative	hydrogen-translocating pyrophosphatase activity, inorganic diphosphatase activity, hydrogen ion transmembrane transporter activity
PF14_0543	412	signal peptide peptidase	aspartic-type endopeptidase activity
PF14_0567	340	conserved Plasmodium protein, unknown function	molecular function
PF14_0655	398	helicase 45	translation initiation factor activity, RNA cap binding, ATP binding, ATP-dependent helicase activity, mRNA binding

Target candidates are listed according to gene IDs. Protein characteristics are from PlasmoDB.org. The sample was treated with ACT-AM-UV, the negative control with ACT-AM-UV-Neg. Proteins detected in samples and negative controls were excluded.

4.6.2 UV-activation of compounds in living cells before saponin lysis

Pull-downs using 3D7 cultures UV-irradiated before saponin treatment were conducted to probe whether the UV-dependent pull-down system is applicable for parasites within intact RBCs. The experiments were essentially carried out as described above under 4.6.1 i). The negative control consisted of cultures incubated with an excess of ACT-AM (competition) prior to the addition of ACT-AM-UV whereas the sample was treated with ACT-AM-UV only. Differentially silver stained areas of the gel (Figure 4.6) were cut out for mass spectrometry. MDR (multidrug resistance protein, PFE1150w) was the only identified protein (samples vs. negative controls).

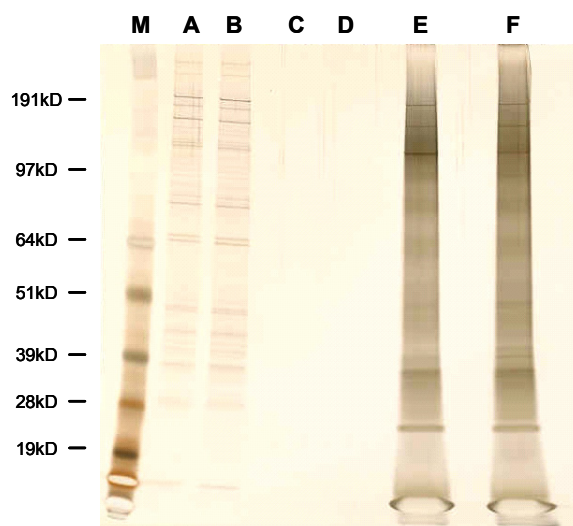


Figure 4.6. Silver staining of pull-down experiments using compounds UV-activated in living cells. The sample was treated with ACT-AM-UV, the negative control with an excess of ACT-AM (competition) prior to the addition of ACT-AM-UV. M) marker, A) first wash, B) first wash of negative control, C) last wash, D) last wash of negative control, E) elution, F) elution of negative control. Differentially stained areas of the gel (in lanes E and F) were cut out for mass spectrometry.

4.7 Pull-down experiments using monomeric avidin systems

Pull-downs with monomeric avidin systems were used in early attempts to find targets of ACT-AM. This method seemed helpful as it enables specific and mild elution conditions using competition with biotin instead of denaturation at 94°C.

Parasites used for pull-downs with monomeric avidin beads were lysed in Triton X-100 lysis buffer. Beads were charged with the biotinylated compounds (ACT-AM-Biotin) and the negative control (less active derivative of ACT-AM-Biotin: same biotin group, different i.e. incomplete parent scaffold) before incubation with lysate. Bound proteins were eluted and separated on a protein gel. As depicted in a representative gel (Figure 4.7), using this method, no differences between samples and controls were visible,

probably due to the fact that parasite lysates which partially exhibit denatured proteins had to be incubated with ACT-AM-Biotin.

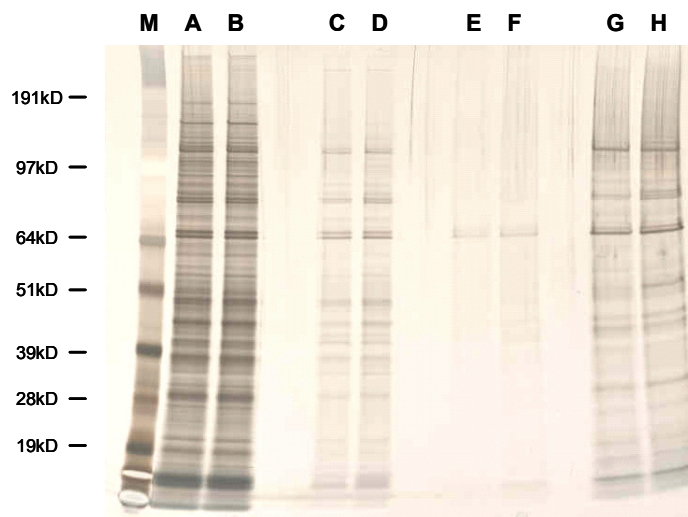


Figure 4.7. Silver staining of pull-down experiments using monomeric avidin systems. The sample beads were charged with ACT-AM-Biotin and the beads of the negative control with a less active derivative of ACT-AM-Biotin (same biotin group, different i.e. incomplete parent scaffold). M) marker, A) first wash, B) first wash of negative control, C) third wash, D) third wash of negative control, E) last wash, F) last wash of negative control, G) elution, H) elution of negative control.

4.8 Early pull-down experiments

Numerous early experiments using non-magnetic streptavidin beads in conjunction with ACT-AM-Biotin or compounds which were directly linked to sepharose beads (ACT-Seph) did not lead to reproducible differences in band patterns (sample vs. control, data not shown). Probably, this was again largely attributable to the fact that lysed i.e. denatured parasites had to be used for both methods.

4.9 Overlap of target candidates

Target candidates which were independently identified at least twice (using at least two different UV-dependent pull-down methods) are listed in Table 4.6.

Table 4.6. Overlap of target candidates identified by several pull-down experiments.

Gene ID	Protein Length	Product Description	Annotated GO Function
MAL7P1.27	424	chloroquine resistance transporter	drug transporter activity
PF07_0101	2190	conserved Plasmodium protein, unknown function	null
PF11_0069	266	conserved Plasmodium protein, unknown function	molecular function
PF13_0143	437	phosphoribosylpyrophosphate synthetase	ribose phosphate diphosphokinase activity, magnesium ion binding
PF13_0272	208	thioredoxin-related protein, putative	protein disulfide isomerase activity
PF14_0105	334	conserved Plasmodium protein, unknown function	molecular function
PF14_0541	717	V-type H(+)-translocating pyrophosphatase, putative	hydrogen-translocating pyrophosphatase activity, hydrogen ion transmembrane transporter activity, inorganic diphosphatase activity
PF14_0655	398	helicase 45	translation initiation factor activity, RNA cap binding, ATP binding, mRNA binding, ATP-dependent helicase activity
PFA0160c	434	nucleoside transporter, putative	null
PFA0375c	1470	lipid/sterol:H+ symporter	hedgehog receptor activity
PFE1150w	1419	multidrug resistance protein	ATP binding, multidrug efflux pump activity, ATPase activity, coupled to transmembrane movement of substances
PFB0210c	504	hexose transporter, PfHT1	monosaccharide transmembrane transporter activity
PFE1285w	300	membrane skeletal protein IMC1-related	null
PFF0435w	414	ornithine aminotransferase	pyridoxal phosphate binding, ornithine-oxo-acid transaminase activity
PFF0690c	853	organic anion transporter	null

Results

PFF1300w	511	pyruvate kinase	magnesium ion binding, potassium ion binding, pyruvate kinase activity
PFI0880c *	396	glideosome-associated protein 50	null
PFI1090w	402	S-adenosylmethionine synthetase	methionine adenosyltransferase activity, ATP binding
PFI1270w	217	conserved Plasmodium protein, unknown function	null
PFL2215w	376	actin I	structural constituent of cytoskeleton, protein binding

Target candidates independently identified at least twice (with at least two different UV-dependent pull-down methods) are listed according to gene IDs. Protein characteristics are from PlasmoDB.org. Proteins detected in samples and negative controls were excluded. * Independently identified three times (with three different pull-down methods).

4.10 Validation of target candidates

Target candidates were chosen for validation based on reproducibility (detected using several methods and experiments: pull-downs and microarray, see 4.12) and feasibility of *in vitro* activity assays. A further criterion for target candidates was expression in all asexual *P. falciparum* blood stages, since ACT-AM was shown to act in a stage unspecific way (Figure 4.1).

4.10.1 Multi drug resistance protein

Interactions of ACT-AM with the multidrug resistance protein (MDR, ID: PFE1150w) were investigated *in vitro* by Corinna Mattheis in the laboratory of David Fidock in New York.

In vitro susceptibility of *P. falciparum* to several antimalarials has been demonstrated to correlate with the gene copy number of *mdr* (Sidhu et al. 2006). This was shown for mefloquine and related drugs by measuring IC₅₀ values against two *P. falciparum* strains with either 1 (strain 1) or 2 (strain 2) *mdr* gene copies, respectively. The gene copy number was found to correlate to the amount of protein and to the respective IC₅₀ values

as strain 2 was significantly less susceptible to mefloquine than strain 1 (Sidhu et al. 2006).

ACT-AM showed the same pattern as the positive control mefloquine with respect to *in vitro* activity against the two strains (Table 4.7), thus implicating an interaction of the compound with MDR.

Table 4.7. *In vitro* antimalarial response of *P. falciparum* strains exhibiting either 1 or 2 multidrug resistance protein (*mdr*) gene copies.

	ACT-AM			mefloquine		
	IC ₅₀ s (nM)		ratio strain 2:1	IC ₅₀ s (nM)		ratio strain 2:1
	strain 2 (2 copies)	strain 1 (1copy)		strain 2 (2 copies)	strain 1 (1copy)	
Exp1	4.9	2.4	2.1	43.1	17.6	2.4
Exp2	3.9	1.9	2.1	34.4	14.1	2.4
Exp3	1.4	0.6	2.1	25.9	13.4	1.9
Exp4	0.8	0.4	1.9	6.7	5.5	1.2

In vitro activities of ACT-AM and mefloquine against *P. falciparum* strains with either 1 or 2 multidrug resistance protein (*mdr*) gene copies were determined by Corinna Mattheis according to Sidhu et al., 2006 in the laboratory of David Fidock in New York. Exp: Experiment.

Statistical analysis showed that the IC₅₀ patterns of ACT-AM and mefloquine are not significantly different (Table 4.8).

The confidence intervals of the geometric mean ratios for ACT-AM and mefloquine include 2, meaning that both geometric mean ratios are not significantly different from 2 at the usual 5%-level. On the other hand, both geometric mean ratios are significantly different from 1 at the 5%-level as their confidence intervals do not include 1.

Finally, the ratio of geometric mean ratios between ACT-AM and mefloquine is very close to 1 and the 95%-confidence interval includes 1, showing that this ratio is not significantly different from 1 at the 5%-level.

Table 4.8. Statistical analysis of *in vitro* activities of ACT-AM and mefloquine against *P. falciparum* strains with either 1 or 2 multidrug resistance protein (*mdr*) gene copies.

	geometric mean ratio ratio: (IC ₅₀ S strain 2: IC ₅₀ S strain 1)	95%-confidence interval
ACT-AM	2.10	1.88 to 2.35
mefloquine	1.94	1.15 to 3.27
	ratio of geometric mean ratios (ACT-AM vs. mefloquine)	
	1.09	0.65 to 1.82

Geometric means of IC₅₀-ratios between *P. falciparum* strains with 1 or 2 multidrug resistance protein (*mdr*) gene copies were statistically analyzed to compare the *in vitro* responses to ACT-AM and mefloquine.

4.10.2 Equilibrative Nucleoside Transporter 4

In vitro interactions of the Equilibrative Nucleoside Transporter 4 (ENT4 gene ID: PFA0160c: nucleoside transporter, putative) with ACT-AM were studied by I. J. Frame in the laboratory of Myles Akabas in New York.

[³H]adenine uptake of *Xenopus laevis* oocytes heterologously expressing PfENT4, PvENT4 (*Plasmodium vivax*) or PfENT1 was measured under treatment with ACT-AM or its enantiomer ACT-AM-EN2 which was less active against *P. falciparum in vitro* (Table 4.1).

In presence of ACT-AM, PfENT4-mediated transport of [³H]adenine was found to decrease in a concentration-dependent manner (Figure 4.8.A).

The effect of ACT-AM seemed more pronounced for PfENT4 than for PvENT4, whereas no effect was observed for PfENT1 (Figure 4.8.B).

ACT-AM and ACT-AM-EN2 were shown to affect [³H]adenine uptake to an equal extent, therefore, both enantiomers seem to similarly interact with the transporter in this assay (Figure 4.8.C).

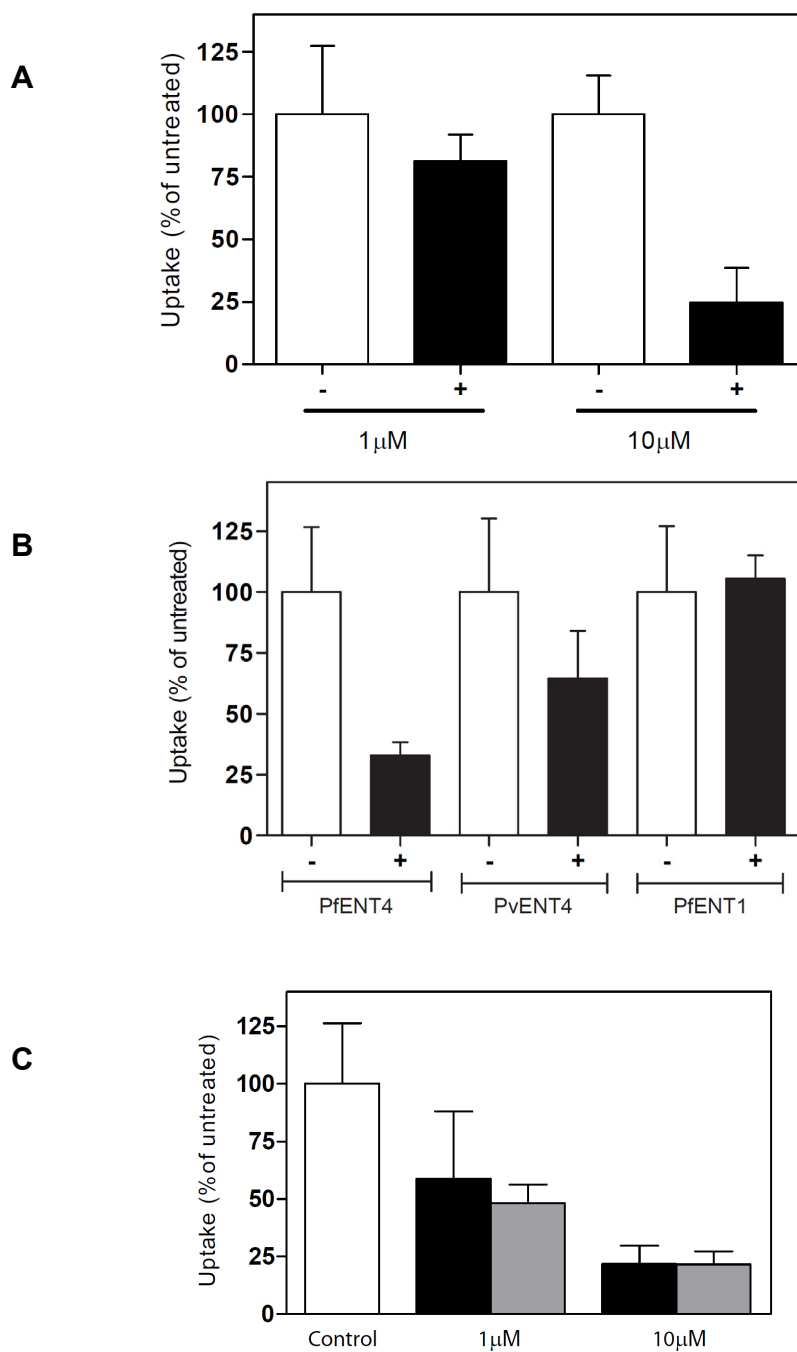
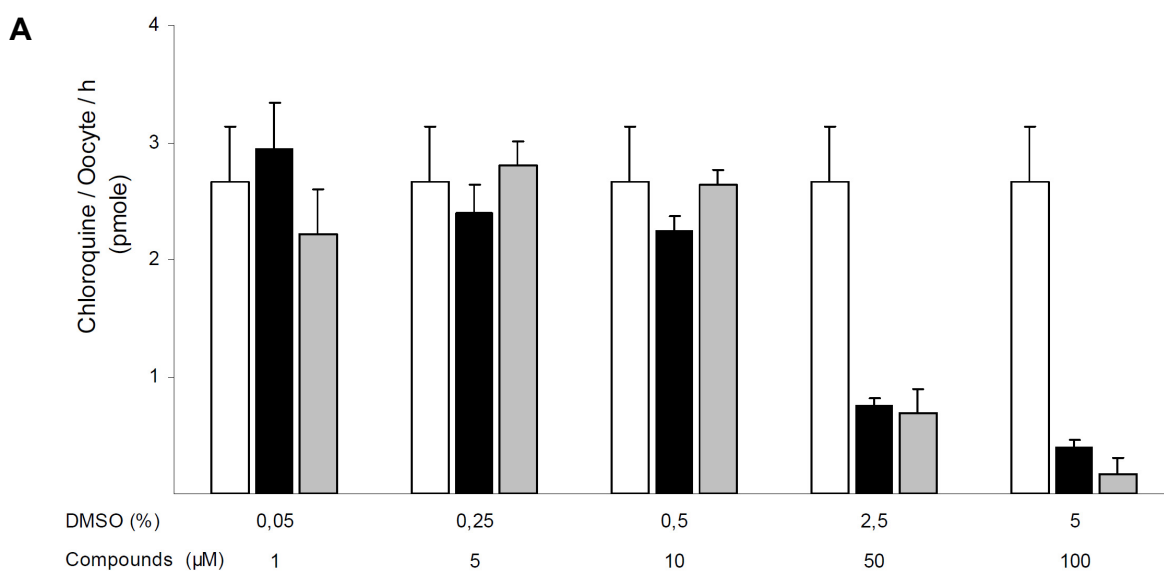


Figure 4.8. *In vitro* effect of ACT-AM on [3 H]adenine transport via *Plasmodium* Equilibrative Nucleoside Transporters expressed in *Xenopus laevis* oocytes. Before exposure to [3 H]adenine, oocytes were preincubated in transport buffer with ACT-AM (black bars), solvent control (white bars) or ACT-AM-EN2 (grey bars). Bars represent the mean uptake of 7 or 8 oocytes and error bars are standard deviations. Tests were performed by I. J. Frame in the laboratory of Myles Akabas in New York.

4.10.3 Chloroquine Resistance Transporter

Interactions of ACT-AM with the Chloroquine Resistance Transporter (CRT, gene ID: MAL7P1.27) were investigated *in vitro* using *Xenopus laevis* oocytes by Sebastiano Bellanca in the laboratory of Michael Lanzer in Heidelberg.

Both, ACT-AM and ACT-AM-EN2, showed a concentration-dependent effect on CRT-mediated [³H]CQ transport suggesting an interaction between the compounds and the transporter (Figure 4.9.A). The observed effect was more attributable to the compounds than to DMSO (Figure 4.9.B).



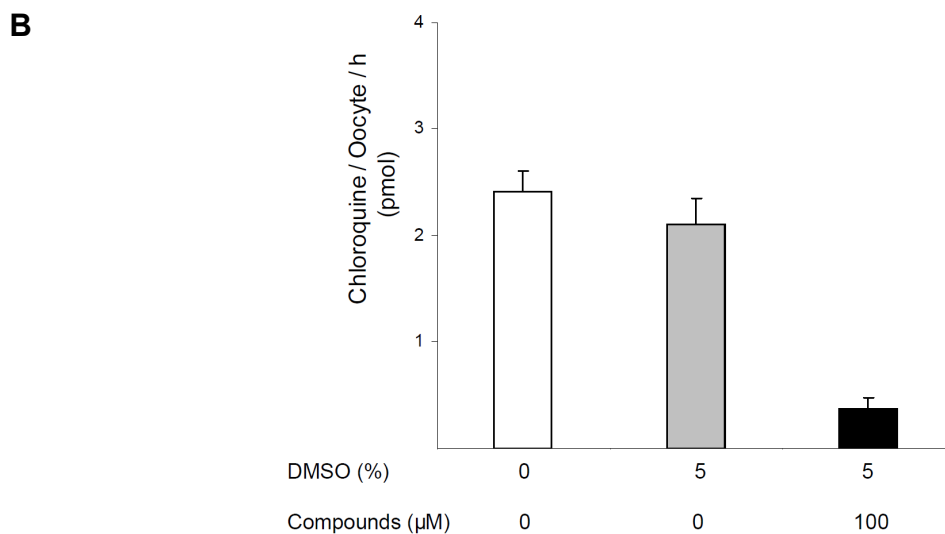


Figure 4.9. *In vitro* effect of ACT-AM on [³H]CQ transport via *P. falciparum* Chloroquine Resistance Transporter expressed in *Xenopus laevis* oocytes. Oocytes were incubated in transport buffer (white bars) with ACT-AM (black bars) or ACT-AM-EN2 (grey bars: Figure A only). Bars represent the mean uptake of 10 oocytes and error bars are standard deviations. Tests were performed by Sebastiano Bellanca in the laboratory of Michael Lanzer in Heidelberg.

4.10.4 Aldolase

Coupled to a NADH-consuming reaction, the *in vitro* activity of aldolase (fructose-bisphosphate aldolase, PF14_0425) can be measured photometrically (3.12.4).

The enzymatic assay itself was first validated using increasing aldolase concentrations while all other factors were kept constant. The activity appeared to be directly proportional to the amount of aldolase (Figure 4.10.A).

To avoid saturation of the tested enzyme, inhibition assays were performed at the experimentally determined K_M (Michaelis Constant). The measured K_M was approx. 21 μM (Figure 4.10.B).

Results

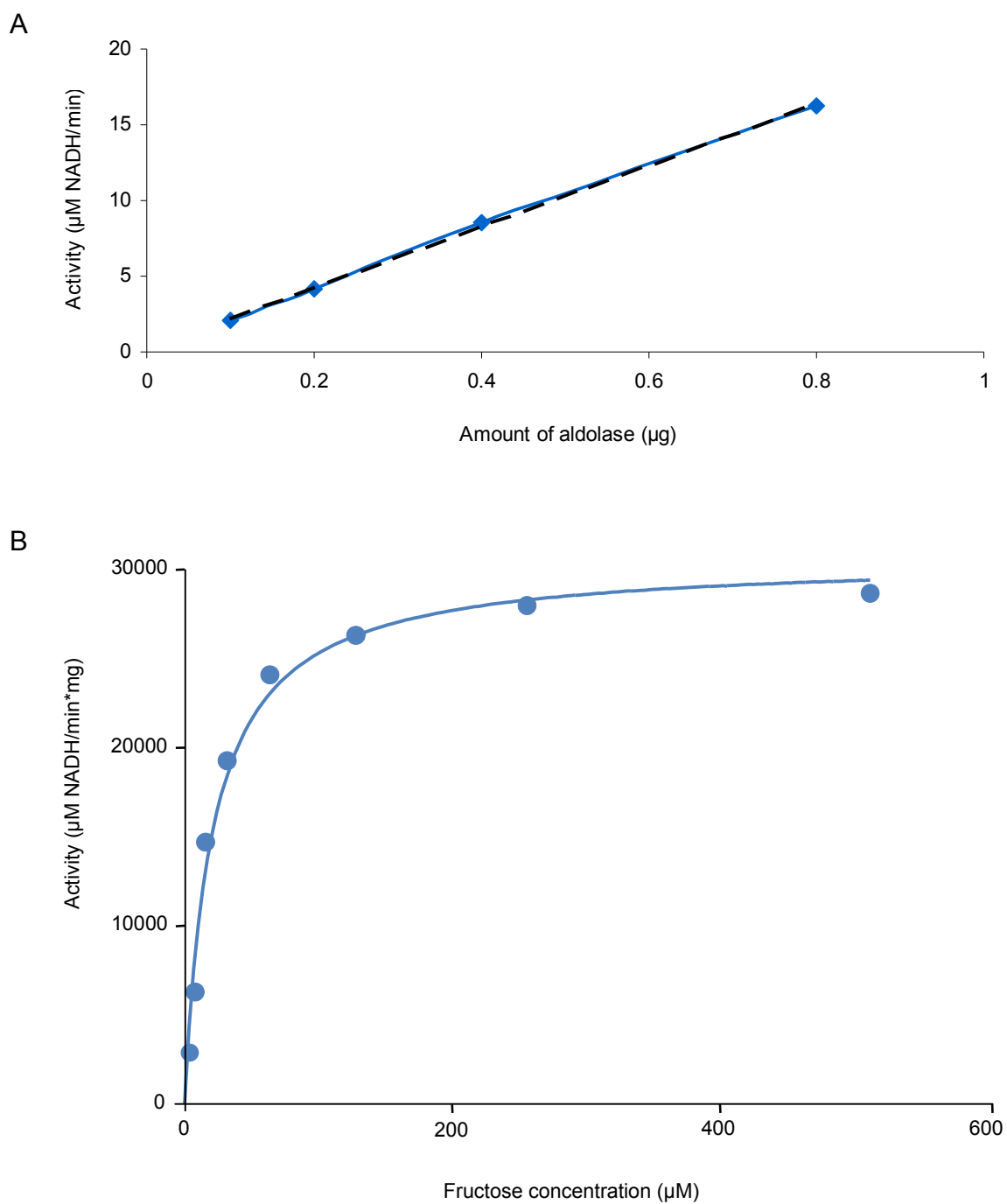


Figure 4.10. *In vitro* fructose-bisphosphate aldolase activity. Aldolase activity was photometrically determined in a NADH-consuming coupled assay. A) Enzyme activity was directly proportional to aldolase concentration (final volume: 725 μl), $R^2 = 0.9993$. B) Saturation curve of aldolase. The kinetics data were fitted and the K_M was determined using Prism software, $K_M = 21 \mu\text{M}$.

To test whether ACT-AM inhibits aldolase activity *in vitro*, the substrate concentration was set equal to the K_M value (approx. $21\mu\text{M}$) while ACT-AM was applied at 1 and $10\mu\text{M}$. For both concentrations (approx. $10\mu\text{M}$ being the highest possible concentration in aqueous solution for solubility reasons), ACT-AM displayed no inhibitory effect on aldolase activity (Table 4.9).

Table 4.9. Effect of ACT-AM on aldolase activity.

	no inhibitor (DMSO)	ACT-AM ($1\mu\text{M}$)	ACT-AM ($10\mu\text{M}$)
Activity ($\mu\text{M NADH}/\text{min}\cdot\text{mg}$)	15777 ± 246	15981 ± 85	16334 ± 32
Activity compared to untreated	-	+ 1.22%	+ 3.5%

Mean *in vitro* activity of fructose-bisphosphate aldolase \pm standard deviations (n = 3 independent experiments) in presence and absence of ACT-AM measured by photometry.

4.10.5 M17 leucyl aminopeptidase

M17 leucyl aminopeptidase (PF14_0439) was tested for its *in vitro* activity under treatment with ACT-AM in the laboratory of Colin Stack in Sydney.

In contrast to the reference compounds, ACT-AM does not seem to inhibit the enzyme (Figure 4.11).

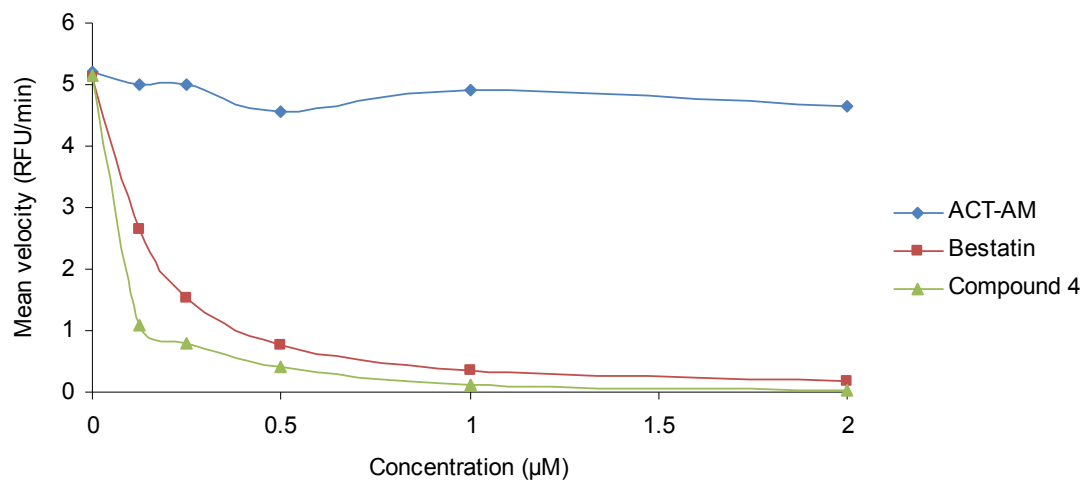


Figure 4.11. Effect of ACT-AM on M17 leucyl aminopeptidase. *In vitro* enzyme activity was determined using several fluorogenic peptide substrates by the method of Stack et al., 2006. Tests were performed in the laboratory of Colin Stack in Sydney. Positive controls: Bestatin and Compound 4. RFU: relative fluorescence units.

4.10.6 Spermidine synthase, S-adenosylmethionine synthetase, and secreted acid phosphatase

In vitro activities of spermidine synthase (PF11_0301), S-adenosylmethionine synthetase (PFI1090w), and secreted acid phosphatase (or glideosome-associated protein 50: PFI0880c) were tested by Ingrid Müller in the laboratory of Rolf Walter in Hamburg. None of the tested enzymes were inhibited by ACT-AM (Figure 4.12, Figure 4.13, Figure 4.14).

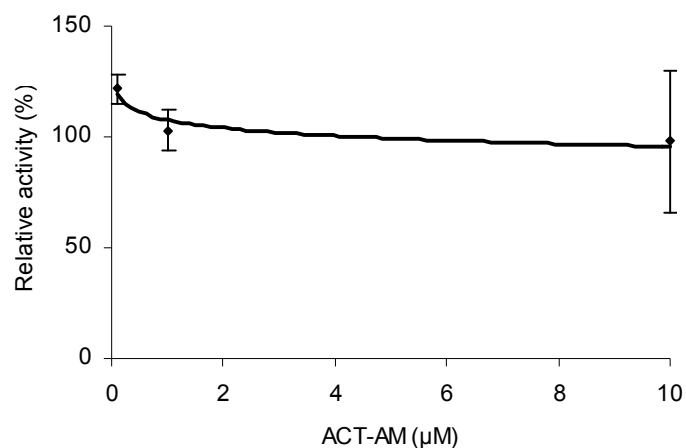


Figure 4.12. Spermidine synthase activity under treatment with ACT-AM. *In vitro* activity of spermidine synthase was tested after Haider et al., 2005 and Dufe et al., 2007 by measuring the formation of [¹⁴C] labeled reaction products from [¹⁴C]putrescine. Tests were performed by Ingrid Müller in the laboratory of Rolf Walter in Hamburg. Data are the means \pm SD of n = 3 independent experiments.

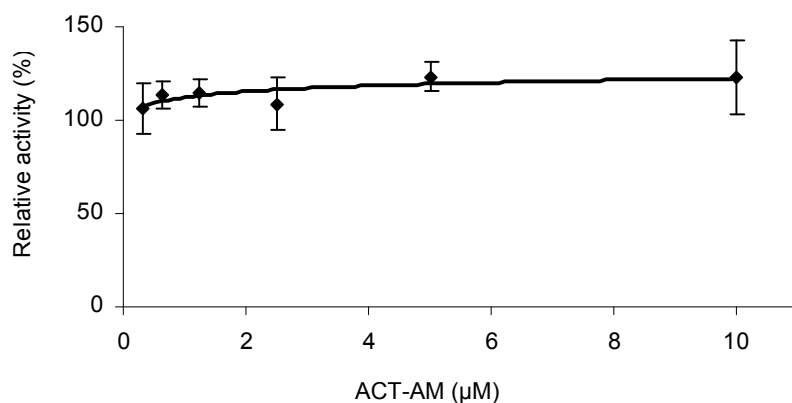


Figure 4.13. Effect of ACT-AM on S-adenosylmethionine synthetase. Enzyme activity was measured *in vitro* using [¹⁴C]S-adenosyl-L-(methyl-)methionine as a substrate according to Das Gupta 2005. Tests were performed by Ingrid Müller in the laboratory of Rolf Walter in Hamburg. Data are the means \pm SD of n = 5 independent experiments.

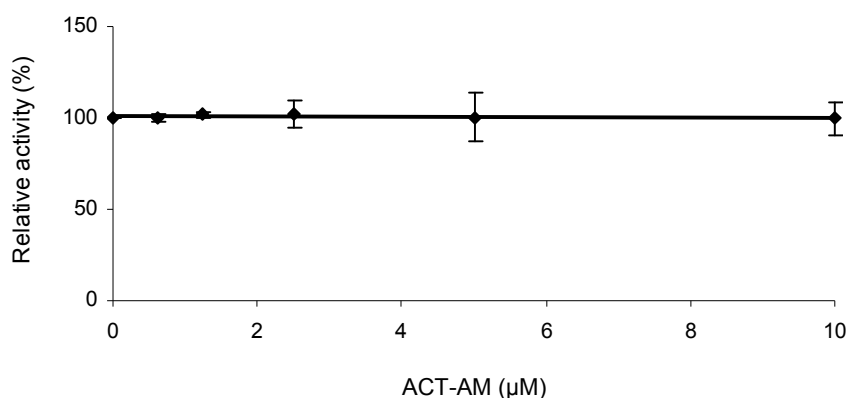


Figure 4.14. Effect of ACT-AM on secreted acid phosphatase. *In vitro* activity of secreted acid phosphatase was measured using [14 C]ATP as a substrate by the method of Müller et al., 2010. Tests were performed by Ingrid Müller in the laboratory of Rolf Walter in Hamburg. Data are the means \pm SD of $n = 3$ independent experiments.

4.11 Hematin interaction studies

An often published MOA of chloroquine and other quinolines involves the inhibition of synthetic hemozoin (beta-hematin) formation (introduction 1.2). To examine if ACT-AM exhibits an MOA similar to that of quinolines, interaction studies of the compound with hematin were conducted.

4.11.1 Inhibition of beta-hematin formation

Quinoline antimalarials were shown to inhibit the formation of synthetic hemozoin from hematin *in vitro*, resulting in unreacted hematin (Egan et al. 1994). This process can be monitored using pyridine which coordinates to unreacted hematin (not to hemozoin) leading to a reddish complex (Ncokazi & Egan 2005).

In vitro beta-hematin (hemozoin) formation can be brought about when hematin is incubated with a saturated acetate solution at 60°C.

Inhibition of beta-hematin formation was shown for chloroquine (positive control, red), whereas ACT-AM and solvent (negative control, colorless) showed no inhibition (Figure 4.15).

The experiment was carried out with Sandra Vargas who had adapted the method from (Ncokazi & Egan 2005) in the laboratory of Karine Ndjoko in Geneva.

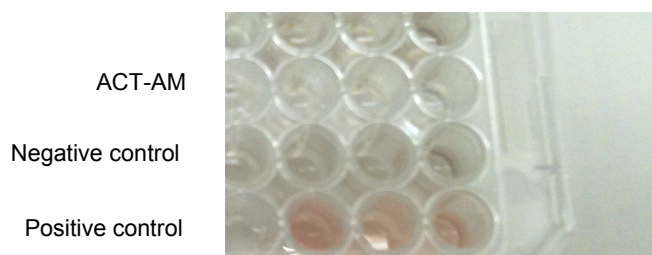


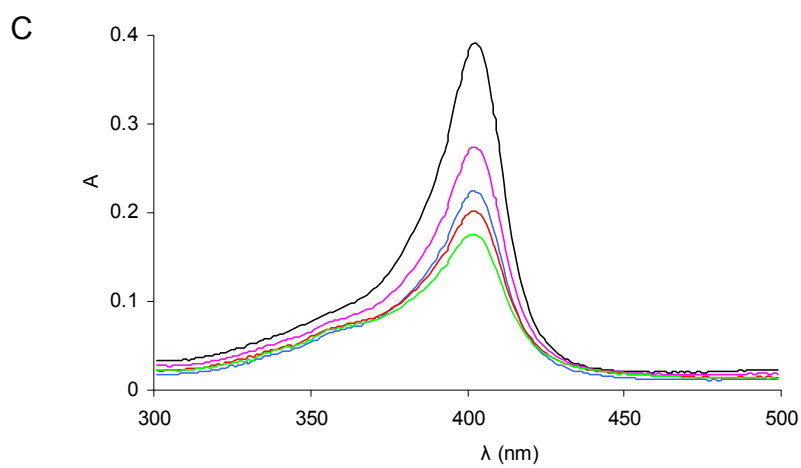
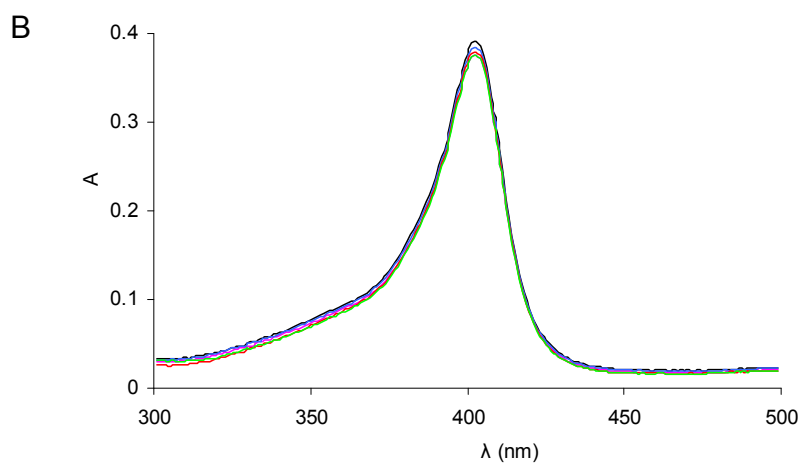
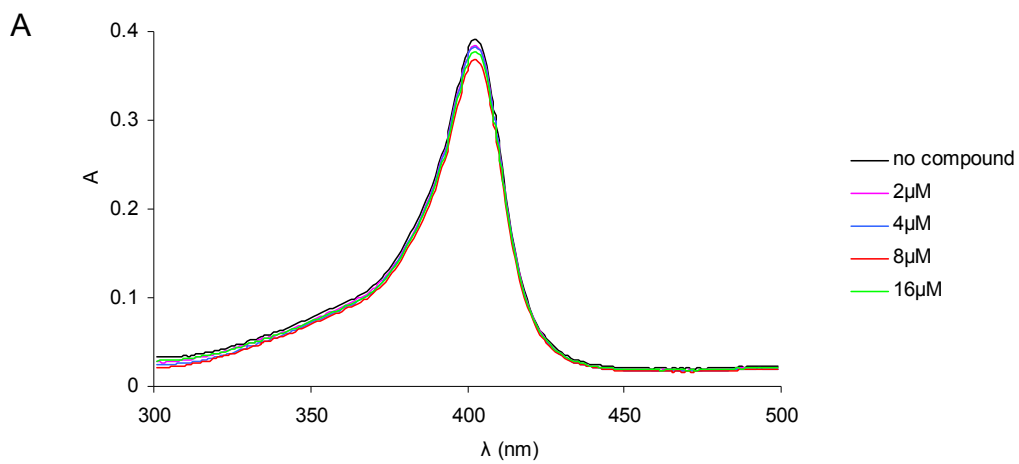
Figure 4.15. Beta-hematin formation assay. Detection of a red complex indicated inhibition of beta-hematin formation, whereas solutions without inhibition remained colorless. Positive control: Chloroquine. Negative control: Solvent.

4.11.2 Spectrophotometric measurement of hematin interactions

Compounds interacting with hematin such as quinolines which inhibit beta-hematin formation were demonstrated to alter the absorbance of hematin solutions *in vitro* (reviewed by Egan 2006). This change in absorbance is thought to be caused by quinolines forming π - π complexes with hematin (Egan & Ncokazi 2004).

Neither ACT-AM nor ACT-AM-EN2 showed a concentration-dependent effect on hematin absorbance (Figure 4.16.A, B, respectively). For the positive controls, chloroquine and mefloquine, a clear dose-dependent effect was observed (Figure 4.16.C, D, respectively), whereas pyrimethamine (negative control) did not alter the absorbance of hematin (Figure 4.16.E).

Results



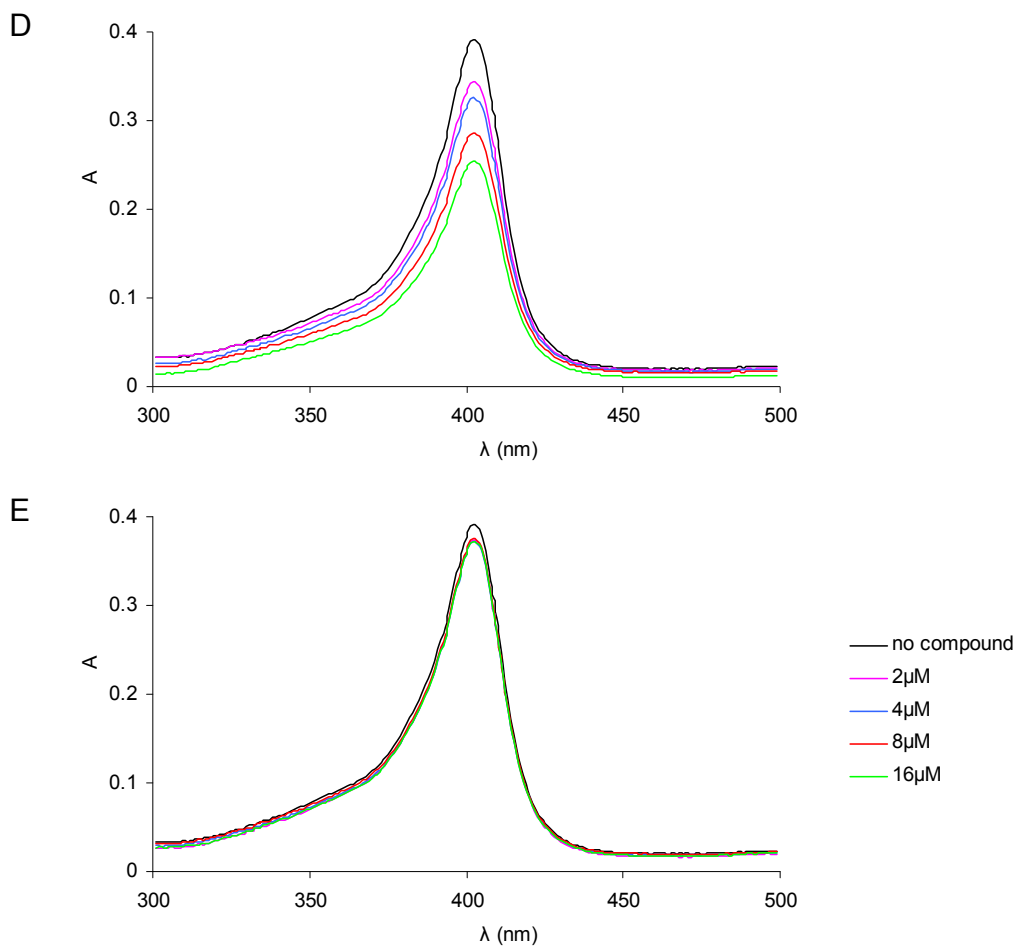


Figure 4.16. Spectrophotometric measurement of hematin interactions. The absorbance of hematin solutions titrated with test compounds was monitored using a UV–visible spectrophotometer. A) ACT-AM, B) ACT-AM-EN2 C) chloroquine, D) mefloquine, E) pyrimethamine.

4.12 Microarray

In order to learn more about the MOA of ACT-AM, microarray studies were performed. *In vitro* gene expression of ACT-AM-treated vs. untreated 3D7 parasites was compared to expression patterns induced by several previously assessed antimalarial compounds (Hu et al. 2010).

Highly synchronized 3D7 *P. falciparum* parasites were treated with an IC₉₀ of ACT-AM and control samples with the respective amount of DMSO starting at $t_0 = 32\text{h}$ post-infection for 1, 2, 4, 6, and 8h.

Hybridization and comparison to expression patterns of 20 different antimalarial compounds were performed by Enghow Lim and Zbynek Bozdech, respectively in Singapore.

Additional analysis of the differentially regulated genes was conducted in-house; the results, including a detailed heat map, are summarized in the appendix (6.1).

For the comparison of transcriptional responses to treatments (ACT-AM vs. other antimalarial compounds), Zbynek Bozdech included genes which were differentially expressed under treatment with ACT-AM by at least two-fold at more than one time point. Applying these criteria, ACT-AM altered the expression of 552 genes of which 407 were up- and 145 down-regulated (Figure 4.17.A). For the up-regulated genes, functional enrichment analysis has revealed statistical overrepresentation of several basic cellular and metabolic pathways (Figure 4.17.B). These include protein synthesis (ribosomal subunits and assembly factors) and posttranslational modifications of proteins (N-myristoylation, S-acylation and prenylation). Furthermore, a major lipid metabolism pathway (phosphatidylethanolamine and phosphatidylserine metabolism) and its supporting glycine and serine metabolic pathway were significantly up-regulated. In addition, a total of 18 protein kinases was found to be up-regulated by ACT-AM. On the other hand, treatment with the compound caused significant down-regulation of numerous components of the merozoite invasion machinery.

Hu and coworkers have recently characterized and profiled gene expression patterns induced by 20 different antimalarial compounds (Hu et al. 2010). The compounds are described in Table 4.10.

The comparison of the transcriptional response induced by ACT-AM to these 20 established profiles is summarized in Figures 4.17.C and D.

Hierarchical clustering analysis revealed four principal groups of the 20 perturbations (Hu et al. 2010) based on similarities in induced expression patterns. The results are depicted as a principal coordinate plot (Figure 4.17.C) or a dendrogram (Figure 4.17.D). ACT-AM clustered closely with a subset of the perturbations which included generic protein kinase inhibitors such as staurosporine and ML-7 on one side and retinol A (a vitamin A alcohol interacting with membranes) or the serine protease inhibitor PMSF on the other side. Importantly, ACT-AM was not found in the same cluster as the antimalarial drugs chloroquine, quinine and artemisinin (Figure 4.17.C and D).

Results

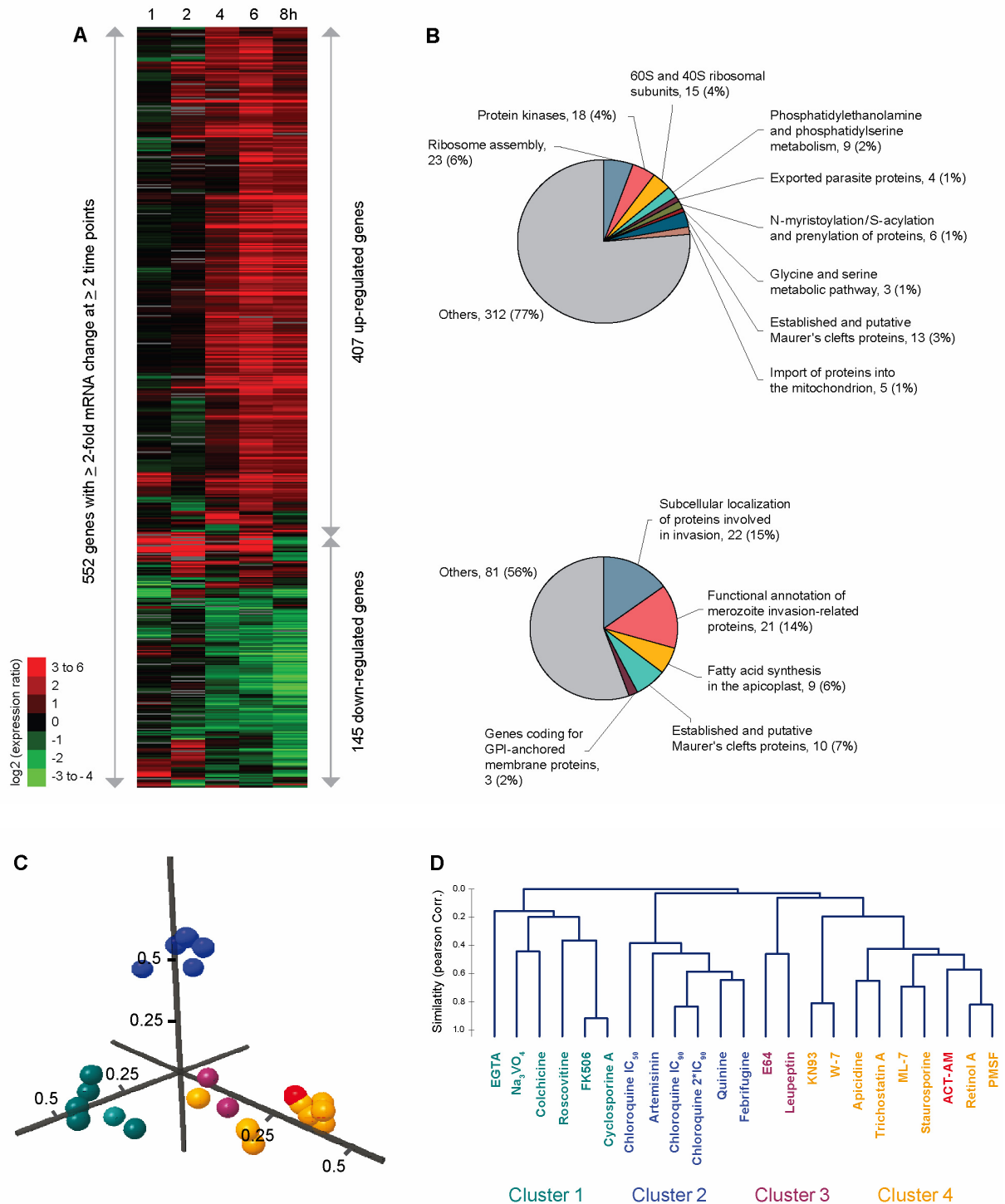


Figure 4.17. Analyses of genome-wide transcriptional response of *P. falciparum* parasites to treatment with ACT-AM. Highly synchronized 3D7 schizonts were treated with ACT-AM (IC₉₀) and control samples with the respective amount of DMSO. RNA was collected after 1, 2, 4, 6 and 8h of treatment. A) The heat map represents clustering of genes found to be differentially expressed by

Results

at least two fold at more than one time point. B) The pie charts show significantly enriched pathways under treatment ($P < 0.05$) identified by functional enrichment analysis. Depicted is the fraction of differentially expressed genes which are within (colored) and not within (grey) the enriched functional pathways, the number and percentage of genes in each cluster are indicated. C) 3-dimensional principal coordinate plot in which distances between points indicate the degree in similarity between transcriptional profiles of individual antimalarial compounds. D) Dendrogram of hierarchical clustering of transcriptional responses to compounds revealed four distinct clusters. The color code is consistent in C and D.

Table 4.10. Comparator compounds of microarray analysis.

Compound	Description
EGTA	ethylene glycol tetraacetic acid, chelating agent, high affinity to calcium (Lau & Gnegy 1982)
Na ₃ VO ₄	sodium orthovanadate, phosphatase inhibitor (Harayama et al. 2004)
Colchicine	microtubule polymerization inhibitor (Margolis & L. Wilson 1977)
Roscovitine	cyclin-dependent kinase inhibitor (Ma et al. 2003)
FK506	tacrolimus, calcineurin pathway inhibitor (Hu et al. 2010)
Cyclosporine A	calcineurin pathway inhibitor (Hu et al. 2010)
Febrifugine	antimalarial activity, unknown MOA (McLaughlin & Evans 2010)
E64	N-(trans-epoxysuccinyl)-l-leucine-4-guanidinobutylamide, cysteine peptidase inhibitor (Parikh et al. 2006)
Leupeptin	cysteine, serine and threonine peptidase inhibitor (Rawlings 2010)
KN93	calmodulin kinase II (CaMKII) inhibitor (Silva-Neto et al. 2002)
W-7	calcium/calmodulin-dependent protein kinase inhibitor (Hu et al. 2010)
Apicidine	histone deacetylase inhibitor (Hu et al. 2010)
Trichostatin A	histone deacetylase inhibitor (Hu et al. 2010)
ML-7	calcium/calmodulin-dependent protein kinase inhibitor (Hu et al. 2010)
Staurosporine	inhibitor of multiple kinases (Karaman et al. 2008)
Retinol A	probable interaction with phospholipid molecules of intracellular membranes (Hamzah et al. 2004)
PMSF	phenylmethanesulfonyl fluoride, serine protease inhibitor (Rupp et al. 2008)

Description of compounds which were used for *P. falciparum* transcriptional profiling by Hu et al. 2010.

4.13 Overlap of pull-down and microarray results

Gene candidates which were identified in both pull-down and microarray experiments are listed in Table 4.11.

Table 4.11. Overlap of gene candidates identified by both pull-down and microarray experiments.

Gene ID	Product Description	Annotated GO Function	
PFA0760w	rifin	molecular function	
PFE1150w	multidrug resistance protein	ATP binding, multidrug efflux pump activity, ATPase activity, coupled to transmembrane movement of substances	
PFF0815w	malate:quinone oxidoreductase, putative	malate dehydrogenase (acceptor) activity	U P
PFF0825c	mitochondrial import receptor subunit tom40	voltage-gated anion channel activity	R
MAL7P1.228	Heat Shock 70 KDa Protein, (HSP70)	ATP binding	E G
PF07_0029	heat shock protein 86	ATP binding, unfolded protein binding	U
PF07_0033	Cg4 protein	ATP binding	L
PF08_0054	heat shock 70 kDa protein	ATP binding	A
PF11_0506	Antigen 332, DBL-like protein	molecular function, receptor activity	T E
MAL13P1.221	aspartate carbamoyltransferase	amino acid binding, aspartate carbamoyltransferase activity	D
MAL13P1.413	membrane associated histidine-rich protein, MAHRP-1	null	
PF14_0076	plasmepsin I	aspartic-type endopeptidase activity	
PFC0120w	Cytoadherence linked asexual protein 3.1	cell adhesion molecule binding	
PFE0080c	rhoptry-associated protein 2, RAP2	null	D O
PFE1285w	membrane skeletal protein IMC1-related	null	W
PFF0870w	conserved Plasmodium membrane protein, unknown function	null	N

Results

PFI0880c	glideosome-associated protein 50	null	
PFI1445w	High molecular weight rhoptry protein-2	null	R
PFL0210c	eukaryotic initiation factor 5a, putative	translation initiation factor activity	E
PFL0720w	conserved Plasmodium membrane protein, unknown function	molecular function	G
PFL2215w	actin I	structural constituent of cytoskeleton, protein binding	U
PF14_0425	fructose-bisphosphate aldolase	fructose-bisphosphate aldolase activity	L
PF14_0439	M17 leucyl aminopeptidase	manganese ion binding	A
			T
			E
			D

Target candidates identified in both pull-down and microarray experiments are listed according to gene IDs. Protein characteristics are from PlasmoDB.org. Candidates of the microarray experiment which showed at least a 2-fold expression change at \geq one time point under treatment were used for analysis.

4.14 qPCR

Microarray results were validated by means of qPCR (Real-Time quantitative PCR) using the $\Delta\Delta C_T$ method. Primers were validated with regard to amplification efficiencies (detailed in appendix 6.2).

The $\Delta\Delta C_T$ method is used to determine the relative target (gene X) quantity in samples and is therefore an often used tool to validate data from microarray experiments.

Six randomly chosen genes of the microarray data set (two up-regulated, two down-regulated, two invariant at timepoint 3 = 4h) were compared (microarray vs. qPCR). For this method, amplification of these genes (here described for one gene X) and of the endogenous control (e.g. a housekeeping gene: HK, here: PFL0900c, arginyl-tRNA synthetase) in samples (treated with ACT-AM) and in a reference sample (untreated) were measured and normalized using the endogenous control. The relative quantity of the genes in every sample was determined by comparing normalized gene X quantity in

every sample to normalized gene X quantity in the reference sample. The amount of gene X (treated), relative to the reference (untreated) and normalized to the endogenous control (HK), is given by:

$$2^{-\Delta\Delta C_T} \text{ whereby}$$

$$\Delta\Delta C_T = \Delta C_{T, \text{ treated}} - \Delta C_{T, \text{ untreated}} =$$

$$(C_T \text{ of gene X, treated} - C_T \text{ of HK, treated}) - (C_T \text{ of gene X, untreated} - C_T \text{ of HK, untreated})$$

According to the validation, the qPCR results are comparable to those of the microarray experiment (Figure 4.18).

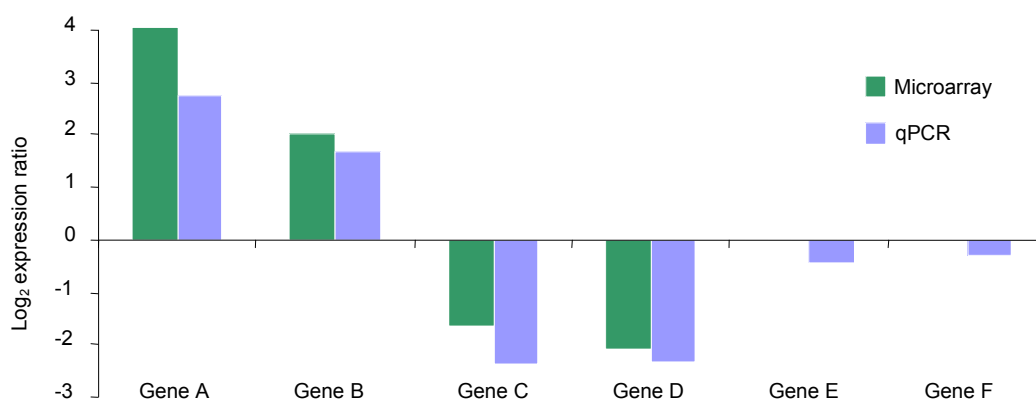


Figure 4.18. Validation of microarray data using qPCR. The fold change (treated with an IC_{90} of ACT-AM vs. untreated) is given by $2^{-\Delta\Delta C_T}$, $\Delta\Delta C_T = \Delta C_{T, \text{ treated}} - \Delta C_{T, \text{ untreated}} = (C_T \text{ of gene X, treated} - C_T \text{ of HK, treated}) - (C_T \text{ of gene X, untreated} - C_T \text{ of HK, untreated})$, HK: housekeeping gene: PFL0900c, arginyl-tRNA synthetase. Six randomly chosen genes of the microarray data set (two up-regulated, two down-regulated, two invariant at timepoint 3 = 4h) were investigated. Gene A: PFL0035c, acyl-CoA synthetase, PfACS7; gene B: PF10_0380, serine/threonine protein kinase, FIKK family; gene C: PF13_0196, MSP7-like protein; gene D: PF14_0545, thioredoxin, putative; gene E: PFA0310c, calcium-transporting ATPase; gene F: PFL1550w, lipoamide dehydrogenase. Bars represent one experiment (microarray) and the mean of $n = 3$ values (wells) of the same experiment (qPCR).

5 Discussion

5.1 *In vitro* activity of ACT-AM and derivatives

The investigated antimalarial lead compound, ACT-AM, showed an IC_{50} against erythrocytic *P. falciparum* in the low single-digit nanomolar range, a value that is comparable to those of the most efficacious registered drugs. Semisynthetic artemisinin derivatives, for instance, which are the base of highly potent and widely used combination therapies (reviewed by Fidock 2010), have similar *in vitro* activities. One example, artesunate, used as a reference drug for this thesis, had IC_{50} values between 1.8 and 7.1nM (determined for seven strains), whereas for ACT-AM, IC_{50} values between 0.4 and 3.8nM were measured (Tables 4.1 and 4.2). Even recently published very promising novel antimalarial pharmacophores have *in vitro* activities comparable to that of ACT-AM, with IC_{50} s in the range of 0.5 to 1.4nM for the spiroindolone NITD609 (Rottmann et al. 2010) and 2.8 to 3.4nM for the ozonide OZ439, respectively (Charman et al. 2011).

Artemisinin derivatives owe their clinical efficacy largely to their fast onset of action and activity against all three asexual blood stages of the parasite (reviewed by White 2008). *In vitro* these two key features are shared with ACT-AM as demonstrated measuring the time-, stage-, and concentration-dependent effect of the molecule on synchronous cultures of *P. falciparum* (Figure 4.1).

Since resistance to conventional malaria treatment is rapidly spreading (reviewed by Fidock 2010), novel lead compounds with antimalarial activity are routinely tested against drug resistant laboratory strains. ACT-AM proved to be highly active against seven tested strains *in vitro*, irrespective of their resistance properties.

Chemical modifications of pharmacophores can dramatically influence their activity (Dumas et al. 1999), therefore, all chemical probes used for the characterization of ACT-AM, were validated with regard to *in vitro* activity. Every applied probe i.e. compounds used for pull-down experiments or fluorescent imaging largely retained the activity of their precursor, suggesting that they still interacted with the same molecular structures of the parasite.

Furthermore, the enantiomer-specific *in vitro* activity of ACT-AM points towards an enantioselective and distinct target.

5.2 UV-activatable compounds

The decision to use photo-activatable capture compounds was a turning point in the project as it enabled the application of biochemical methods such as pull-downs, Far Western blotting, and fluorescent imaging which were not feasible with conventional non-UV-activatable chemical probes. The main advantage of UV-activatable compounds lies in their ability to covalently bind to interacting molecular structures upon activation (Lenz et al. 2010). This allows the use of harsh conditions in sample processing, such as SDS lysis or fixation without loss of the interaction. On the contrary, weaker interactions between compounds and their binding partners can easily be broken, as was presumably the case for earlier unsuccessful pull-down and fluorescent imaging studies using non-UV-activatable compounds. These probes have most likely lost contact to their targets after extensive washes or fixation with acetone/methanol.

The formation of a covalent bond between target and compound allows another crucial feature of UV-activatable molecules which is the ability to use living or partially (saponin) lysed cells. Working under physiological conditions offers the advantage that target structures are in their native conformation at the time of activation of the compound, i.e. prior to lysis of the parasite. This is in sharp contrast to conventional methods for which lysates are mostly prepared before incubation with chemical probes whereby target structures may lose their original conformation (see discussion of pull-down experiments).

Before being used in biochemical binding assays, the UV-activatable capture compound ACT-AM-UV was tested for its *in vitro* activity and pharmacodynamic properties. Not only did the compound largely retain the activity of the original antimalarial, it also showed a similar *in vitro* pharmacodynamic pattern and therefore was qualified for characterization studies. Moreover, using Far Western blot, fluorescent imaging and pull-

down experiments (see results section), it could be demonstrated that photo-activatable compounds are applicable for *P. falciparum* in a UV-dependant manner, dispelling the concern that UV-light might be unable to penetrate RBCs densely packed with hemoglobin (Hawkey et al. 1991). To my knowledge, this is the first time that this advantageous UV-dependent system has been implemented for *P. falciparum*- notably for living and partially (saponin) lysed cells.

5.3 Fluorescent imaging

Experiments using fluorescent probes were conducted to determine the intracellular localization of the site of action of the ACT-AM and to define which fraction of the parasite extract was to be used for pull-down experiments. Since pull-downs were eventually performed with methods based on photo-activation, compatible to lysis of the whole cell using SDS, the fractionation of lysates was omitted.

The applied fluorescent imaging methods were either direct, using a fluorescein-labeled derivative of ACT-AM, or indirect, using a UV-activatable derivative of ACT-AM followed by detection of the latter with a streptavidin conjugate.

With both methods, fluorescent signals were obtained for all investigated parasite stages (Figures 4.2 and 4.3) which was in line with the lead compound being effective against all asexual blood stages of the parasite. The signals mainly suggested a cytosolic distribution of the compound but fluorescence seemed to be detectable in membranous structures as well. Membrane localization of ACT-AM would be in agreement with the observation of several transporters in pull-down experiments.

Fluorescent imaging can shed some light on the site of action of a compound, but even using electron microscopy, it is difficult to draw conclusions about the MOA based on imaging techniques alone. More thorough imaging experiments aimed at target identification were therefore not undertaken.

5.4 Far Western blotting

Far Western blotting was largely applied to validate the use of UV-activatable compounds in *P. falciparum*.

It could be shown that the method was compound-, control- and UV-dependent. These findings were in accordance with the results of the fluorescent imaging studies and therefore encouraged the application of UV-activatable compounds for downstream experiments.

In order not to provoke unspecific signals and to maintain experimental conditions comparable to those of pull-down experiments, the concentration of ACT-AM-UV was kept low (approx. 2x IC₉₀). Probably due to the low compound concentrations, the limited loading capacity of the protein gel and the blotting procedure, the resulting signals were generally weak and not congruent with respective gel-patterns of pull-down experiments. These limiting factors of the method, in conjunction with the fact that proteins bound to blotting membranes are not suitable for mass spectrometry led to the omission of this technique for direct target identification studies.

5.5 Pull-down experiments

Pull-downs were performed employing a variety of systems with respect to chemical probes, controls, lysates and beads. Intriguingly, all significant results of pull-down experiments stem from methods using UV-activatable capture compounds, whereas attempts with conventional pull-down methods were not successful (sections 4.7 and 4.8). The main reason for this observation might be that target structures were in their native conformation at the time of interaction with ACT-AM-UV, whereas in the case of conventional techniques, cells have to be lysed before interactions can be studied. Especially complex structures with multiple membrane-spanning domains easily lose their native conformation after detergent-based lysis of membranes (Mancia & Love 2010). It is therefore plausible that the three identified interaction partners of ACT-AM, being complex transporters, were only identifiable using the UV-dependent approach.

Moreover, the covalent bond formed between UV-activatable compounds and their binding partners allows for harsh washing conditions thereby drastically reducing unspecific background, which is usually not feasible with conventional methods without losing target candidates.

5.5.1 Validation of target candidates

Numerous target candidates were identified using pull-down experiments (section 4.6). Eight target candidates could be tested *in vitro*, three of which were positive (probable interaction with ACT-AM) and five were negative (probably no interaction with ACT-AM). The three probable interaction partners are discussed below and in the MOA section:

MDR (multidrug resistance protein, PFE1150w)

It could be demonstrated that the *in vitro* susceptibility of *P. falciparum* to ACT-AM correlated with the gene copy number of *mdr* suggesting an interaction between the compound and the transporter (Tables 4.7 and 4.8). Notably, the effect of ACT-AM on MDR was studied using *P. falciparum*, offering a system much closer to natural conditions than e.g. heterologous expression in *E. coli*. The kind of interaction, however, cannot be determined with this system. Either ACT-AM is transported by MDR or the compound acts as an inhibitor of the transporter. A straight forward experiment addressing the question of how ACT-AM and MDR interact would involve *in vitro* transport studies. Sanchez and coworkers have established such an *in vitro* system based on MDR-expressing *Xenopus laevis* oocytes to measure the transport of several ³H-labeled antimalarials (Sanchez et al. 2008). By means of this system and radiolabeled ACT-AM, it would be feasible to

- A) Validate the *mdr* gene copy number-dependent results
- B) Demonstrate transport of ACT-AM
- C) Show inhibition (if MDR-activity decreases in an ACT-AM-dependent way without simultaneous transport of the compound)

D) Test the enantioselectivity of the protein

ENT4 (Equilibrative Nucleoside Transporter 4, PFA0160c)

Using *Xenopus laevis* oocytes, it was found that PfENT4-mediated transport of [³H]adenine decreased in an ACT-AM-concentration-dependent manner (Figure 4.8). The measured effect of the compound was more pronounced for PfENT4 than for PvENT4 (*P. vivax*), and no effect was observed for PfENT1 implying a specific interaction. As discussed above for MDR, the nature of interaction (transport or inhibition) between ACT-AM and ENT4, needs to be elucidated using a radiolabeled version of the compound.

Several limitations of the observed inhibition can be considered:

First, in this assay, both enantiomers of ACT-AM affected the transporter to a similar extent even though they differ in *in vitro* activity by a factor of about 50 (Table 4.1). It can be speculated that this clear difference in *in vitro* activity against the parasite should be reproducible when studying the isolated target. From this point of view, ENT4 could be deleted from the list of target candidates. On the other hand, it could still be that the enantiomer-specific activity of ACT-AM is caused by a mechanism upstream of the actual target, e.g. by an enantiomer-specific transporter which moves the compound to its enantiomer-unspecific site of action. Enantiomer-specific transporters are not uncommon; the proton-coupled folate transporter (PCFT) has been shown to stereoselectively transport methotrexate (ratio: L- / D-form: 40) in mammalian cells (Narawa & Itoh 2010).

A second limitation of the experimental system itself was the application of a synthetic gene that displayed optimized codons for *Xenopus laevis* expression, meaning that the studied transporter may differ from the genuine PfENT4.

Third, the concentrations of ACT-AM leading to a clearly reduced activity of the transporter were in the low micromolar range rather than the low nanomolar *in vitro* activity observed against the parasite (Figure 4.8 and Table 4.1). This observation does however not completely rule out ENT4 as a target of ACT-AM. A similar discrepancy

between on-target (in *Xenopus*) and *in vitro* growth assays was published for artemisinins against PfATP6 (introduction 1.2), in which case the authors concluded that the protein is the target of artemisinins (Eckstein-Ludwig et al. 2003).

The observed discrepancy could be explained in the following ways:

A) ENT4 is not the target but a transporter of ACT-AM.

B) The assay conditions in *Xenopus oocytes* differ from those of the *in vitro* growth assays, therefore the resulting activities may not be directly compared. The key differences between the two assays are (*Xenopus*- vs. *Plasmodium*-based system, respectively):

- Oocytes vs. parasites
- Time of exposure to compound (1h vs. 72h)
- Amount / concentration of the transporter (arbitrary vs. natural)
- Experimental temperature (16°C vs. 37°C)
- Recodoned sequence of the transporter (synthetic vs. natural, see above)

C) Artemisinins were demonstrated to be concentrated within the parasite by several hundred-fold (Gu et al. 1984). This might also be the case for ACT-AM leading to a lower apparent IC₅₀ against the parasite in contrast to the actual IC₅₀ against the isolated target.

D) The transporter might need other cell-derived co-factors in order to exhibit its proper function which might not be provided by *Xenopus oocytes*.

CRT (Chloroquine Resistance Transporter, MAL7P1.27)

As for ENT4, *in vitro* interactions of ACT-AM (and its enantiomer) with CRT were observed using *Xenopus oocytes* (Figure 4.9). Mainly therefore, essentially the same limitations as discussed for ENT4 (see above, 1, 2, and 3A-D) regarding experimental conditions and results also apply to CRT. An exception was the amino acid sequence of the investigated CRT which was cloned from the chloroquine-resistant *P. falciparum* strain Dd2 (Wellems et al. 1990) thereby differing in several codons from the actually identified one of the 3D7 strain (Gardner et al. 2002).

As the name implies, the transporter is associated with resistance (Fidock et al. 2000); especially therefore, it should be clarified if the type of interaction between ACT-AM and CRT is based on transport or on inhibition. This could again (see above) be studied with the same experimental *Xenopus*- setting using a radiolabeled version of the compound.

5.6 Microarray

In order to gain more information about the MOA of ACT-AM and, above all, potentially exclude several specific MOAs, the *in vitro* gene expression under treatment with ACT-AM was compared to previously established expression patterns induced by 20 different compounds with antimalarial activity (Hu et al. 2010). The comparison was based on the assumption that compounds with different MOAs induce different gene expression patterns.

The transcriptional response of *in vitro* treated 3D7 parasites to ACT-AM involved more than 550 differentially expressed genes, most of which were deregulated in a time-dependent manner (Figure 4.17). Functional enrichment analysis of deregulated genes has revealed an overrepresentation of several pathways (Figure 4.17.B). In the case of up-regulated genes, these pathways were mainly associated with synthesis and posttranslational modifications of proteins as well as lipid metabolism and kinase-dependent signaling. Down-regulation on the other hand was predominantly observed for several components of the merozoite invasion machinery, suggesting that the parasite holds the development of the late schizont under treatment with ACT-AM.

The actual comparison of ACT-AM to the other 20 antimalarial compounds revealed that ACT-AM very tightly clustered with generic protein kinase inhibitors (staurosporine and ML7), retinol A (a vitamin A alcohol interacting with membranes) and the serine protease inhibitor PMSF (Figure 4.17.D). Given that ACT-AM is exceptionally lipophilic (data not shown), the clustering with retinol A is noteworthy (see below). On the other hand, ACT-AM did not exhibit *in vitro* activity against several mammalian kinases in a commercial screen (data not shown) nor did the compound inhibit any of the investigated *P. falciparum* proteases [M17 leucyl aminopeptidase (Figure 4.11), plasmepsin 1, 2 and 4

(tested at Actelion, data not shown)]. Furthermore, apart from the above stated enzymes, there was no significant overlap between results of pull-down and microarray experiments with respect to kinases and proteases (Table 4.11), indicating that the similarity of the induced expression changes to that seen with inhibitors of kinases and proteases is most likely only due to downstream effects of the compound.

Remarkably, ACT-AM was not found in the same cluster as the antimalarials chloroquine, quinine and artemisinin (Figure 4.17.C and D). This result is of particular importance when it comes to choosing a potential partner drug for combination therapies. It should be noted that even though the experimental protocols of the compared microarray studies (ACT-AM vs. the 20 comparator molecules) were essentially the same, the individual experiments have been carried out in different laboratories at different times. This limitation should be considered when interpreting the comparisons of the studies and follow-up experiments confirming the effect of ACT-AM on the different pathways will therefore be required. Nevertheless, taking solely microarray data into account, it could be hypothesized that ACT-AM may interfere with parasite membranes, as proposed for retinol A (Hamzah et al. 2004) or through intracellular signaling similar to kinase inhibitors.

5.7 Mode of action

Knowing the mode of action of a molecule is of significant importance in drug development.

In general, if a novel molecule is to be combined with an existing drug, the combination partners should have different MOAs and not interfere with the MOA of the partner. This applies in particular to antimalarials, for which monotherapies ought to be avoided to prevent further spread of resistance (reviewed by White 1999). In addition, identification of the specific target of a substance could allow molecular modeling of novel compounds and, if assays using the purified target are feasible, direct structure activity relationship studies can be conducted *in vitro*. If the human counterpart of the target is testable *in*

in vitro as well, the selectivity of the compound can be determined, which enables an early estimation of side effects prior to clinical trials.

Furthermore, detailed knowledge about the MOA could facilitate the registration of a novel treatment, largely for the above stated reasons. Nevertheless, the definition of the exact MOA is not a prerequisite for registration of antimalarial drugs; there are various examples of antimalarials which were approved without knowledge of their targets (see introduction).

The results of this thesis contribute to the formation of several hypotheses of how ACT-AM might exert its action and to the exclusion of a number of known MOAs:

5.7.1 MOA of ACT-AM: Hypotheses

Pull-down experiments with UV-activatable derivatives of ACT-AM revealed three binding partners which were shown to interact with the original lead compound *in vitro* (results section 4.10). Hypotheses of how these target candidates might be involved in the MOA of ACT-AM are discussed below.

MDR (multidrug resistance protein, PFE1150w)

MDR consists of 12 transmembrane domains, is predominantly located at the membrane of the digestive vacuole and partially present at the parasite plasma membrane (Cowman et al. 1991; Sanchez et al. 2007).

The identification of MDR via pull-down experiments has two opposing implications: MDR could either represents a target of ACT-AM or confer resistance to the compound.

The target hypothesis is favored by the observation that the transporter is probably essential (Sidhu et al. 2005). The natural function of MDR in *P. falciparum* remains elusive but MDRs are well known from cancer cells and microorganisms, in which contexts they have been shown to actively expel chemotherapeutic agents (Higgins 2007). In any case, MDRs seem to enable their organisms to dispose of harmful

substances, i.e. to detoxify themselves. Compounds interfering with this process could thus be detrimental. A current example making use of a similar mechanism is the registered drug bortezomib which leads to proteotoxic stress within cancer cells by inhibiting the abolishment of misfolded or damaged proteins (Neznanov et al. 2009).

MDR has been associated with resistance to several antimalarials such as quinine and mefloquine (Wilson et al. 1993; Cowman et al. 1994; Sidhu et al. 2006). ACT-AM probably interacting with the transporter might therefore suggest as well that the compound is prone to resistance development. This possibility needs to be carefully investigated (see outlook).

ENT4 (Equilibrative Nucleoside Transporter 4, PFA0160c)

According to PlasmoDB.org, ENT4 is predicted to have 11 transmembrane domains; apart from that, very little has been published about the structure or localization of the transporter. It is however known that *P. falciparum* cannot synthesize purines including adenosine, hypoxanthine and inosine *de novo* (Baldwin et al. 2007). The parasite thus depends on salvage of these essential nutrients from its host (reviewed by de Koning et al. 2005). Purine salvage is thought to be mediated by transporters such as ENTs, which makes them promising and often cited potential drug targets (Parker et al. 2000; Baldwin et al. 2007). In this light, it might be that ACT-AM interferes with purine salvage via ENT4, however, since it is not proven if the transporter is essential in the first place, this hypothesis is very speculative and needs further validation.

CRT (Chloroquine Resistance Transporter, MAL7P1.27)

CRT has 10 predicted transmembrane domains and was shown to localize to the digestive vacuole of the parasite (Fidock et al. 2000).

The transporter confers resistance to chloroquine and the failure to create CRT knockout strains implies that the protein is essential for parasite survival (Fidock et al. 2000; Sanchez et al. 2008). The essential function of CRT is not completely understood but is thought to involve the transport of ions and amino acids or peptides across the digestive

vacuole membrane (Zhang et al. 2002; Martin & Kirk 2004; Zhang et al. 2004). Whatever the natural role of CRT turns out to be, if it truly is essential, ACT-AM might be targeting it.

As discussed for MDR (see above), the interaction of ACT-AM with CRT might also indicate a tendency towards resistance development of the compound, which needs to be carefully addressed.

It is striking that all three positively tested target candidates are transporters. This prompts the hypothesis that ACT-AM has a general affinity to transporters of *P. falciparum* and that the actual target is a transporter. It is therefore possible that the target is either one of the three tested transporters or can be found among the not yet tested / not yet testable transporter candidates (results section). Moreover, one could postulate that only the inhibition of more than one of the three discussed transporters is sufficient to kill the parasite. Nevertheless, it can as well be speculated that the three mentioned transporters are merely indirectly involved in the MOA of ACT-AM e.g. transporting the compound to its site of action, suggesting that the actual target still remains to be identified.

5.7.2 Exclusion of published MOAs

First, ACT-AM most likely has a mode of action distinct from that of stage-specific antimalarials because it is effective against all three asexual blood stages of the parasite. Examples of stage-specific antimalarials are Pyrimethamine (Dieckmann & Jung 1986; Maerki et al. 2006) or the novel spiroindolone NITD609 (Rottmann et al. 2010).

Second, according to hemozoin interaction experiments, ACT-AM does not interfere with the formation of beta-hemozoin *in vitro*, which is in contrast to chloroquine, mefloquine and other molecules of the quinoline class (Egan 2006).

Microarray studies offered a third way to exclude MOAs of other compounds with antimalarial activity, since ACT-AM seemed to induce an expression pattern distinct from previously assessed molecules (Hu et al. 2010). MOAs which can probably be

excluded on the basis of the microarray data are associated with e.g. inhibitors of phosphatases, inhibitors of microtubule polymerization and importantly quinine, chloroquine and artemisinin (Figure 4.17).

In addition, several distinct target candidates can be excluded based on negative *in vitro* inhibition assays, namely fructose-bisphosphate aldolase, M17 leucyl aminopeptidase, spermidine synthase, S-adenosylmethionine synthetase, and secreted acid phosphatase (Figures 4.11-4.14, respectively).

5.8 Outlook

Most of the following experiments are planned for the near future or are already ongoing.

MOA studies

- Interaction between MDR and ACT-AM was demonstrated in an *mdr* gene copy number-dependent assay and should be validated by means of MDR-expressing *Xenopus laevis* oocytes.
- It is crucial to experimentally define the nature of interaction (inhibition vs. transport) between ACT-AM and the three transporters MDR, ENT4 and CRT. This could ideally be addressed using radiolabeled ACT-AM for *Xenopus*- based transporter studies.
- Interaction of ACT-AM with MDR and CRT raises concerns about resistance development. It is therefore critical to assess the ability of *P. falciparum* to develop resistance against ACT-AM which can be performed by continuously applying sub-lethal concentrations of the compound to *in vitro* cultures of the parasite (Jiang et al. 2008).

- Numerous target candidates were identified using pull-down experiments and are listed in the results section. Some of the candidates have been successfully tested, others were not testable or even unknown. The candidate lists ought to be carefully reassessed with regard to probability of interaction with ACT-AM and feasibility of *in vitro* assays.

- Microarray: MOAs associated with compounds which have induced gene expression patterns similar to that of ACT-AM should be considered for further investigations. An interesting example would be the MOA of retinol A, since both ACT-AM and retinol A are highly lipophilic and show expression patterns which cluster closely.

- In order to reduce the complexity of lysates i.e. of putative binding partners of ACT-AM, pull-down experiments using UV-activatable compounds should be repeated with highly synchronized parasites. It is noteworthy that this has already been attempted using synchronized rings. Unfortunately, competition with an excess of ACT-AM led to a drastic growth reduction of the negative control. The resulting difference in amount of proteins (sample vs. negative control) did not allow for an unbiased comparison of protein band intensities after gel electrophoresis (data not shown). Therefore, similar experiments should be conducted using later stages of synchronized parasites as the difference in biomass (sample vs. negative control) might turn out to be less pronounced in the latter case.

Fluorescent imaging

To provide a more detailed view of the site of action of ACT-AM, colocalization studies using ACT-AM-UV and e.g. cytosolic or membrane markers such as GAPDH (Daubenberger et al. 2003) or MDR (Cowman et al. 1991), respectively should be conducted. Especially to dissect signals from membranous structures, confocal or electron microscopy using ACT-AM-UV should be performed in addition.

Far Western blotting

Signals obtained from Far Western blots using UV-activatable compounds were relatively weak. This might partly be explained by the low concentration of ACT-AM-UV and the limited capacity of the protein gels. Since increasing the concentration of the compound could result in more unspecific signals, a way of obtaining stronger signals per gel might be to pool several lysate samples which can be concentrated using a vacuum centrifuge or protein precipitation techniques.

5.9 Conclusion

The purpose of this thesis was the characterization of a novel antimalarial lead compound with respect to MOA and *in vitro* properties.

This molecule, ACT-AM, which was discovered in a collaboration between Actelion Pharmaceuticals Ltd and the Swiss TPH was shown to display promising *in vitro* activity. First, ACT-AM inhibited erythrocytic *P. falciparum* growth at low nanomolar concentrations. Second, the compound was effective against a panel of drug resistant strains and third, equally affected all asexual blood stages of the parasite with a fast onset of action. These *in vitro* qualities are similar to those of artemisinins, the most potent currently used antimalarials. In addition, the results of this thesis indicate that ACT-AM has an MOA which differs from that of known antimalarial drugs.

MOA studies involved pull-down methods aimed at directly identifying molecular targets and techniques such as microarray and hematin interaction studies to exclude MOAs of existing antimalarials. Through pull-down experiments, more than 50 target candidates were revealed. Three of these candidates were shown to interact with ACT-AM *in vitro*: MDR (multidrug resistance protein), ENT4 (equilibrative nucleoside transporter 4) and CRT (chloroquine resistance transporter). The nature of interaction (inhibition vs. transport) between ACT-AM and these transporters remains unknown and will need to be characterized in the future, ideally using radiolabeled ACT-AM for experiments in *Xenopus laevis* oocytes.

MOAs related to several antimalarial compounds and registered drugs including chloroquine, quinine, and artemisinin can probably be ruled out based on differences in gene expression patterns and hemozoin interaction studies. This is of particular importance for potential combination therapies. Given that ACT-AM seems to have an MOA distinct from artemisinins but shares properties of these peroxides i.e. fast onset of action and activity against all asexual blood stages, ACT-AM or analogues could be substitutes of this class of drugs threatened by resistance development.

Taken together, the results described in this thesis suggest that ACT-AM has promising *in vitro* activity and is likely to have a novel mode of action against *P. falciparum*. The findings therefore warrant further efforts to explore the potential of ACT-AM or other molecules of the same chemical class as therapeutic agents for the treatment of malaria.

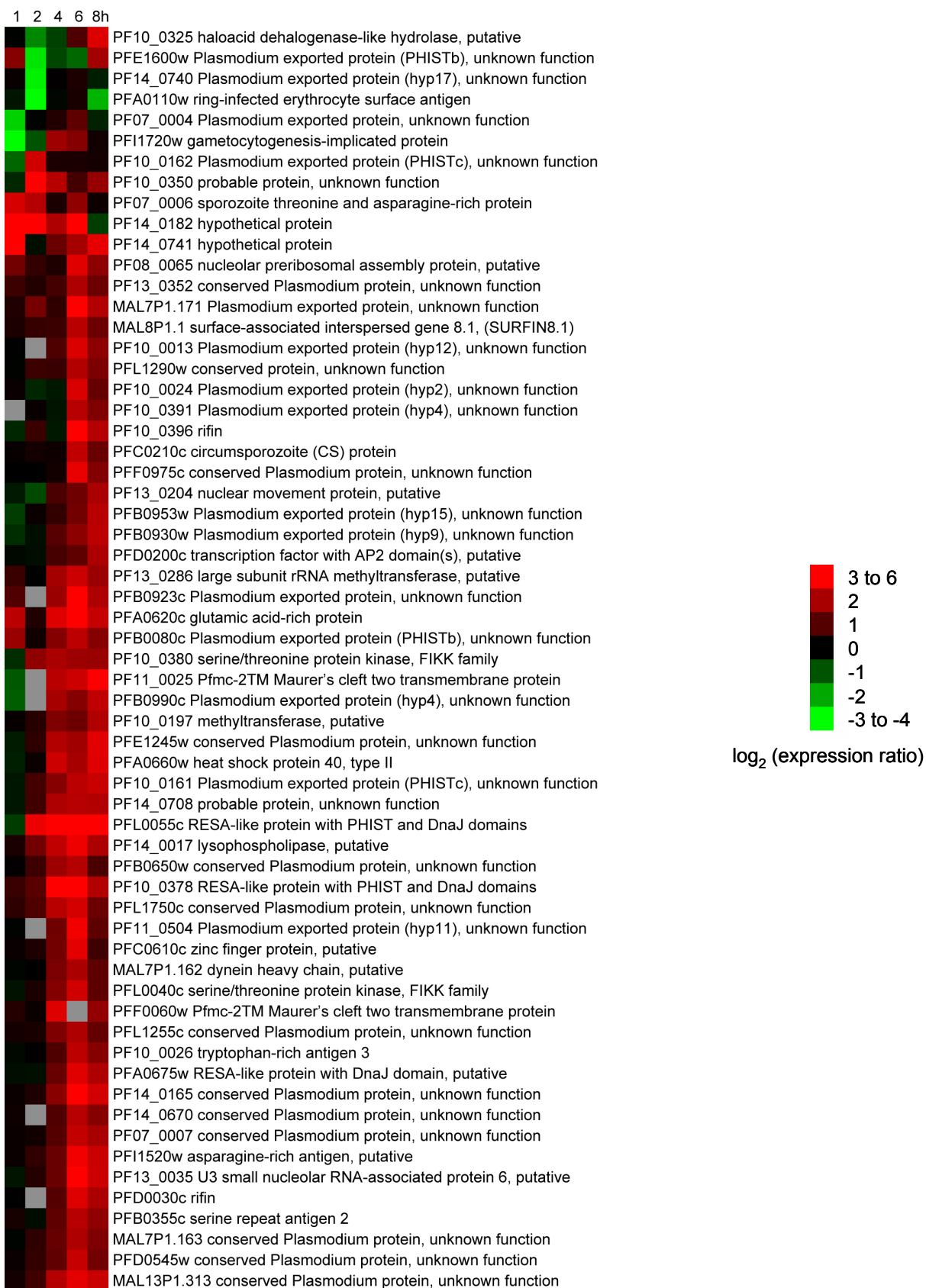
6 Appendix

6.1 Microarray

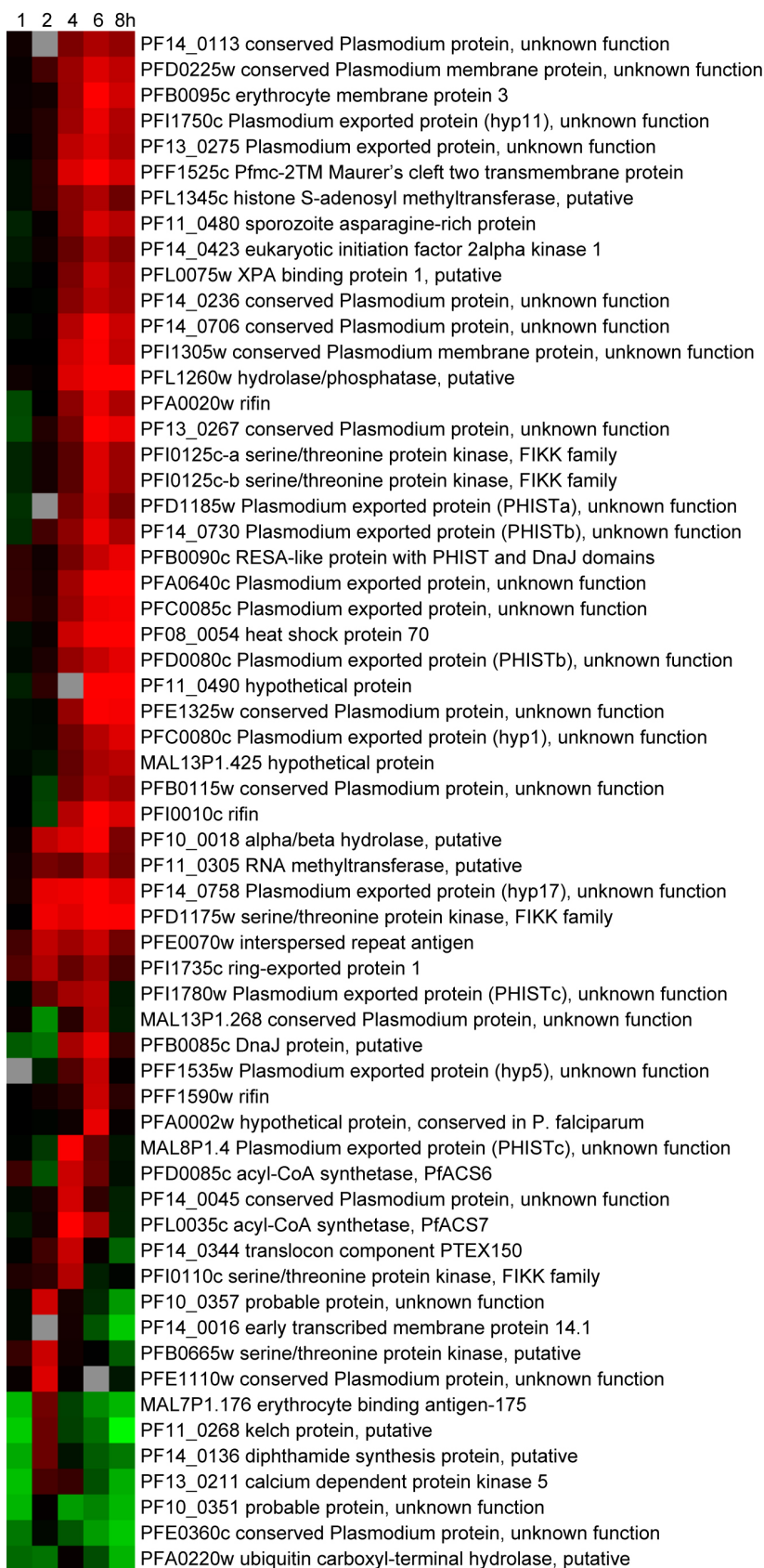
The transcriptional response of *P. falciparum* 3D7 parasites to ACT-AM involved 1299 differentially expressed genes (expression altered by at least two-fold at \geq one time point, max. one of five time point values missing). Of these 1299 genes, 874 were up- and 350 down-regulated. Genes were considered up-regulated if up-regulation (at least two-fold) was observed for at least one time point and if no down-regulation was observed at all; the opposite applied for genes considered down-regulated. For the remaining 75 genes, both up-and down-regulation was observed at different time points.

In Figure 6.1, 165 genes with a four or greater fold expression change (treated vs. untreated) at \geq one time point are shown. Up-regulated, down-regulated, and both up-and down-regulated at different timepoints were 101, 36, and 28 genes, respectively. Up-and down-regulation was defined as described in the above paragraph, except for the four or greater fold expression change criterion.

Appendix



Appendix



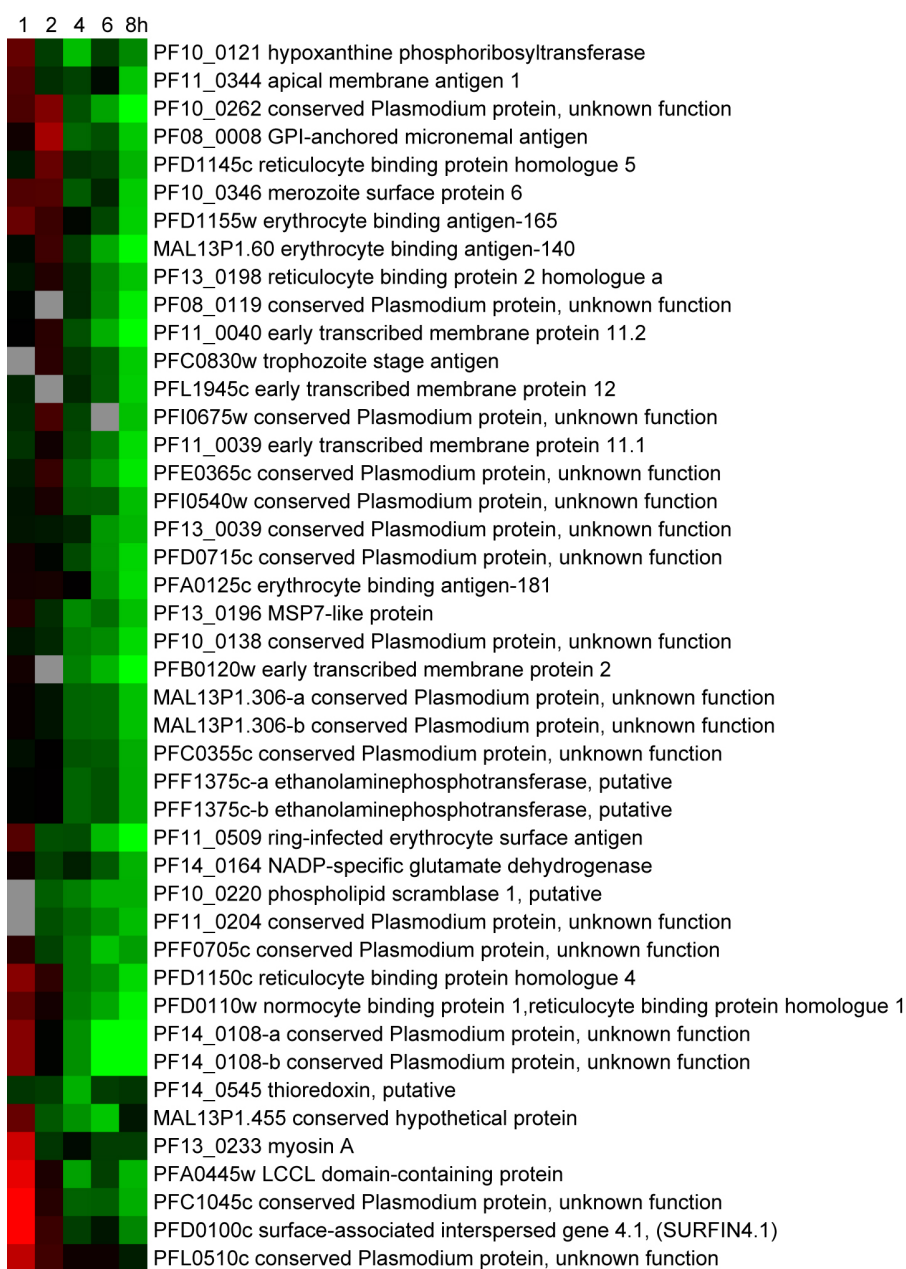


Figure 6.1. Transcriptional response of *P. falciparum* 3D7 to ACT-AM. Highly synchronized parasites were treated with ACT-AM (IC₉₀) and control samples with the respective amount of DMSO. RNA was collected after 1, 2, 4, 6 and 8h of treatment. Genes with a four or greater fold expression change (treated vs. untreated) at \geq one time point are shown. Grey: No signal. Hybridization was performed in the laboratory of Zbynek Bozdech in Singapore.

6.2 qPCR: Primer validation

Primers can only be used for the qPCR $\Delta\Delta C_T$ method if their amplification efficiencies are comparable.

To validate primers, C_T values were determined with DNA templates spanning 5 logs (base 10) for every gene. ΔC_T values [C_T of target gene – C_T of endogenous control (PFL0900c, arginyl-tRNA synthetase)] were calculated for every log of template amount. According to the manufacturer of the qPCR system (Applied Biosystems) the absolute value of the slope of the resulting graph (ΔC_T vs. log of template amount) should not exceed 0.1 which was shown for all used genes (Table 6.2).

Table 6.2. Validation of primers used for qPCR.

Primer	Gene ID Product description	Absolute value of slope (ΔC_T vs. log of template amount)
PFL0035c	acyl-CoA synthetase, PfACS7	0.02
PF10_0380	serine/threonine protein kinase, FIKK family	0.04
PF13_0196	MSP7-like protein	0.001
PF14_0545	thioredoxin, putative	0.01
PFA0310c	calcium-transporting ATPase	0.05
PFL1550w	lipoamide dehydrogenase	0.03
PFL0900c	arginyl-tRNA synthetase, adapted from Frank et al. 2006	N.A.

Primers for qPCR were validated using the absolute value of the slope of the graph ΔC_T vs. log10 of template amount. Values below 0.1 were acceptable. $\Delta C_T = [C_T \text{ of target gene} - C_T \text{ of endogenous control (PFL0900c, arginyl-tRNA synthetase)}]$.

7 References

- Baldwin, Stephen A et al., 2007. Nucleoside transport as a potential target for chemotherapy in malaria. *Current Pharmaceutical Design*, 13(6), pp.569-580.
- Baruch, D I, 1999. Adhesive receptors on malaria-parasitized red cells. *Baillière's Best Practice & Research. Clinical Haematology*, 12(4), pp.747-761.
- Bosch, J. et al., 2007. Aldolase provides an unusual binding site for thrombospondin-related anonymous protein in the invasion machinery of the malaria parasite. *Proceedings of the National Academy of Sciences*, 104(17), pp.7015 -7020.
- Boss, C et al., 2003. Inhibitors of the Plasmodium falciparum parasite aspartic protease plasmepsin II as potential antimalarial agents. *Current Medicinal Chemistry*, 10(11), pp.883-907.
- Burr, W., 2011. WHO to develop plan to curb artemisinin resistance. *CMAJ*, 183(2), pp.E81-82.
- Charman, S.A. et al., 2011. Synthetic ozonide drug candidate OZ439 offers new hope for a single-dose cure of uncomplicated malaria. *Proceedings of the National Academy of Sciences of the United States of America*. Available at:
- Chen, P.Q. et al., 1994. The infectivity of gametocytes of Plasmodium falciparum from patients treated with artemisinin. *Chinese Medical Journal*, 107(9), pp.709-711.
- Ciak, J. & Hahn, F.E., 1966. Chloroquine: mode of action. *Science (New York, N.Y.)*, 151(708), pp.347-349.
- Corminboeuf, O. et al., 2006. Inhibitors of Plasmepsin II-potential antimalarial agents. *Bioorganic & Medicinal Chemistry Letters*, 16(24), pp.6194-6199.
- Cowman, A F, Galatis, D. & Thompson, J.K., 1994. Selection for mefloquine resistance in Plasmodium falciparum is linked to amplification of the pfmdr1 gene and cross-resistance to halofantrine and quinine. *Proceedings of the National Academy of Sciences of the United States of America*, 91(3), pp.1143-1147.
- Cowman, A F et al., 1991. A P-glycoprotein homologue of Plasmodium falciparum is localized on the digestive vacuole. *The Journal of Cell Biology*, 113(5), pp.1033-1042.
- Cowman, Alan F & Crabb, B.S., 2006. Invasion of red blood cells by malaria parasites. *Cell*, 124(4), pp.755-766.

- Crompton, P.D., Pierce, S.K. & Miller, L.H., 2010. Advances and challenges in malaria vaccine development. , 120(12), pp.4168-4178.
- Cunha-Rodrigues, M. et al., 2006. Antimalarial drugs - host targets (re)visited. *Biotechnology Journal*, 1(3), pp.321-332.
- Dahl, E.L. & Rosenthal, P.J., 2008. Apicoplast translation, transcription and genome replication: targets for antimalarial antibiotics. *Trends in Parasitology*, 24(6), pp.279-284.
- Das Gupta, R., 2005. Polyamine in Plasmodium falciparum (Welch, 1897): Einfluss von Inhibitoren der Syntheseenzyme auf Polyamingehalt und Wachstum. *PhD Thesis*, p.61.
- Daubenberger, C.A. et al., 2003. The N⁷-terminal domain of glyceraldehyde-3-phosphate dehydrogenase of the apicomplexan Plasmodium falciparum mediates GTPase Rab2-dependent recruitment to membranes. *Biological Chemistry*, 384(8), pp.1227-1237.
- Desjardins, R.E. et al., 1979. Quantitative assessment of antimalarial activity in vitro by a semiautomated microdilution technique. *Antimicrobial Agents and Chemotherapy*, 16(6), pp.710-718.
- Dieckmann, A. & Jung, A., 1986. Stage-specific sensitivity of Plasmodium falciparum to antifolates. *Zeitschrift Für Parasitenkunde (Berlin, Germany)*, 72(5), pp.591-594.
- Ding, X.C., Beck, H.-P. & Raso, G., 2011. Plasmodium sensitivity to artemisinins: magic bullets hit elusive targets. *Trends in Parasitology*, 27(2), pp.73-81.
- Döbeli, H. et al., 1990. Expression, purification, biochemical characterization and inhibition of recombinant Plasmodium falciparum aldolase. *Molecular and Biochemical Parasitology*, 41(2), pp.259-268.
- Dondorp, A.M. et al., 2009. Artemisinin resistance in Plasmodium falciparum malaria. *The New England Journal of Medicine*, 361(5), pp.455-467.
- Dondorp, A.M. et al., 2010. Artemisinin resistance: current status and scenarios for containment. *Nat Rev Micro*, 8(4), pp.272-280.
- Dorn, A et al., 1995. Malarial haemozoin/beta-haematin supports haem polymerization in the absence of protein. *Nature*, 374(6519), pp.269-271.
- Downie, M.J. et al., 2006. Transport of nucleosides across the Plasmodium falciparum parasite plasma membrane has characteristics of PfENT1. *Molecular Microbiology*, 60(3), pp.738-748.
- Dufe, V.T. et al., 2007. Crystal Structure of Plasmodium falciparum Spermidine Synthase in Complex with the Substrate Decarboxylated S-adenosylmethionine and the

- Potent Inhibitors 4MCHA and AdoDATO. *Journal of Molecular Biology*, 373(1), pp.167-177.
- Dumas, J. et al., 1999. Synthesis and structure activity relationships of novel small molecule cathepsin D inhibitors. *Bioorganic & Medicinal Chemistry Letters*, 9(17), pp.2573-2578.
- Eckstein-Ludwig, U. et al., 2003. Artemisinins target the SERCA of Plasmodium falciparum. *Nature*, 424(6951), pp.957-961.
- Egan, T J, Ross, D.C. & Adams, P.A., 1994. Quinoline anti-malarial drugs inhibit spontaneous formation of beta-haematin (malaria pigment). *FEBS Letters*, 352(1), pp.54-57.
- Egan, Timothy J, 2006. Interactions of quinoline antimalarials with hematin in solution. *Journal of Inorganic Biochemistry*, 100(5-6), pp.916-926.
- Egan, Timothy J et al., 2002. Fate of haem iron in the malaria parasite Plasmodium falciparum. *The Biochemical Journal*, 365(Pt 2), pp.343-347.
- Egan, Timothy J & Ncokazi, K.K., 2004. Effects of solvent composition and ionic strength on the interaction of quinoline antimalarials with ferriprotoporphyrin IX. *Journal of Inorganic Biochemistry*, 98(1), pp.144-152.
- van Eijk, A.M. & Terlouw, D.J., 2011. Azithromycin for treating uncomplicated malaria. *Cochrane Database of Systematic Reviews (Online)*, 2, p.CD006688.
- Eisen, M.B. et al., 1998. Cluster analysis and display of genome-wide expression patterns. *Proceedings of the National Academy of Sciences of the United States of America*, 95(25), pp.14863-14868.
- Elmendorf, H.G. & Haldar, K., 1993. Identification and localization of ERD2 in the malaria parasite Plasmodium falciparum: separation from sites of sphingomyelin synthesis and implications for organization of the Golgi. *The EMBO Journal*, 12(12), pp.4763-4773.
- Eng, J.K., McCormack, A.L. & Yates III, J.R., 1994. An approach to correlate tandem mass spectral data of peptides with amino acid sequences in a protein database. *Journal of the American Society for Mass Spectrometry*, 5(11), pp.976-989.
- Enserink, M., 2010. Malaria's drug miracle in danger. *Science (New York, N.Y.)*, 328(5980), pp.844-846.
- Feachem, R.G. et al., 2010. Shrinking the malaria map: progress and prospects. *The Lancet*, 376(9752), pp.1566-1578.

- Ferone, R., Burchall, J.J. & Hitchings, G.H., 1969. Plasmodium berghei dihydrofolate reductase. Isolation, properties, and inhibition by antifolates. *Molecular Pharmacology*, 5(1), pp.49-59.
- Fidock, D A et al., 2000. Mutations in the P. falciparum digestive vacuole transmembrane protein PfCRT and evidence for their role in chloroquine resistance. *Molecular Cell*, 6(4), pp.861-871.
- Fidock, David A, 2010. Drug discovery: Priming the antimalarial pipeline. *Nature*, 465(7296), pp.297-298.
- Frank, M. et al., 2006. Strict Pairing of var Promoters and Introns Is Required for var Gene Silencing in the Malaria Parasite Plasmodium falciparum. *Journal of Biological Chemistry*, 281(15), pp.9942 -9952.
- Fry, M. & Beesley, J.E., 1991. Mitochondria of mammalian Plasmodium spp. *Parasitology*, 102 Pt 1, pp.17-26.
- Fry, M. & Pudney, M., 1992. Site of action of the antimalarial hydroxynaphthoquinone, 2-[trans-4-(4'-chlorophenyl) cyclohexyl]-3-hydroxy-1,4-naphthoquinone (566C80). *Biochemical Pharmacology*, 43(7), pp.1545-1553.
- Gamo, F.-J. et al., 2010. Thousands of chemical starting points for antimalarial lead identification. *Nature*, 465(7296), pp.305-310.
- Gardner, M.J. et al., 2002. Genome sequence of the human malaria parasite Plasmodium falciparum. *Nature*, 419(6906), pp.498-511.
- van Geertruyden, J.-P. et al., 2004. The contribution of malaria in pregnancy to perinatal mortality. *The American Journal of Tropical Medicine and Hygiene*, 71(2 Suppl), pp.35-40.
- Gu, H.M., Warhurst, D.C. & Peters, W., 1984. Uptake of [3H] dihydroartemisinin by erythrocytes infected with Plasmodium falciparum in vitro. *Transactions of the Royal Society of Tropical Medicine and Hygiene*, 78(2), pp.265-270.
- Guiguemde, W.A. et al., 2010. Chemical genetics of Plasmodium falciparum. *Nature*, 465(7296), pp.311-315.
- Haider, N. et al., 2005. The spermidine synthase of the malaria parasite Plasmodium falciparum: Molecular and biochemical characterisation of the polyamine synthesis enzyme. *Molecular and Biochemical Parasitology*, 142(2), pp.224-236.
- Hamzah, J. et al., 2004. Characterization of the effect of retinol on Plasmodium falciparum in vitro. *Experimental Parasitology*, 107(3-4), pp.136-144.
- Harayama, H., Muroga, M. & Miyake, M., 2004. A cyclic adenosine 3',5'-monophosphate-induced tyrosine phosphorylation of Syk protein tyrosine kinase

- in the flagella of boar spermatozoa. *Molecular Reproduction and Development*, 69(4), pp.436-447.
- Hawkey, C.M. et al., 1991. Erythrocyte size, number and haemoglobin content in vertebrates. *British Journal of Haematology*, 77(3), pp.392-397.
- Higgins, C.F., 2007. Multiple molecular mechanisms for multidrug resistance transporters. *Nature*, 446(7137), pp.749-757.
- Hofer, S. et al., 2008. In vitro assessment of the pharmacodynamic properties of DB75, piperazine, OZ277 and OZ401 in cultures of *Plasmodium falciparum*. *The Journal of Antimicrobial Chemotherapy*, 62(5), pp.1061-1064.
- Hu, G. et al., 2010. Transcriptional profiling of growth perturbations of the human malaria parasite *Plasmodium falciparum*. *Nature Biotechnology*, 28(1), pp.91-98.
- Hu, G. et al., 2007. Selection of long oligonucleotides for gene expression microarrays using weighted rank-sum strategy. *BMC Bioinformatics*, 8, p.350.
- Huber, W. & Koella, J.C., 1993. A comparison of three methods of estimating EC50 in studies of drug resistance of malaria parasites. *Acta Tropica*, 55(4), pp.257-261.
- Hudson, A.T., 1993. Atovaquone - a novel broad-spectrum anti-infective drug. *Parasitology Today (Personal Ed.)*, 9(2), pp.66-68.
- Jiang, H. et al., 2008. Genome-Wide Compensatory Changes Accompany Drug- Selected Mutations in the *Plasmodium falciparum* crt Gene. *PLoS ONE*, 3(6), p.e2484.
- Kappe, S.H.I. et al., 2010. That Was Then But This Is Now: Malaria Research in the Time of an Eradication Agenda. *Science*, 328(5980), pp.862 -866.
- Karaman, M.W. et al., 2008. A quantitative analysis of kinase inhibitor selectivity. *Nat Biotech*, 26(1), pp.127-132.
- de Koning, H.P., Bridges, D.J. & Burchmore, R.J.S., 2005. Purine and pyrimidine transport in pathogenic protozoa: from biology to therapy. *FEMS Microbiology Reviews*, 29(5), pp.987-1020.
- Korsinczky, M. et al., 2000. Mutations in *Plasmodium falciparum* Cytochrome b That Are Associated with Atovaquone Resistance Are Located at a Putative Drug-Binding Site. *Antimicrobial Agents and Chemotherapy*, 44(8), pp.2100-2108.
- Kubo, M. & Hostetler, K.Y., 1985. Mechanism of cationic amphiphilic drug inhibition of purified lysosomal phospholipase A1. *Biochemistry*, 24(23), pp.6515-6520.
- ter Kuile, F. et al., 1993. *Plasmodium falciparum*: in vitro studies of the pharmacodynamic properties of drugs used for the treatment of severe malaria. *Experimental Parasitology*, 76(1), pp.85-95.

- Lambros, C. & Vanderberg, J P, 1979. Synchronization of Plasmodium falciparum erythrocytic stages in culture. *The Journal of Parasitology*, 65(3), pp.418-420.
- Lau, Y.S. & Gnegy, M.E., 1982. Chronic haloperidol treatment increased calcium-dependent phosphorylation in rat striatum. *Life Sciences*, 30(1), pp.21-28.
- Laveran, 1880. Note sur un nouveau parasite trouvé dans le sang de plusieurs malades atteints de fièvre palustres. *Bull Acad Med*, 9, pp.1235-1236.
- Laxminarayan, R. et al., 2010. Should new antimalarial drugs be subsidized? *Journal of Health Economics*, 29(3), pp.445-456.
- Lenz, T. et al., 2010. Profiling of methyltransferases and other S-adenosyl-L-homocysteine-binding Proteins by Capture Compound Mass Spectrometry (CCMS). *Journal of Visualized Experiments: JoVE*, (46). Available at:
- Looareesuwan, S. et al., 1996. Clinical studies of atovaquone, alone or in combination with other antimalarial drugs, for treatment of acute uncomplicated malaria in Thailand. *The American Journal of Tropical Medicine and Hygiene*, 54(1), pp.62-66.
- Ma, C., Cummings, C. & Liu, X.J., 2003. Biphasic Activation of Aurora-A Kinase during the Meiosis I- Meiosis II Transition in Xenopus Oocytes. *Molecular and Cellular Biology*, 23(5), pp.1703-1716.
- Maerki, S. et al., 2006. In vitro assessment of the pharmacodynamic properties and the partitioning of OZ277/RBx-11160 in cultures of Plasmodium falciparum. *The Journal of Antimicrobial Chemotherapy*, 58(1), pp.52-58.
- Mancia, F. & Love, J., 2010. High-throughput expression and purification of membrane proteins. *Journal of Structural Biology*, 172(1), pp.85-93.
- Margolis, R.L. & Wilson, L., 1977. Addition of colchicine-tubulin complex to microtubule ends: The mechanism of substoichiometric colchicine poisoning. *Proceedings of the National Academy of Sciences of the United States of America*, 74(8), pp.3466-3470.
- Martin, R.E. & Kirk, K., 2004. The malaria parasite's chloroquine resistance transporter is a member of the drug/metabolite transporter superfamily. *Molecular Biology and Evolution*, 21(10), pp.1938-1949.
- Martin, R.E. et al., 2009. Chloroquine transport via the malaria parasite's chloroquine resistance transporter. *Science (New York, N.Y.)*, 325(5948), pp.1680-1682.
- McGregor, I.A., 1974. Mechanisms of acquired immunity and epidemiological patterns of antibody responses in malaria in man. *Bulletin of the World Health Organization*, 50(3-4), pp.259-266.

- McLaughlin, N.P. & Evans, P., 2010. Dihydroxylation of Vinyl Sulfones: Stereoselective Synthesis of (+)- and (-)-Febrifugine and Halofuginone. *The Journal of Organic Chemistry*, 75(2), pp.518-521.
- Meshnick, S R, Taylor, T.E. & Kamchonwongpaisan, S., 1996. Artemisinin and the antimalarial endoperoxides: from herbal remedy to targeted chemotherapy. *Microbiological Reviews*, 60(2), pp.301-315.
- Meshnick, Steven R, 2002. Artemisinin: mechanisms of action, resistance and toxicity. *International Journal for Parasitology*, 32(13), pp.1655-1660.
- Miller, L.H. et al., 2002. The pathogenic basis of malaria. *Nature*, 415(6872), pp.673-679.
- Mita, T., Tanabe, K. & Kita, K., 2009. Spread and evolution of Plasmodium falciparum drug resistance. *Parasitology International*, 58(3), pp.201-209.
- MMV, 2008. Compound Progression Criteria – August 2008, Medicines for Malaria Venture, Geneva. Available at: http://www.mmv.org/sites/default/files/uploads/docs/essential_info_for_scientists/Compound_progression_criteria.pdf.
- MMV, 2011. Science Portfolio, Medicines for Malaria Venture, Geneva. Available at: <http://www.mmv.org/research-development/science-portfolio>.
- Mota, M.M. et al., 2001. Migration of Plasmodium Sporozoites Through Cells Before Infection. *Science*, 291(5501), pp.141 -144.
- Müller, I.B. et al., 2010. Secretion of an acid phosphatase provides a possible mechanism to acquire host nutrients by Plasmodium falciparum. *Cellular Microbiology*, 12(5), pp.677-691.
- Narawa, T. & Itoh, T., 2010. Stereoselective transport of amethopterin enantiomers by the proton-coupled folate transporter. *Drug Metabolism and Pharmacokinetics*, 25(3), pp.283-289.
- Ncokazi, K.K. & Egan, Timothy J, 2005. A colorimetric high-throughput beta-hematin inhibition screening assay for use in the search for antimalarial compounds. *Analytical Biochemistry*, 338(2), pp.306-319.
- Neznanov, N. et al., 2009. Anti-malaria drug blocks proteotoxic stress response: anti-cancer implications. *Cell Cycle (Georgetown, Tex.)*, 8(23), pp.3960-3970.
- Okie, S., 2008. A new attack on malaria. *The New England Journal of Medicine*, 358(23), pp.2425-2428.
- Olliario, P., 2001. Mode of action and mechanisms of resistance for antimalarial drugs. *Pharmacology & Therapeutics*, 89(2), pp.207-219.

- Pagola, S. et al., 2000. The structure of malaria pigment beta-haematin. *Nature*, 404(6775), pp.307-310.
- Painter, H.J. et al., 2007. Specific role of mitochondrial electron transport in blood-stage *Plasmodium falciparum*. *Nature*, 446(7131), pp.88-91.
- Pandey, A.V. et al., 1999. Artemisinin, an endoperoxide antimalarial, disrupts the hemoglobin catabolism and heme detoxification systems in malarial parasite. *The Journal of Biological Chemistry*, 274(27), pp.19383-19388.
- Parikh, S. et al., 2006. Antimalarial Effects of Human Immunodeficiency Virus Type 1 Protease Inhibitors Differ from Those of the Aspartic Protease Inhibitor Pepstatin. *Antimicrobial Agents and Chemotherapy*, 50(6), pp.2207-2209.
- Parker, M.D. et al., 2000. Identification of a nucleoside/nucleobase transporter from *Plasmodium falciparum*, a novel target for anti-malarial chemotherapy. *The Biochemical Journal*, 349(Pt 1), pp.67-75.
- Peters, J.M. et al., 2002. Mutations in Cytochrome b Resulting in Atovaquone Resistance Are Associated with Loss of Fitness in *Plasmodium falciparum*. *Antimicrobial Agents and Chemotherapy*, 46(8), pp.2435-2441.
- Plowe, C.V. et al., 1997. Mutations in *Plasmodium falciparum* dihydrofolate reductase and dihydropteroate synthase and epidemiologic patterns of pyrimethamine-sulfadoxine use and resistance. *The Journal of Infectious Diseases*, 176(6), pp.1590-1596.
- Rawlings, N.D., 2010. Peptidase inhibitors in the MEROPS database. *Biochimie*, 92(11), pp.1463-1483.
- Rottmann, M. et al., 2010. Spiroindolones, a potent compound class for the treatment of malaria. *Science (New York, N.Y.)*, 329(5996), pp.1175-1180.
- Rupp, I. et al., 2008. Effect of protease inhibitors on exflagellation in *Plasmodium falciparum*. *Molecular and Biochemical Parasitology*, 158(2), pp.208-212.
- Saldanha, A.J., 2004. Java Treeview--extensible visualization of microarray data. *Bioinformatics (Oxford, England)*, 20(17), pp.3246-3248.
- Sanchez, C.P. et al., 2008. Polymorphisms within PfMDR1 alter the substrate specificity for anti-malarial drugs in *Plasmodium falciparum*. *Molecular Microbiology*, 70(4), pp.786-798.
- Sanchez, C.P., Stein, W.D. & Lanzer, M., 2007. Is PfCRT a channel or a carrier? Two competing models explaining chloroquine resistance in *Plasmodium falciparum*. *Trends in Parasitology*, 23(7), pp.332-339.

- Sharma, A. & Mishra, N.C., 1999. Inhibition of a protein tyrosine kinase activity in *Plasmodium falciparum* by chloroquine. *Indian Journal of Biochemistry & Biophysics*, 36(5), pp.299-304.
- Sidhu, A.B.S. et al., 2006. Decreasing pfmdr1 copy number in plasmodium falciparum malaria heightens susceptibility to mefloquine, lumefantrine, halofantrine, quinine, and artemisinin. *The Journal of Infectious Diseases*, 194(4), pp.528-535.
- Sidhu, A.B.S., Valderramos, Stephanie Gaw & Fidock, David A, 2005. pfmdr1 mutations contribute to quinine resistance and enhance mefloquine and artemisinin sensitivity in *Plasmodium falciparum*. *Molecular Microbiology*, 57(4), pp.913-926.
- Silva-Neto, M.A.C., Atella, G.C. & Shahabuddin, M., 2002. Inhibition of Ca²⁺/calmodulin-dependent protein kinase blocks morphological differentiation of plasmodium gallinaceum zygotes to ookinetes. *The Journal of Biological Chemistry*, 277(16), pp.14085-14091.
- Singh, B. et al., 2004. A large focus of naturally acquired Plasmodium knowlesi infections in human beings. *Lancet*, 363(9414), pp.1017-1024.
- Skinner, T.S. et al., 1996. In vitro stage-specific sensitivity of *Plasmodium falciparum* to quinine and artemisinin drugs. *International Journal for Parasitology*, 26(5), pp.519-525.
- Slater, A.F. & Cerami, A., 1992. Inhibition by chloroquine of a novel haem polymerase enzyme activity in malaria trophozoites. *Nature*, 355(6356), pp.167-169.
- Slater, A.F. et al., 1991. An iron-carboxylate bond links the heme units of malaria pigment. *Proceedings of the National Academy of Sciences of the United States of America*, 88(2), pp.325-329.
- Snow, R W & Marsh, K, 1998. New insights into the epidemiology of malaria relevant for disease control. *British Medical Bulletin*, 54(2), pp.293-309.
- Solomon, V.R. & Lee, H., 2009. Chloroquine and its analogs: a new promise of an old drug for effective and safe cancer therapies. *European Journal of Pharmacology*, 625(1-3), pp.220-233.
- Soulard, A. et al., 2010. The Rapamycin-sensitive Phosphoproteome Reveals That TOR Controls Protein Kinase A Toward Some But Not All Substrates. , 21(19), pp.3475-3486.
- Srivastava, I.K., Rottenberg, H. & Vaidya, A B, 1997. Atovaquone, a broad spectrum antiparasitic drug, collapses mitochondrial membrane potential in a malarial parasite. *The Journal of Biological Chemistry*, 272(7), pp.3961-3966.

- Stack, C.M. et al., 2007. Characterization of the Plasmodium falciparum M17 leucyl aminopeptidase. A protease involved in amino acid regulation with potential for antimalarial drug development. *The Journal of Biological Chemistry*, 282(3), pp.2069-2080.
- Sullivan, D J et al., 1996. On the molecular mechanism of chloroquine's antimalarial action. *Proceedings of the National Academy of Sciences of the United States of America*, 93(21), pp.11865-11870.
- Sullivan, David J., 2002. Theories on malarial pigment formation and quinoline action. *International Journal for Parasitology*, 32(13), pp.1645-1653.
- Taylor, S.M., Juliano, J.J. & Meshnick, Steven R, 2009. Artemisinin resistance in Plasmodium falciparum malaria. *The New England Journal of Medicine*, 361(18), p.1807; author reply 1808.
- Toovey, S., 2004. The Miraculous Fever-Tree. The Cure that Changed the World Fiametta Rocco; Harper Collins, San Francisco, 2004, 348 pages, Paperback, ISBN 0-00-6532357. *Travel Medicine and Infectious Disease*, 2(2), pp.109-110.
- Trager, W. & Jensen, J.B., 1976. Human malaria parasites in continuous culture. *Science*, 193(4254), pp.673-675.
- Tuteja, R., 2007. Malaria - an overview. *The FEBS Journal*, 274(18), pp.4670-4679.
- Vaidya, A B et al., 1993. Structural features of Plasmodium cytochrome b that may underlie susceptibility to 8-aminoquinolines and hydroxynaphthoquinones. *Molecular and Biochemical Parasitology*, 58(1), pp.33-42.
- Van den Eede, P. et al., 2009. Human Plasmodium knowlesi infections in young children in central Vietnam. *Malaria Journal*, 8, p.249.
- Vennerstrom, J.L. et al., 2004. Identification of an antimalarial synthetic trioxolane drug development candidate. *Nature*, 430(7002), pp.900-904.
- Wellems, Thomas E. et al., 1990. Chloroquine resistance not linked to mdr-like genes in a Plasmodium falciparum cross. *Nature*, 345(6272), pp.253-255.
- White, N J, 1999. Delaying antimalarial drug resistance with combination chemotherapy. *Parassitologia*, 41(1-3), pp.301-308.
- White, N J, 2008. Qinghaosu (artemisinin): the price of success. *Science (New York, N.Y.)*, 320(5874), pp.330-334.
- White, Nicholas J, 2010. Artemisinin resistance-the clock is ticking. *The Lancet*, 376(9758), pp.2051-2052.

- Wilson, C.M. et al., 1993. Amplification of *pfmdr 1* associated with mefloquine and halofantrine resistance in *Plasmodium falciparum* from Thailand. *Molecular and Biochemical Parasitology*, 57(1), pp.151-160.
- Wirth, Dyann F., 2002. The parasite genome: Biological revelations. *Nature*, 419(6906), pp.495-496.
- Wongsrichanalai, C. et al., 2002. Epidemiology of drug-resistant malaria. *The Lancet Infectious Diseases*, 2(4), pp.209-218.
- World Health Organization, 2010. Malaria Factsheet Nr. 94. *World Health Organization, Geneva*.
- Zhang, H., Howard, E.M. & Roepe, Paul D., 2002. Analysis of the Antimalarial Drug Resistance Protein Pfert Expressed in Yeast. *Journal of Biological Chemistry*, 277(51), pp.49767 -49775.
- Zhang, H., Paguio, M. & Roepe, Paul D., 2004. The Antimalarial Drug Resistance Protein Plasmodium falciparum Chloroquine Resistance Transporter Binds Chloroquine. *Biochemistry*, 43(26), pp.8290-8296.
- Zhang, Y. & Meshnick, S R, 1991. Inhibition of *Plasmodium falciparum* dihydropteroate synthetase and growth in vitro by sulfa drugs. *Antimicrobial Agents and Chemotherapy*, 35(2), pp.267-271.

Curriculum vitae

Name Ralf Oskar Brunner
Date of birth 18.05.1979
Citizenship Swiss
Private address Palmenstrasse 15, 4055 Basel, Switzerland

Education and employment

2008 – 2011 PhD in cell biology, Swiss Tropical and Public Health
Institute, University of Basel, and Actelion Pharmaceuticals Ltd
Supervisor: Prof. Reto Brun
“A Novel Antimalarial Lead Compound:
In Vitro Properties and Mode of Action Studies”

2005 – 2008 Medical and Product Management (oncology),
F. Hoffmann-La Roche Ltd

1999 – 2004 MSc in molecular biology, Biocenter, University of Basel
Supervisor: Prof. Nicole Schaeren-Wiemers
“Characterization of Differentially Expressed Genes in Multiple
Sclerosis Brain Tissues”

Publication

2010 “Rapid anaemia control with epoetin: results of a Swiss survey on
treatment of chemotherapy-induced anaemia”

Popescu R, von Rohr A, Piguet D, Irlé C, Giger M, Brunner R, Ahnesorg P, Zappa F. *Acta Haematologica*. 2010; 123(2), pp.129-134

Conferences

2010 Attendance: Molecular Parasitology Meeting: Woods Hole, MA, USA

Talk: PhD student meeting of the Swiss Society of Tropical Medicine and Parasitology (SSTMP): Spiez, Switzerland

2009 Talk: PhD student meeting of the Swiss Society of Tropical Medicine and Parasitology (SSTMP): Basel, Switzerland

2008 Attendance: Malariatreffen der Paul Ehrlich Gesellschaft (PEG) und der Deutschen Gesellschaft für Tropenmedizin und Internationale Gesundheit (DTG): Tübingen, Germany

Talk: PhD student meeting of the Swiss Society of Tropical Medicine and Parasitology (SSTMP): Jongy, Switzerland

During my studies I attended lectures by the following lecturers:

U. Aebi, M. Affolter, S. Arber, T. Bickle, G. Cornelis, C. Dehio, M. Dürrenberger, A. Engel, W. Gehring, S. Grzesiek, H. J. Güntherodt, M. Hall, M. Hamburger, H. P. Hauri, H. C. Im Hof, U. Jenal, W. Keller, T. Kiefhaber, J. Pieters, H. Reichert, A. Rolink, M. Rüegg, T. Schirmer, A. Seelig, J. Seelig, U. Séquin, I. Sick, H. Sigel, M. Spiess, M. Tanner, C. Thompson.